CRANFIELD UNIVERSITY

Martina Mohseni

HELIX – SIMULATION FRAMEWORK DEVELOPMENT FOR ASSESSMENT OF ROTORCRAFT ENGINES

SCHOOL OF ENGINEERING

PhD THESIS

CRANFIELD UNIVERSITY

SCHOOL OF ENGINEERING

DEPARTMENT OF POWER AND PROPULSION

PhD THESIS

2008-2011

Martina Mohseni

HELIX – SIMULATION FRAMEWORK DEVELOPMENT FOR ASSESSMENT OF ROTORCRAFT ENGINES

Supervisors: Dr. Vassilios Pachidis

Professor Pericles Pilidis

March 2011

This thesis is submitted in partial fulfilment of the requirements for the degree of Doctor of Philosophy

Executive Summary

The inevitable growth of air traffic resulting from the increasing demands on utilization of the aircraft for various purposes has introduced public awareness and concern about the contribution of air traffic towards climate change. The increase of aircraft emissions enhancing the greenhouse effect and decreasing the air quality in general, is no longer considered sustainable and steps are being taken towards the mitigation of this problem. Although a significant research activity takes place in the development of new technologies, the most readily available solution to this problem is seen in applying changes to aircraft operational rules and procedures and in optimizing the flight paths using the aircraft currently in service.

The helicopter, although comprising a significantly smaller portion of the aircraft market in comparison with the fixed-winged aircraft, is experiencing the same concerns with respect to the amount of gaseous emissions produced. The helicopter plays a specific and irreplaceable role in the air transportation and it is often being used for purposes where the environmental concerns are secondary (such as during medical rescue operations or during police missions). It is however being increasingly employed for non-urgent operations, such as executive business travel or for the transportation of personnel to and from oil rigs. In all cases, the most readily available solution (and also perhaps the least costly) to lowering the gaseous emissions is to evaluate the helicopter engine performance along a given flight path using a computer program in order to investigate the effect on fuel burn and gaseous emissions.

For this purpose, the development of a helicopter engine performance assessment tool has been established as the main objective of this research in order to evaluate the helicopter and engine performance at any given condition along the flight path. This tool has been developed in a way that allows the integration into the larger platform together with other performance and optimization programs in order to assess and quantify the environmental effect of a given helicopter mission.

In order to accomplish this objective a helicopter performance scheme, HELIX, was developed. This performance tool was subsequently incorporated into a larger

integration platform, HECTOR, comprising of several other performance models, namely engine and emission prediction models and of an optimization toolbox. Subsequently several performance analyses and evaluation processes on engine performance and its effects on helicopter missions/operations have been carried out and their results presented.

The main contribution of this research work is the development of a helicopter performance simulation scheme capable of predicting the helicopter performance at any given point along its flight path. The secondary contribution is seen in the development of the library of helicopter engine models.

Based on the results obtained from the performance analyses and comparative studies conducted during this research work, it is concluded that these studies aid significantly in determining the environmental impact of a certain flight path and represent a useful tool for assessing helicopter trajectories at system level and identifying “greener” trajectories. As such they represent a feasible option for reducing the environmental impact of aviation. The precise amount of these reductions is however to be determined yet through a detailed analysis of various mission scenarios.

The further development and the improvements of HELIX’s capabilities should continue in order to represent the helicopter and engine performance with even increased accuracy so that it can be used for the purposes of comparative helicopter performance studies or for the determination of more efficient helicopter trajectories that will help to minimise the environmental impact of the helicopter operations. The future steps in this direction and the enhancements of HELIX’s capabilities were recommended.

Acknowledgements

In the Name of God, the Most Gracious, the most Merciful

I would like to express my gratitude to Prof. Pilidis, for giving me the opportunity of pursuing this PhD, and for his useful advice throughout this research work. I would like to express my gratitude to my supervisor, Dr. Pachidis, for his patient guidance, constructive criticism, suggestions and support. I am also indebted to Dr. Sethi for very useful advice.

I will be forever indebted to my beloved husband, Seyed Mohammad, whose never ending encouragement, patience, love and support have helped me enormously during these years and whose presence by my side has given me and continues to give me the drive to move forward.

My big thanks goes also to our families, especially to my mum and mother-in-law, who have provided me with assistance in looking after our baby and in this way prepared the way for the completion of this thesis. I am grateful to the rest of our families for their patient endurance of separation from them.

Finally, my thanks goes to Katerina and Giusy for our tea breaks together, which represented pleasant experiences in the predominantly male environment; and to our secretaries Gill, Maria and Claire who were always there to help.

List of Contents

List of figures

List of Tables

Nomenclature

ACARE	Advisory Council for Aeronautics Research in Europe
ATAG	Air Transport Action Group
AW	Aircraft weight
CFD	Computational fluid dynamics
CO	Carbon monoxide
CO_2	Carbon dioxide
DL	Disc loading
FUL	Fixed useful load
GTOW	Gross take-off weight
GWP	Global warming potential
EI	Emission index
ICAO	The International civil aviation organization
IGE	In-ground effect
IPCC	Intergovernmental panel on climate change
ITD	Integrated technology demonstrator
JTI	Joint technology initiative
MTOW	Maximum take off weight
NOTAR	NoTAilRotor
NO_X	Nitrogen oxides
OEI	One engine inoperative
OEW	Operating empty weight
OGE	Out-of-ground effect
PL	Power loading
POST	Parliamentary office of science and technology
RPM	Revolutions per minute
SAR	Search and rescue
SFC	Specific fuel consumption
SO_2	Sulphur dioxide
SP	Search pattern

TE	Technology Evaluator
TERA	Techno Economic and Environmental Risk Analysis
TET	Turbine entry temperature
T-O	Take-off
UHC	Unburned hydrocarbons
VTOL	Vertical Take-off and Landing
WGS	World Geodetic System

Symbols

A	rotor disk area
a_s	Speed of sound
B	Tip loss factor
c	Blade chord
	Blade root chord
°C	Degree Celsius
C_D	Drag coefficient
C_L	Lift coefficient
C_P	Specific heat at constant pressure
	Thrust coefficient
C_V	Specific heat at constant volume
D	Rotor diameter (or drag where stated)
E	Endurance
f	Equivalent flat plate area
h	altitude
hPa	hectoPascal
k	Induced power factor
K	Kelvin
L	Lift
m	Meter
M	Mach number
N	Newton
N_b	Number of blades
p	Static pressure
p_0	Ambient static pressure
P_{comp}	Compressibility effects factor
P_h	Power required in hover
P_i	Induced power
P_o	Induced power

P_i	Profile power
P_p	Parasite power
P_{TR}	Tail rotor power
R	Radius (or gas constant where stated)
S	Reference area
t	Static temperature
T	Rotor thrust
t_0	Ambient static temperature
V	Speed
v_c	Climb rate
	Induced velocity
V_{ne}	Never-exceed speed
	Tip speed
W_E	Weight empty
W_F	Weight of fuel
x_{TR}	Main and tail rotor shaft distance
Z	Rotor height above the ground
	angle of attack
	Hover inflow ratio
	Blade solidity
	Blade taper ratio
	Advance ratio
	Azimuth angle
	Angular speed
	Density
	Ambient density
	Ratio of specific heats C_v/C_p

Chapter 1: Introduction

This chapter defines the context of the research together with its scope and objectives. Various environmental impacts of aviation are briefly discussed along with suggested approaches of their mitigation. Consequently, one of the technology initiatives launched to reduce the environmental impacts- Clean Sky JTI - is introduced. Cranfield University's involvement in this programme and the relatedness of this research is then explained and the focus is directed towards the objectives and novel contribution of this study. The chapter is concluded by outlining the thesis structure.

1.1 Aviation and the Environment

Like virtually every area of human activity, air transport has an impact on the environment. Among the environmental impacts of aviation that have a significant effect on the lives of people, especially those living in a close proximity to the airports, are noise, air pollution and other local environmental impacts such as waste management, water pollution and land seizure. Each of these impacts is briefly discussed below:

1.1.1 Aircraft Noise

According to the Parliamentary Office of Science and Technology the UK government states that: "noise is one of the most objectionable impacts of airport development and for many airports, taking effective measures to mitigate and control aircraft noise is fundamental to their sustainable development." (POST, 2010)

The industry has been tackling the challenge of noise reduction for the past few decades. According to the studies done by Boeing or Airbus, on average, aircraft are already 50% quieter today than they were 10 years ago. The International Civil Aviation Organization (ICAO), the United Nations' intergovernmental body on aviation, introduced a new noise certification standard, that aimed to ensure new aircraft were at least 10 decibels (or one third) quieter than those built to previous standard.

The solution to reduce aircraft noise typically comes from more than one approach. This includes noise reduction at source; land-use planning and management; operational procedures and flight restrictions. The intention is to maximize the environmental benefit at lowest cost.

1.1.2 Air Pollution

Major concerns for the aviation industry present greenhouse gas emissions and their implication on climate change. Despite the continuing improvements in emission levels from aircraft engines, the forecasted growth in air travel implies that the emissions from the aircraft are apt to become a more considerable source of air pollution around the airports. (POST, 2010)

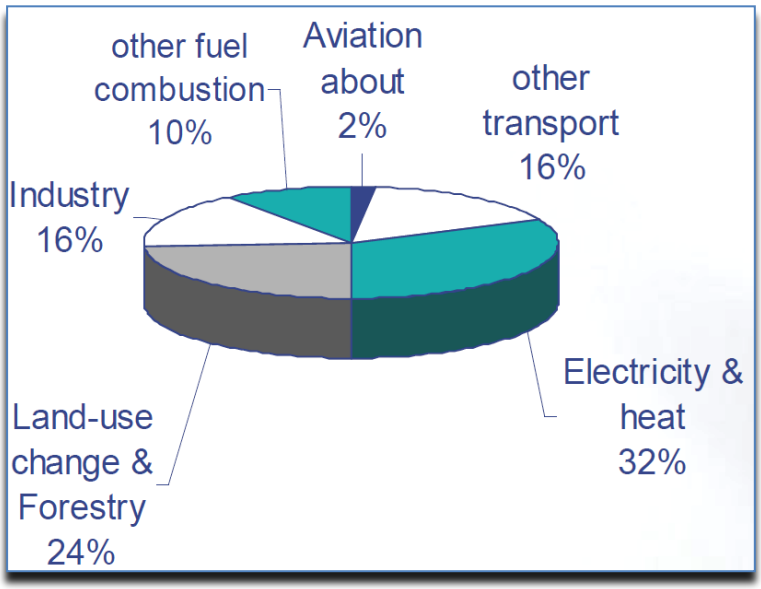

Figure 1. 1– Global man-made CO2 emissions (source: World Resources Institute) (Kumar, 2007)

Aircraft engines emit a mixture of gases, with carbon dioxide (CO_2), nitrogen oxides (NO_x) and water vapour among the most pertinent when considering effects on the global atmosphere.

Aviation produces approximately 2% of the world's manmade emissions of carbon dioxide according to the United Nations Intergovernmental Panel on Climate Change (IPCC). With the predicted growth of aviation to meet the increasing demand, its share of global manmade CO_2 emissions is expected to rise to around 3% in 2050, according to IPCC. (Kumar, 2007)

The quantities of CO_2 and water vapour emitted from aircraft engines are proportional to the amount of fuel used. Hence, a possible mitigation strategy to reduce these emissions is to increase the fuel efficiency of aircraft. The fuel efficiency gain can potentially be achieved by improvements in:

• technology – via increase in engine efficiency, use of alternative fuels and power sources and improvements in aircraft aerodynamics

• operational procedures represented by alterations of current air traffic control practices and flight arrangements. (ATAG, 2010)

It is broadly accepted that tackling the environmental impacts of aviation requires a 'balanced approach' which can be seen as an integration of both technological improvements and nontechnical means such as modifications to aircraft operations. (POST, 2010)

1.1.3 Other Local Environmental Impacts

Although aircraft noise and air pollution are the most significant environmental impacts that need to be dealt with, there are other local ones that also need to be taken into consideration. Examples of these include:

- Land seizure for building airports would have an effect on wildlife habitats and landscape
- Water pollution, particularly from de-icing the aircraft, runways and other parts of the airport site
- Waste management of the waste generated inside the terminal buildings (POST, 2010)

These local environmental impacts are however in most cases subject to mitigation by local authorities and are more or less controllable effects of the infrastructure development.

The reduction of the environmental impacts of aviation often introduces contradictory requirements and certain compromises need to be made. For example, the aviation industry needs to comply with strict measures with regards to noise

abatement and therefore flights have to be directed over less populated areas, which often means prolonging the aircraft route and consequently increasing the amount of fuel used. (ATAG, 2010)

1.2 Clean Sky JTI

Government policy and legislation relating to environmentally friendly air travel is mostly focused on emissions trading and other economic measures, such as taxation. Governments are focusing on positive economic measures such as incentives for using more fuel-efficient aircraft and funding for research and development. This research activity is part of the European Union's "Clean Sky" Joint Technology Initiative (JTI), a large program that is planning to develop breakthrough technologies to significantly improve the impact of air transport on the environment. This project aims to demonstrate and validate the technology breakthroughs that are necessary to make major steps towards the environmental goals sets by ACARE - Advisory Council for Aeronautics Research in Europe - to be reached in 2020. (Clean Sky JTI, 2009). The goals include reduction of emissions, improvement of flight performance, noise reduction, improvement of safety and cost reduction (Wildi, 2008). Within its planned duration of 7 years Clean Sky JTI aims are to reduce fuel consumption and CO_2 by 50%, NO_X by 80% and perceived external noise by 50%. (Quentin, 2009) This research programme involves 86 organisations in 16 countries, including Cranfield University. It consists of 6 projects –Integrated Technology Demonstrators (ITD) and the Technology Evaluator (TE).

The expected impacts of the Clean Sky JTI project are twofold:

- Environmental

  - faster introduction of innovative technologies, less noise, lower emissions, lower fuel consumption and greener design, production and maintenance

- Socio-economic impact

  - integrating European industry, major contribution to sustainable growth in Europe, a competitive European industry leading to introduction of more environmentally friendly products and sustaining the creation of highly qualified jobs

More information about Clean Sky JTI project is provided in Chapter 2.

Cranfield University is involved in the *Technology Evaluator* and is interacting strongly with the Green Rotorcraft ITD. The general objectives of the Green Rotorcraft technology domain are to tackle the noise reduction via design of innovative rotor blades and engine installation, lower airframe drag, integration of diesel engine technology and advanced electrical systems for elimination of noxious hydraulic fluids and fuel consumption reduction. (Clean Sky JTI, 2009).

The Technology Evaluator, on the other hand, is visualised as a shared and integrated methodology, consistently quantifying the environmental impact of each of the innovative technologies proposed. Its role is to provide an overall assessment of the value of Clean Sky JTI activities performed within the ITDs in order to comply with the ACARE environmental goals and to help substantiate consistency between all ITDs and maximize synergies between them.

More information about the TE is provided in Chapter 2.

Cranfield University also actively participates in the *Systems for Green Operations (SGO)* Integrated Technology Demonstrator of the Clean Sky project. The SGO focuses on two key areas: Management of Aircraft Energy (MAE), and Management of Trajectory and Mission (MTM). The main contributions of Cranfield University to the SGO ITD are seen in the development of computational algorithms not only for the management of aircraft trajectory and mission, but also for the modelling of various disciplines involved in the optimisation processes, such as aircraft performance, engine performance, or pollutants formation (ACARE, 2007).

1.2.1 TERA

A number of concepts are being put forward to mitigate or eliminate CO_2 emissions. As an aid for assessment of advantages and disadvantages of these strategies, detailed plant and component mathematical models need to be used. This is an idea behind TERA (Technoeconomic and Environmental Risk Analysis) that Cranfield University has initiated and is deploying within the European power and propulsion context. Aircraft TERA is a set of models comprising of the thermodynamic model of the engine coupled with the noise, weight, aircraft, environment, economic and risk models. It is an effective tool at the preliminary stage of the design process to identify most promising solutions (via design space exploration, sensitivity/trade off studies, etc.). Final decisions for designs need to be made by the engine manufacturers following rigorous simulations using their proprietary data and higher fidelity tools. (Ogaji et al., 2007)

Currently, a few versions of TERA exist. Apart from aircraft TERA, its marine and industrial versions were also formed by altering some of the models within the TERA environment. One of the objectives of this research project was to create a helicopter thermodynamic performance simulation model that could in the future replace the aircraft model within TERA and that could be integrated with the rest of the models and as such give rise to the helicopter version of TERA for turboshaft engine performance calculations including noise, emissions, fuel burn, integration and installation studies. As such, this helicopter version of TERA could be used in the context or Cranfield University's work within the TE to assess the helicopter mission fuel burn and emissions.

More detailed discussion on TERA concept can be found in Chapter 2.

1.3 Objectives and Scope

Evaluating the available options to reduce the aircraft impact, it can be seen that certain approaches are more readily applicable than others. While enhancements of the current technology and improvements of aircraft design might take many years

and may be very costly, the aircraft trajectory analysis with respect to identifying more fuel efficient flight paths and reducing aircraft emissions along these flight paths might represent a more readily implementable solution. The above discussed Clean Sky JTI project and in particular the objectives of the TE provide a framework for a research study that would aid the establishment of the environmentally friendly flight paths for a helicopter. Consequently, a need arises to develop a computational model that would be capable of predicting the thermodynamic performance of the helicopter and its engine at a given flight condition and that would be suitable for a helicopter flight path analysis. This tool can in the future be utilized for flight path optimizations with respect to lower fuel burn or lower emissions. Hence, the objectives of this research study were defined as follows:

- Development of a tool with the capabilities to simulate the performance of the most common helicopter configuration. The tool will calculate basic performance parameters along the user-specified helicopter flight path. The performance prediction program will have the capability to assess current helicopter designs as well as novel concepts. Design of this tool needs to be carried out in mind with the potential of integration with the optimizer and also with the TERA environment. This tool could then be used in the context of Cranfield University's involvement in the TE work of the Clean Sky JTI project in order to assess helicopter mission fuel burn and emissions.
- Enhancement of the tool capabilities to enable a three-dimensional definition of a helicopter mission trajectory. In other words, to express the position of the helicopter at any given time by using the recognized geodetic system – WGS84.
- Conducting the evaluation and analysis of the results of the developed helicopter performance model in connection with the integrated framework.
- Development of a library of thermodynamic helicopter engine models that can be used for the helicopter performance prediction tool's evaluation studies: active role (development of four engine models) and passive role (advisory approach over several MSc projects).

1.4 Thesis Structure

The thesis is structured in the following manner:

Literature review of the topics providing a background for the research is discussed in Chapter 2. The chapter starts with the review of works describing *aviation's impact on the environment*, and suggests possible mitigation strategies and solutions. The chapter then moves on to discussing the European *Clean Sky JTI* project in more detail as well as the involvement of Cranfield University in it, primarily through the work on the *Technology Evaluator.* The helicopters are described in terms of their *configurations, their roles and applications* as well as the standard way of their *classification*. *Helicopter basic aerodynamics* and flight dynamics is briefly touched upon further in the chapter to provide the reader with the minimum required information in order to follow the research findings. The relatively scarce studies that are addressing a *helicopter performance* are reviewed. The description of the two most commonly used *helicopter performance modelling methodologies* is offered and finally, an insight into the *helicopter mission performance* is provided.

The methodology used for this research study is touched upon in Chapter 3. The first part of this chapter describes the *interaction and interconnection between various tools and models* used as well as their brief description. Following that, *HECTOR*, an optimization framework, developed in Cranfield University, is referred to in relation to this research study and its synthesis with the developed tool is described.

Helicopter performance model – HELIX – the core of this study is the topic of the fourth chapter. The *requirements* of this model are laid out, followed by a brief *description of the model*, its architecture and the description of the workflow. The attention is then focused on the *model structure*, including the description of the functions, subroutines and other parts of the model. The next part of the chapter details a further development of this model in a sense of implementation of the *three-dimensional trajectory simulation*. The chapter is then concluded by a discussion of the *synthesis* of HELIX with the integrated simulation platform HECTOR.

Helicopter engine modelling is mentioned in chapter 5. A necessary part of the performance simulation of the helicopter is the thermodynamic model of its engine. Hence a library of helicopter engine thermodynamic models was required in order to enable accurate performance simulations of helicopters of any size. The development of the *library of the helicopter engine models* in cooperation with MSc students is addressed and *the contribution of MSc students* is highlighted. The chapter is concluded with the *results of simulations* of selected engine models, using TURBOMATCH - the Cranfield University performance simulation software (Palmer, 1990).

Results of the HELIX performance simulation studies are summarized in chapter 6. A number of *comparative studies* were conducted using HELIX as part of the HECTOR framework in order to verify the results. The lack of data in the open literature that the HELIX results could be compared against means that a validation studies were not possible, however, certain parametric studies were performed in order to gain confidence in the calculated results. The effect of cruise altitude, and gross take-off weight on the fuel burn and emissions were investigated as well as the effect of forward velocity, cruise range and the climb and descent angle. The results were compared to the general performance characteristics available in the open literature.

Conclusions and future work are discussed in the final chapter (chapter 7). The novel contribution of this research study is highlighted in context of current state of findings within the field of helicopter performance. The process of creating the helicopter performance tool HELIX is summarized and suggestions and recommendations for its enhancement and for the future work in this area are offered.

Chapter 2: Literature Review

This chapter starts with the review of works describing aviation's impact on the environment, and discusses possible mitigation strategies and solutions. The chapter then moves on to discussing the European Clean Sky JTI project in more detail as well as the involvement of Cranfield University in it, primarily through the work in the Technology Evaluator. The basic necessary background for the relevant study of the helicopter performance is provided, including the overview of helicopter configurations, their roles and applications as well as the standard way of their classification, followed by a review of helicopter basic aerodynamics and flight dynamics. The term helicopter performance is explained and its basic aspects are reviewed. Finally, an insight into the helicopter mission performance is provided.

2.0 Glossary of Used Terms

Angle of attack - the angular difference between the chord of the blade and the relative airflow (also known as the relative wind)

Blade angle (pitch angle) – the angular difference between the chord of the blade and the plane of rotation

Collective control – means of mechanical rotor control to decrease or increase the blade angle of all the rotor blades simultaneously

Cyclic control – means of mechanical rotor control to alter the blade angle of individual blades

Drag coefficient – the dimensionless number which represents the drag characteristics of an aerodynamic body. It is determined mainly by its shape and angle of attack

Ground effect – A beneficial gain in lifting power when operating near the surface – caused by the rotor downwash field being altered from its free air state by the presence of the surface

Induced flow - the mass of air that is forced down by the rotor action. It travels down through the rotor when the helicopter is in normal powered flight and is the result of lift that has deflected the airflow downward

Lift coefficient – the dimensionless number representing the lifting ability of an airfoil. It is determined mainly by the airfoil's shape and angle of attack

Relative airflow – the velocity vector of the airflow approaching the blades

Tip path – the circular path described by the tips of the rotor blades

Tip speed – the rotational speed of the rotor at its blade tips

Torque – the moment of a force or combination of forces that tends to produce rotational motion

Yaw – movement of the aircraft around its vertical axis

2.1 Atmospheric Effects of Aviation

It is widely recognized that the emissions formed by civil air traffic may cause climate changes by an increase of ozone in the upper troposphere and enhance greenhouse effect. Although advances in gas turbine technology are continually being made the challenge to improve energy efficiency and emissions performance remain high priorities. Research and interest in the environment by scientists and, increasingly the general public has evolved from concern for the deterioration in air quality to broader issues of ozone depletion and global warming.

The major pollutants are considered to be CO_2 and water vapour that are produced by the combustion of jet fuel. Water vapour plays a role in the ozone depletion process. It can cause a formation of contrails when combined with soot particles in the jet engine exhaust. The formation of contrails is due to ambient temperature, humidity and engine efficiency. (Sadiq, 2007), (Noppel et.al, 2008)

The emission levels are proportionate to the amount of fuel consumed and the amount of hydrogen and carbon contained in the fuel. Other products of combustion include nitrogen oxides (NO_x), carbon monoxide (CO), and unburned hydrocarbons (UHC). Nitrogen oxides are produced in the high-temperature regions of the combustor primarily through the oxidation of atmospheric nitrogen. The amount of emissions produced depends on the engine power setting.

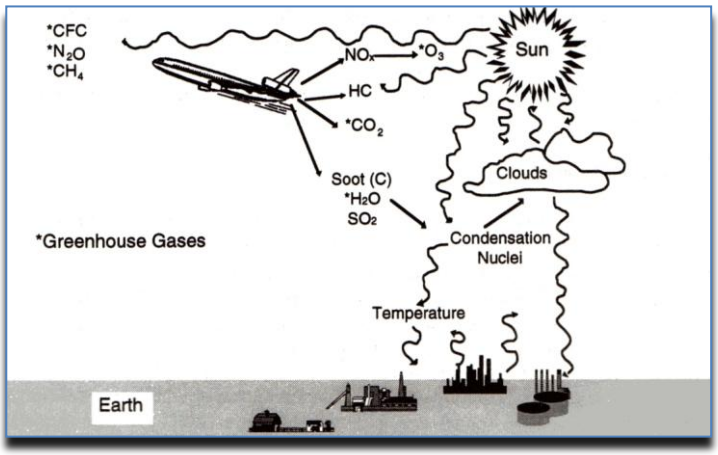

Figure 2. 1 – Climate effect of emissions (Thompson et al., 1996)

Other emissions, such as sulphur dioxide (SO_2) from aircraft engines are determined by the levels of sulphur contained in the jet fuel.

As part of the certification process for each commercial aircraft engine type two categories of emissions are controlled: smoke and gaseous emissions, such as UHC, NO_x and CO. The smoke is measured and assessed in terms of Smoke Number, whereas the gaseous pollutants are measured at power settings of 7% (taxi/ground idle), 30% (approach), 85% (climb out) and 100% (take off) and the measurements are reported in grams. These measurements have been developed to evaluate aircraft emissions in the vicinity of airports, rather than for cruise altitude conditions. They do, however, provide a comprehensive database for interpolation to cruise conditions. (Thompson et al. 1996), (ICAO, 2008)

The situation has to be viewed differently for the helicopters. The helicopter industry has to face the policy challenge of no clear regulatory imperatives being in place. As

mentioned above, the emissions-trading systems for airliners are putting significant pressure on aircraft manufacturers to reduce the emission output of their products, but no similar rules apply for rotorcraft. However, the industry officials are largely in agreement that well defined restrictions also have to be imposed to helicopters. (Wall, 2009)

2.1.1 Clean Sky JTI

Improvements in engine component efficiencies have led to additional progress in engine fuel efficiency and other advances in technology in the past few decades have played their role in decreasing the aircraft emissions; however, the inevitable growth in air travel means that the amount of greenhouse gases emitted by the aircraft is increasing. The overall society trend indicates that further increase in emissions is unacceptable. This approach also affects the aviation despite its relatively small contribution to man-made CO_2 emissions (currently approximately 2%). A number of worldwide initiatives have stemmed from the need to resolve the emission problem. Focus of these initiatives is directed towards finding the best alternatives to reduce the environmental impact of the aircraft operations.

The industry together with the governmental bodies are trying to procure mechanisms and incentives for further technological and operational improvements. These include:

• voluntary agreements – collective agreements between the industry and governments on target reductions in emissions, either at European Union or at international level

• emissions charges – fees charged to the airlines and subsequently passengers that reflect the amount of emissions produced by a particular flight

• emissions trading –buying and selling of the emissions permits related to a quantity of greenhouse gas emissions between the airlines

• aviation fuel tax –This measure can only affect domestic or European flights as under ICAO regulations, fuel tax cannot be introduced on fuel for international flights.

The actual impact of these mechanisms on the reduction of aviation emissions varies. Some of the mechanisms would have a short-term, while others would have a long-term effect. In the short term, voluntary agreements may be attainable on issues such as increasing the efficiency of air traffic management and using aircraft most appropriate for specific journeys. However, these options are unlikely to reduce emissions significantly in the long term. Further improvements in engine design, airframe aerodynamics, and a European Union-based emissions charge could be effective - although the latter would not reflect the full climate change impact of long-haul flights. In the longer term, it is widely suggested that a move towards an international global emissions trading scheme could stimulate radical innovation and help manage demand.

Among the technological means that could reduce aircraft emissions are:

• quieter aircraft engines and airframes

• improving the efficiency of the engines and consequently reducing the emissions of air pollutants and greenhouse gases

• the environmental impacts of airport operations can be lessened through careful engineering and mitigation (e.g. recycling wastes, ensuring energy efficiency in buildings and locating infrastructure away from sensitive habitats).

Government policy and legislation relating to environmentally friendly air travel is mostly focused on emissions trading and other economic measures, such as taxation. Governments are focusing on positive economic measures such as incentives for using more fuel-efficient aircraft and funding for research and development. This research activity is part of the European Union's "Clean Sky" Joint Technology Initiative (JTI), a large program that is planning to develop breakthrough technologies to significantly improve the impact of air transport on the environment. This project

aims to demonstrate and validate the technology breakthroughs that are necessary to make major steps towards the environmental goals sets by ACARE - Advisory Council for Aeronautics Research in Europe - to be reached in 2020. (Clean Sky JTI, 2009). The goals include reduction of emissions, improvement of flight performance, noise reduction, improvement of safety and cost reduction. (Wildi, 2008) Within its planned duration of 7 years Clean Sky JTI aims are to reduce fuel consumption and CO_2 by 50%, NO_X by 80% and perceived external noise by 50%. (Quentin, 2009) This research programme involves 86 organisations in 16 countries, including Cranfield University. It consists of 6 projects – ITDs (Integrated Technology Demonstrators) and the Technology Evaluator.

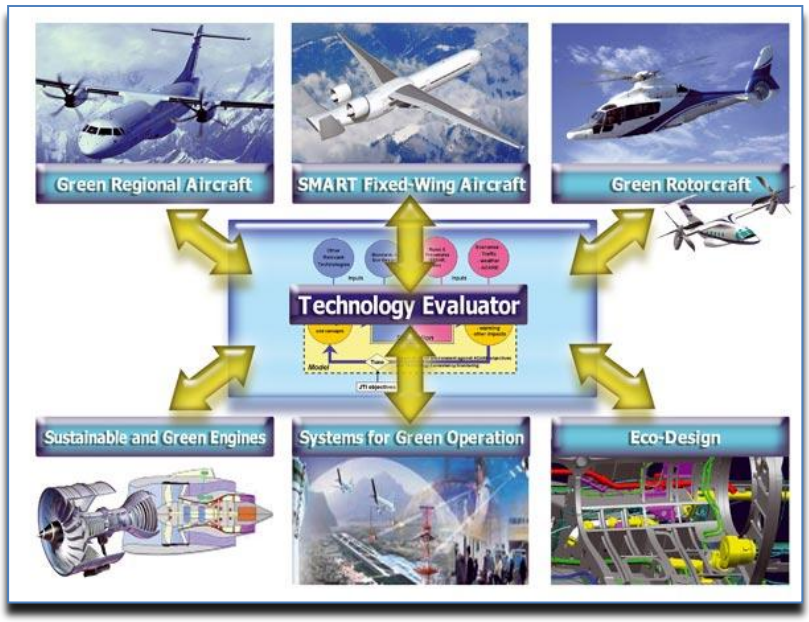

Figure 2. 2 – The ITDs and the Technology Evaluator (Clean Sky JTI, 2009)

The expected impacts of the Clean Sky JTI project are both environmental (faster introduction of innovative technologies, less noise, lower emissions, lower fuel consumption and greener design, production and maintenance) and socio-economic (integration of the European industry, major contribution to sustainable growth in Europe, a creation of competitive European industry leading to introduction of more environmentally friendly products and sustaining the creation of highly qualified jobs).

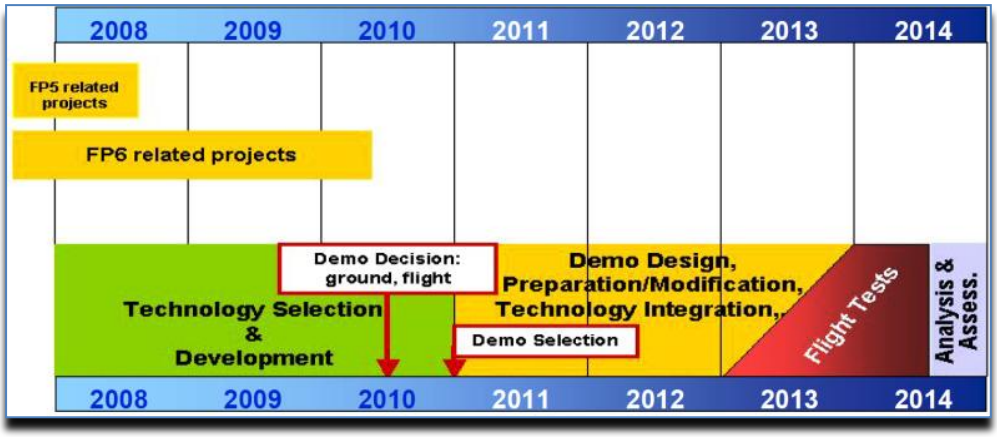

Figure 2. 3 – Timetable for Clean Sky JTI project (Clean Sky JTI, 2009)

Cranfield University is interacting strongly with the *Green Rotorcraft ITD*. The general objectives of this technology domain are to tackle the noise reduction via design of innovative rotor blades and engine installation, lower airframe drag, integration of diesel engine technology and advanced electrical systems for elimination of noxious hydraulic fluids and fuel consumption reduction. (Clean Sky JTI, 2009). Some of the proposed mitigation strategies of this technology domain are outlined below:

(1) Environmentally friendly flight paths

- Optimization of the take-off and landing procedures to and from helipads or airports located within densely populated areas in order to significantly reduce external noise and fuel consumption.
- Optimization of the mission profiles for lower fuel consumption and reduced NO_X and CO_2 emissions.
- Optimizations of flight procedures for tilt rotor configurations with respect to noise during approach and departure.
- Optimization of low altitude navigation needed on short flights and for non-pressurised cabins

(2) Focus on Technology Development

- External noise reduction by optimisation of rotor blade design and the design of air intakes and exhaust nozzles of turboshaft engines, especially in hovering conditions
- Cleaner and more efficient power use by improvements to the airframe for the reduction of aerodynamic drag and download in cruise flight conditions; by engine integration, based on adaptation of diesel engine technology to light helicopters and turboshaft engine installation optimised for minimal power loss; and finally by larger employment of the electrical systems. (Clean Sky JTI, 2009)

Another ITD that the Cranfield University takes part in is the *Systems for Green Operations (SGO)* Integrated Technology Demonstrator of the Clean Sky project. This ITD will create value for improved aircraft operation through the management of aircraft energy and the management of mission and trajectory. The highest overall benefits will be appreciated during the approach, on-ground and departure phases, where the environmental impact near built-up areas is felt the most. (Clean Sky JTI, 2009)

The SGO focuses on two key areas: Management of Aircraft Energy (MAE), and Management of Trajectory and Mission (MTM). The Cranfield University contributes to the MTM platform by developing a multi-objective aircraft trajectory optimization algorithm that would be used as a core optimizer of the MTM platform. The main goal is to produce a standard optimization tool which is conveniently suited to the aircraft trajectory problem. Developing such a tool, called Green Aircraft Trajectory under ATM Constraints (GATAC) will represent a step towards fulfilling the objectives of the SGO ITD. (Marzal Espi, 2010)

All ITDs are linked to the *Technology Evaluator (TE),* in which the Cranfield University actively participates. The Technology Evaluator is a shared and integrated methodology, consistently quantifying the environmental impact of each of the innovative technologies proposed. Its role is to provide an overall assessment of the

value of Clean Sky JTI activities performed within the ITDs in order to comply with the ACARE environmental goals; help substantiate consistency between all ITDs and maximize synergies between them.

The principles of the TE activities and its involvement within the Clean Sky JTI can be described in the following steps:

- Standalone technologies will be initially evaluated at ITD design level.
- The pre-designs of new aircraft using one or a combination of Clean Sky technologies will be prepared by the ITDs.
- The TE will insert these new "Conceptual aircraft" into evaluation scenarios, using traffic growth and route forecasts going to 2020 and beyond.
- The TE will then assess the environmental improvements brought about by these technology combinations, by substituting conceptual aircraft, stemming from Clean Sky, for some of the reference aircraft of present design. (Clean Sky JTI, 2009)

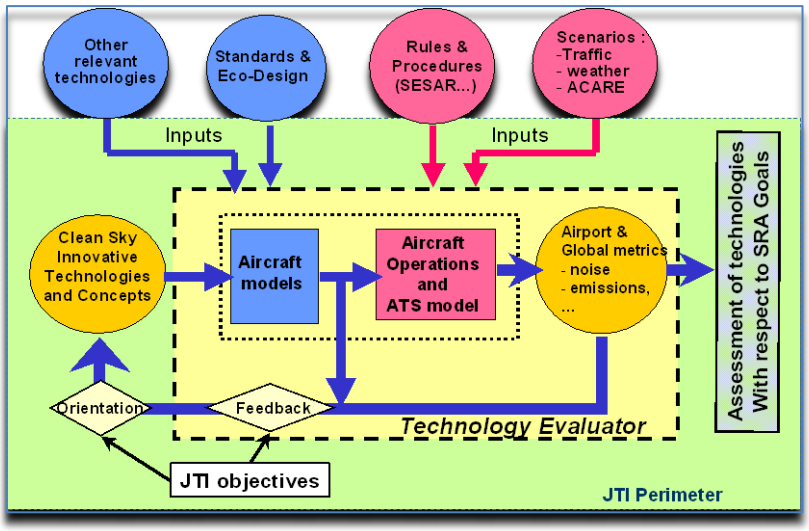

Figure 2. 4 – General principle of using TE for feedback on ITDs design, adapted from (Clean Sky JTI, 2009)

2.1.2 Techno-economic and Environmental Risk Assessment (TERA)

As mentioned in Chapter 1, one of the objectives of this research is the creation of a helicopter thermodynamic performance simulation model that could in the future replace the aircraft model within TERA and that could be integrated with the rest of

the models and as such give rise to the helicopter version of TERA for turboshaft engine performance calculations including noise, emissions, fuel burn, integration and installation studies. As such, this helicopter version of TERA could be used in the context or Cranfield University's work within TE to assess the helicopter mission fuel burn and emissions.

Techno-Economic and Environmental Risk Assessment model (TERA) is used for assessing and optimizing existing and potential engine designs in order to reduce the cost of development and ownership. TERA incorporates modules for modelling gas turbine and aircraft performance, estimation of engine weight, noise and emissions as well as environmental impact and operating economics.

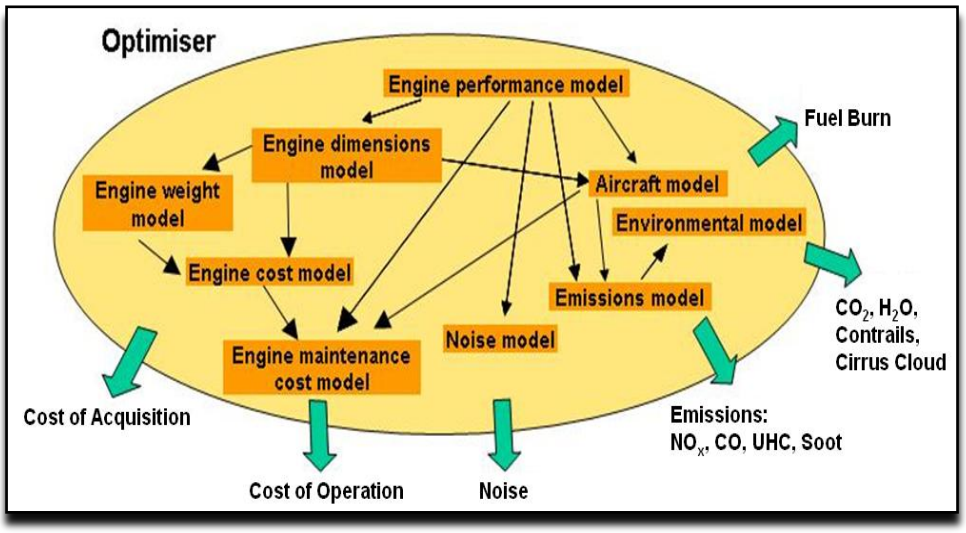

Figure 2. 5 – TERA concept (Ogaji, 2007)

TERA' role is to aid in assessment of the engines with minimum global warming impact and lower cost of ownership in a variety of emission legislation scenarios, emissions taxation policies, fiscal and air traffic management environments.

The core of the TERA is a detailed thermodynamic model of the power plant. This is represented by detailed component algorithms assembled into a thermodynamic whole. This delivers a representative view of component and whole engine performance in a wide range of operating conditions. Surrounding this core there is a layer of additional models, aircraft, economic, emissions, noise, weight, etc. Risk

analysis is then carried out at two levels. Firstly financial risk is examined through variability of income, costs and prices. The second level of risk examine is from the perspective of the technologies employed. These use the detailed and reliable thermodynamic results produced over a wide range of operating conditions. The outcome is an economic and environmental picture of power plant performance that takes into account variable demand patterns.

Below is a brief insight into the TERA modules:

Aircraft Performance (HERMES)

The model calculates aircraft performance data such as lift and drag coefficients, distance for take-off, etc. from available information on the geometry and mass of the aircraft. The model also calculates the fuel usage, time elapsed and distance covered for the baseline and derivative aircraft performing a given mission. Modelling of different aircrafts and engines is possible. For specified maximum take-of weight, payload and fuel load the model should compute the range of the aircraft. More information can be found in (Laskaridis et al., 2005)

Engine Performance (TURBOMATCH)

Cranfield university in-house gas turbine performance code, TURBOMATCH, has been adopted for use in the current TERA. TURBOMATCH is a gas turbine performance modelling code for assessing performance of existing and also novel cycles. (Palmer, 1990)

Economics

The economic model is composed of three modules: a lifing module, an economic module and a risk module. The lifing module estimates the life of the high pressure turbine disk and blades through the analysis of creep and fatigue over a full working cycle of the engine. The economic module uses the time between overhauls together with the cost of labour and the cost of the engine (needed to determine the cost of spare parts) to estimate the cost of maintenance of the engine. The risk module uses

the Monte Carlo method with a Gaussian distribution to study the impact of the variations in some parameters on the net present cost of operation.

Environment

The environmental impact for a given mission is assessed in terms of global warming potential (GWP). The GWP index represents an attempt to integrate the differential radiative forcing effect due to an anthropogenic emission along a pre-defined time horizon. The effect is then related to the emission of an equivalent mass of CO_2. In TERA, a parametric model has been used in the assessment of the GWP.

Noise

An acoustic prediction code called SOPRANO is used to estimate the aircraft noise. SOPRANO is primarily developed by the company ANOTEC Consulting for noise reduction technologies assessment. It is a semi-empirical code incorporating public noise prediction methods.

With SOPRANO as the noise estimation program, interfaces were developed to link it with the other modules in TERA, particularly the Economic model from which the noise tax is estimated.

Emissions (HEPHAESTUS)

Empirical approaches, of which there are numerous available, are used to provide the exhaust concentrations of pollutants of interest such as NO_x, CO and UHC. Several methods were assessed and one of them was selected for emissions modelling in TERA. The Emission module provides the data required by the Economic and Environment modules for the estimation of emission taxes and GWP respectively.

Weight and Geometry (WEICO)

The weight and geometry module provides an extensive list of engine and component weights, geometry and material which are required by other TERA modules i.e. Plant cost to estimate engine and component cost, Aircraft for

computation of aircraft maximum take-off weight and nacelle drag as well as Noise for computation of noise magnitudes from the turbomachinery.

Manufacturing Plant Cost

The plant cost module used in TERA primarily provides a direct production cost which reflect realistic cost trending and scaling but do not predict absolute cost or selling prices. Validation of this module has been carried out using a bottom–up approach i.e. estimating the costs from component to engine level.

Detailed information about TERA can be found in (Ogaji et al., 2007) or (Pascovici et al., 2007).

2.2 Helicopter Role and its Applications

The helicopter is a unique vehicle due to its capability to hover and fly vertically and at low altitudes, its manoeuvrability or ability to land on water. However, the helicopter is not only useful in difficult terrain; it is often the most efficient solution for urban areas because of its immediate availability. Helicopter are widely used for civilian operations such as scheduled flight services between airports and heliports, they are being more extensively used in relieving ground transportation in many cities serving as air taxi and for the business travel, they play irreplaceable role in search and rescue operations, disaster relief, traffic monitoring, agricultural applications, press and TV coverage, aerial photography, power line inspection, pipeline inspection, lifting (skycranes), law enforcement, fire fighting, motorway patrol, air ambulance, air taxi or policing and executive services. (Sonneborn, 2003)

They are also used for military and naval purposes, e.g. support of ground troops, transfer of armament or personnel, attacking, reconnaissance etc. In battlefield operations often different types of helicopters operate together, for example attack helicopters and escort support helicopters. (Brown, 1981)

Many times the helicopters need to operate from and to challenging landing sites, in adverse weather conditions or to fly over a terrain with no emergency landing sites. Due to this reason the helicopters need to be certified for take off with one engine inoperative (OEI) (Filippone, 2006). This important feature is especially important for navy applications where flyaway recovery with one engine inoperative is vital.

Low energy consumption per unit of generated thrust, i.e. high hovering efficiency gives the helicopter advantage over other vertical take-off and landing (VTOL) vehicles. (Stepniewski et al., 1984)

Hovering efficiency for a range of VTOL aircraft is depicted in the figure below.

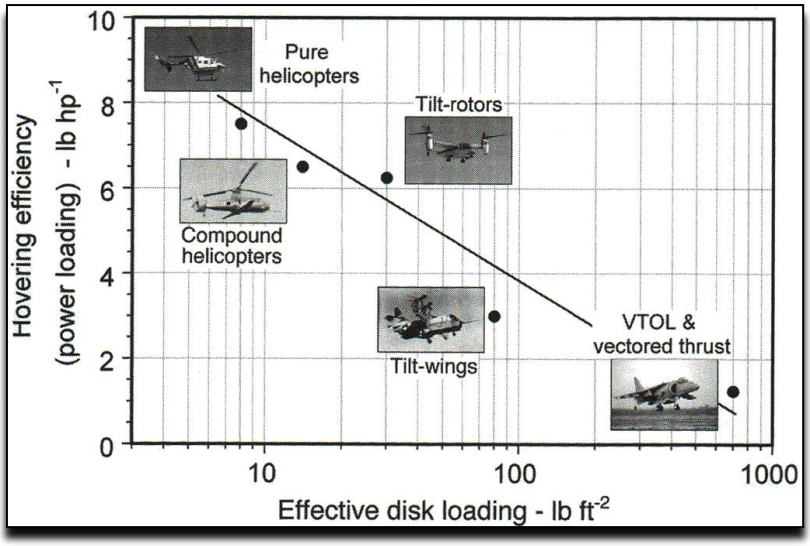

Figure 2. 6 – Hovering efficiency versus disk loading for a range of vertical lift aircraft. (Leishmann, 2006)

In this figure the effective disk loading (DL), defined as rotor thrust/rotor area is plotted against the power loading (PL =rotor thrust/ power required). The vertical lift aircraft that have a low DL have high PL, i.e. the rotor requires less power to generate any given amount of thrust, and hence is more efficient.

2.3 Classification of the Helicopters

The commonly used classification of the helicopters is based on their gross take-off weight and the type of operation they perform (civil, commercial, and military).

Helicopter with a maximum take-off weight of approximately 5,500 kg falls into the category of a light helicopter; a medium helicopter has a maximum take-off weight up to 10,000kg and the weight above this value characterizes heavy-lift helicopters. The vast majority of helicopters currently in service (95%) fall into the category of light helicopters. (Filippone, 2006)

The medium and light helicopters are equipped either with one or two engines. The question of whether to have single or twin engine propulsion system must be evaluated on the basis of the mission requirements. The reasons for having a single-engined helicopter include cheaper and lighter propulsion system and hence smaller, lighter and cheaper helicopter, lower fuel consumption and also lower maintenance cost of one engine. The obvious advantage of the twin-engined helicopter shows in the event of one engine's failure – the helicopter can still land safely or even complete the given mission. There is also no need to optimize the rotor system for autorotation (see section 2.5.4) which results in a smaller rotor. In the event of the foreign object damage or exposure to enemy fire there is a higher probability of one engine remaining operational. The disadvantage of such configuration is clearly in its higher weight, higher fuel consumption and maintenance cost. (Bree et al., 1981)

2.4 Helicopter Configurations

The single main rotor/tail rotor configuration

During the flight the single main rotor helicopter fuselage is subjected to a torque couple that causes the helicopter to rotate in a direction opposite to that of main rotor rotation (see section 2.7).The thrust needs to be provided to overcome main rotor torque; this is achieved by using a small tail rotor mounted vertically on the tail boom. The tail rotor (also called antitorque rotor) also permits the helicopter to have hover turn capability and balances the helicopter's tendency to yaw in forward flight. The main rotor provides lift, propulsive force and vertical control for this configuration. (Wagtendonk, 1996), (Prouty, 1984), (Newman, 1994)

The single main rotor/tail rotor configuration is by far the most commonly used helicopter configuration. Despite its versatility there are other configurations which offer advantages in specific flight situations and are therefore more suitable for certain purposes than the traditional configuration. Below is a brief description of the alternative configurations.

Figure 2. 7– Single main rotor/tail rotor (Mil Mi-171, courtesy of Mil Design) (www.airplane-pictures.net)

The twin main rotor configuration

Anti-torque control can be achieved by having two main rotors rotating in opposite directions, thereby cancelling out the torque from each other. The *tandem* configuration has a main rotor located at each end of the fuselage, with the rear rotor raised on a pylon above the level of the front rotor in order to decrease the interference of the fore rotor. The advantage of the tandem is that hovering is much less sensitive to wind direction. This proves advantageous especially in military operations. The disadvantage of this configuration lies in not having perfect torque balance and hence a need of some yaw control. In addition, the inevitable interference of the rotors however, represents a stability issue especially in forward flight. (Watkinson, 2004)

Figure 2. 8– Tandem configuration (CH-47 Chinook, courtesy of Boeing Helicopters) (www.chinook-helicopter.com)

The *side by side* configuration has the main contra-rotating rotors placed on pylons. The lateral disposition of the main rotors means that the mutual interference is substantially reduced. The disadvantage is that the pylon structure needed to carry the rotors inevitably causes drag.

Figure 2. 9 – Side-by-side configuration (Mil V– 12, courtesy of Mil Design)(www.aviastar.org)

In the *coaxial* configuration the two main rotors are placed on the same axis. The absence of the tail rotor allows for a more compact hull making this configuration especially suitable for use on the ships where hangar space is limited. It has also been used with success on unmanned helicopters. However because of smaller rotors the hovering efficiency is lower and also because the lower rotor is affected by the flow from the upper rotor the power consumption tends to be higher. This configuration is only used for special applications where compactness is of utmost importance. (Watkinson, 2004), (Newman, 1994)

Figure 2. 10– Coaxial configuration (Kamov K32-A, courtesy of Kamov Design)(www.heliweb.ca)

The ***synchropter*** configuration (intermeshing) helicopter has two contra-rotating synchronized rotors mounted side by side. The rotors are at the same height which represents a more compact hub arrangement over the coaxial configuration. The more complicated rotor heads cause a drag penalty and hence rules out the synchropter from high speed applications. However, as the synchropter is practically limited to two-blade rotors to achieve appropriate blade clearance, it naturally suggests low disc loading which makes it suitable for low speed, high altitude work or heavy lifting. (Watkinson, 2004)

Figure 2. 11 – Synchropter (HH-43, courtesy of Kaman aircraft) (www.h43-huskie.info)

Compound configuration

The compound helicopter, is one in which the rotor does not produce any forward trust in cruise. Instead the thrust is provided by addition of wings or other means. The thrust required from the rotor is reduced and it is only carrying the weight of the machine and not overcoming drag as well. The main advantage is aerodynamic. As the rotor remains edge-on to the airflow, there is no need to increase the blade pitch to account for inflow as speed rises. This minimizes the effect of retreating blade stall

(see section 2.5.6) and reduces vibration, allowing a higher airspeed to be reached. (Watkinson, 2004), (Leishmann, 2006)

Figure 2. 12 – Compound configuration (S-72, courtesy of Sikorsky Aircraft) (www.sikorsky.com)

2.5 Basic Helicopter Aerodynamics and Flight Dynamics

The following review is intended to offer the reader an insight into the basic helicopter aerodynamics and flight dynamics in order to be familiar with the terms used within this research study. It by no means replaces a helicopter textbook, a thorough discussion of this topic is beyond the scope of this thesis.

The helicopter is an aircraft that uses rotating blades to provide lift, control and forward speed. The rotor blades rotate about a vertical shaft and produce the required aerodynamic forces and moments by the relative motion of the rotor blades with the inflow velocity. The ability of the helicopter to produce lift without forward motion distinguishes it from fixed wing aircraft and determines its specific roles and applications.

The vertical flight capability, however, inevitably introduces a higher power requirement than for purely level flight and therefore a need for a large transmission system in order to deliver the extra power to the rotors at low speed.

The helicopter must obviously have the capability of flying forward and thus a mechanism is required to produce a force capable of opposing the rotor and fuselage drag. This force is produced by the forward tilting of the main rotor (see section 2.4.4). (Crouch et al., 1994), (Payne, 1959)

2.5.1 Lift

The production of lift through deflection of the relative airflow as it passes an object is the result of changes in the atmospheric pressure which occur around the surface of that object. When the airflow is deflected downwards by an airfoil, the air pressure

above becomes less than the pressure below. The airfoil then tends to move into the area of lower pressure. An upward force is produced, which is called lift. The standard formula for calculating the lift is:

$$\text{Lift} = \quad - \qquad (1)$$

Where C_L is the lift coefficient, a factor that represents the ability of an object to deflect, or bend the airflow. The lift coefficient depends on the shape of the airfoil and the angle of attack. (Wagtendonk, 1996)

2.5.2 Drag

Drag, in the broadest sense, is resistance to motion. It is formulated as

$$\text{Drag} = \quad - \qquad (2)$$

C_D represents the drag coefficient that means the potential of an object to interfere with a flow of fluid. The amount of interference is determined by the object's shape and its angle of attack.

The total helicopter drag is a combination of three types of drag: parasite, profile and induced drag.

All helicopter components that do not provide lift (helicopter cabin, skids, tail boom etc.) experience parasite drag. Parasite drag is proportional to the square root of the forward speed which means the faster the aircraft flies the greater is the parasite drag. It is essential to keep parasite drag to minimum to avoid large losses in engine power. This can be achieved by choosing aerodynamically clean shapes of the fuselage; skids, wheels etc.

Profile drag consists of form drag and skin friction. Form drag is the resistance caused by frontal and rear areas of the rotor blades, while skin friction is associated with the deceleration of the airflow in close proximity to the surface of the blades. Profile drag is related to the rotor rotational speed and since this is more or less constant, profile drag is essentially constant, too.

To produce net lift, there must be a positive deflection of air, which is assured when the downwash behind the airfoil is greater than the upwash in front. This downwash has a fundamental influence on induced drag, which is a drag associated with lift production. (Wagtendonk, 1996)

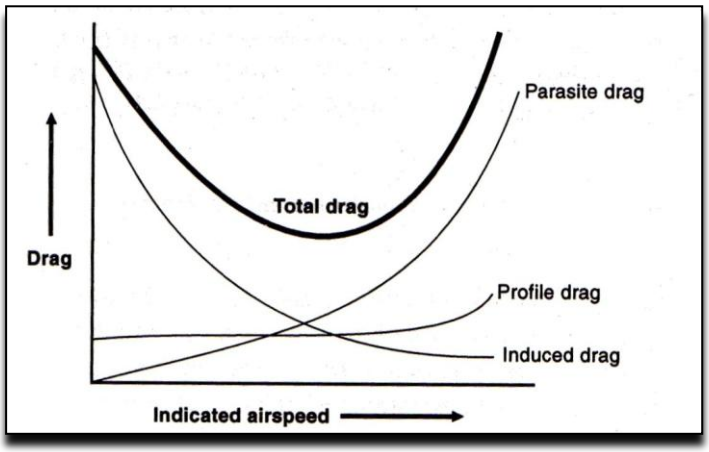

Figure 2. 13 – Parasite, profile and induced drag combine into total drag (Wagtendonk, 1996)

2.5.3 Helicopter Rotor

Helicopter rotor serves three purposes – it generates lift in the vertical direction (in opposite direction to the helicopter weight), it provides propulsive force in the horizontal direction in forward flight and also provides suitable forces to control the altitude and position of the helicopter. A rotor allows a helicopter to fly in any direction, to hover, climb and descend. Rotors consist of two or more identical blades spaced around a central rotor hub which are maintained in uniform rotational motion. (Dreier, 2007), (Wahab et al., 2006)

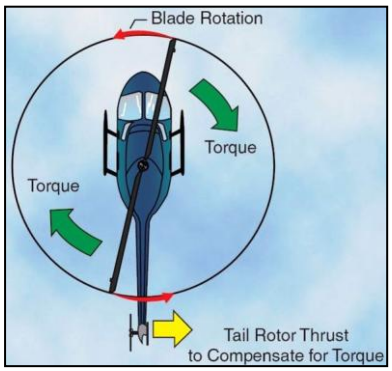

The rotor disc is divided into two parts by the a*zimuth angle* (ψ): the *advancing side* (0°≤ψ≤180°, with 0° being measured from the point when the blade is pointing over the tail in the direction of the blade rotation) and the *retreating side* (180°≤ψ≤360°).

Figure 2. 14 – Rotor torque and antitorque forces

2.5.4 Helicopter Aerodynamic Phenomena Which Affect its Performance

There are specific aerodynamic phenomena associated with the helicopter which have an effect on its handling and performance. Only some of these phenomena are touched upon below.

(A) Dissymmetry of lift

During hover the lift created by the rotor blades is the same at all corresponding positions around the rotor disc (area swept by the rotor blades). During forward flight, however, on the advancing side the sum of two inflow velocities would lead to an increased dynamic pressure and therefore and increased lift potential. The retreating side will then experience the difference of the inflow velocities, and its lift potential will therefore be decreased. The lift production over the disc is thus asymmetrical with approximately four-fifths of the total lift produced on the advancing side. If not compensated, the consequences of this imbalance would lead to large oscillatory bending stresses at the blade roots and a large rolling moment on the helicopter. The situation is remedied by blade flapping. It is a cyclical variation in blade incidence angle, achieved by hinging the rotor blades at the hub attachment. This motion reduces the effective blade incidence, and thus the lift is reduced and the blade can flap down again. On the retreating side the reverse process occurs. (Brown, 1981), (Newman, 1994), (Seddon et al., 2002)

(B) Ground effect

The effect of ground or any other boundary that can constrain the flow into the rotor has long been recognized, but the aerodynamics of the rotor under these conditions is still not fully understood. When a rotor is hovering in close proximity to the ground (up to the height of one rotor diameter) the rotor blades move air downward through the disc faster than it can escape from beneath the helicopter. This builds up an area of denser air between the ground and the helicopter. This affects the induced velocity in the plane of the rotor, and consequently the rotor thrust and power are altered. The rotor thrust is increased for a given power, or alternatively the power is reduced for a given thrust. Hence helicopter hovering in ground effect (IGE)

consumes less power and can therefore operate at a higher gross weight or density altitude than would be possible out of ground effect (OGE). The ground effect is significant during hover. At approximately 5-8 km/h

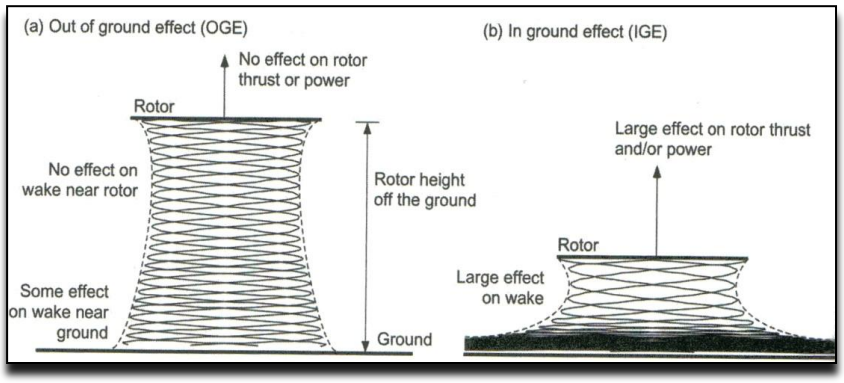

Figure 2. 15 – Hovering rotor wake (a) out of ground effect and (b) in ground effect (Leishmann, 2006)

groundspeed the helicopter will leave its ground cushion. At low forward speeds, a region of flow recirculation is formed upstream of the rotor near the ground. As forward speed increases, this recirculation develops into a small vertical flow region between the ground and around the leading edge of the rotor. This recirculation would return some of the air back to the disk and as a consequence, the induced power requirements will exceed those required for hover IGE. Above a critical value of advance ratio, which depends on aircraft weight (rotor thrust) and proximity to the ground, a well-defined horseshoe vortex (ground vortex) is formed under the leading edge of the rotor near the ground. When the forward speed is further increased this phenomenon disappears as the rotor wake is tilted back by the oncoming flow. During the performance calculations because of the mathematical complexity of the problem, semi-empirical methods are usually used to evaluate the ground effect. The correction factors are developed from flight tests. (Leishmann, 2006) , (Stepniewski & Keys, 1984), (Brown, 1981), (Saunders, 1975), (McCormick, 1995), (Layton, 1984)

(C) Reverse flow and Retreating Blade Stall

The figure shows a typical variation of local angle of attack within the rotor disk during the forward flight. The grey area represents the region of reversed flow where the forward velocity component, which is subtracted from the rotational velocity on

the retreating blade side, is negative. In other words, this blade section has greater speed of air going from trailing edge to leading edge. Reverse flow does not produce effective rotor thrust which is as if that part of the retreating blade was lost. No lift can be developed in this region. In order to remedy the situation and to increase the rotor thrust in the unaffected part of the blade the angle of attack is increased by blade flapping. The increase in angle of attack has got a limit, however, and consequently there is a critical helicopter forward speed where the retreating blade reaches its maximum angle of attack and the blade stalls. This is known as retreating blade stall.

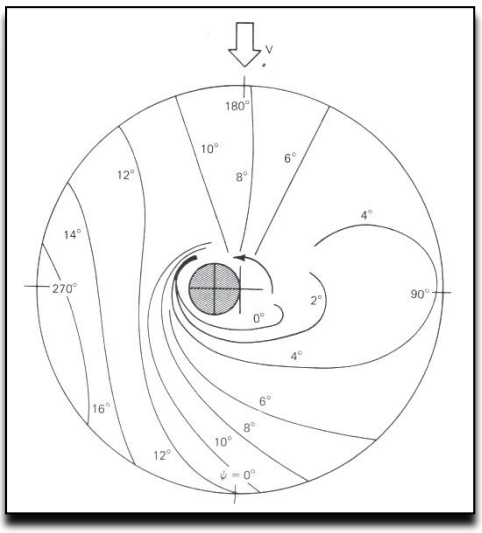

Figure 2. 16 – Variation of local angle of attack in a forward velocity environment (Layton, 1984)

As a consequence of this condition the rotor experiences vibration, pitch-up of the nose, and tendency to roll in the direction of the stalled side. In order to recover from retreating blade stall either the rotational velocity of the rotor needs to be increased (this is not practicable as the rotor RPM is usually kept constant) or the forward velocity has to be decreased. The retreating blade stall thus represents a limit on the forward velocity of a helicopter. The V_{ne} (never exceed airspeed) is for this reason clearly stated in the cockpit of every helicopter. (Brown, 1981), (Layton, 1984), (Stepniewski et al. 1984), (Wagtendonk, 1996)

(D) Tip loss

In order to produce lift, an airfoil (rotor) must have a difference in pressure between the upper and lower surfaces. At the tip of the rotor blade, air tends to flow from the high pressure region (lower surface) to the low pressure region (upper surface). This rotary flow combines with the blade velocity to leave a corkscrew-like flow known as vortex. The loss of pressure differential due to this vortex generation cancels out the lift generated at the blade tip; an effect known as tip loss. Nearly 10% of the blade

length is useless. There is also a vortex at the inboard end of the blade but it is less powerful because the lift gradient is much lower. Tip loss may be reduced by tapering and by twisting the blade near the tip in order to decrease the angle of attack. A tapered blade has a smaller tip area than the rectangular blade and hence the tip loss is smaller. In performance calculations this reduction in lift may be taken into account by either of two ways: by reducing the lift an amount proportional to the tip losses or by considering a decreased blade radius by a factor. (Layton, 1984), (Watkinson, 2004)

(E) Vortex ring state

Vortex ring state or settling with power can be experienced during high vertical rates of descent and the addition of more power during recovery leads to further descent and loss of height. When the helicopter descends vertically at a fast rate, it can get caught in its own wake and the rotor vortices are not swept away, but result in recirculation in a motion known as vortex ring. This recirculation increases inflow and so more collective pitch (increased angle of attack) is needed to provide the same lift and thus more torque will be needed. This situation leads to a highly unsteady flow through the rotor that can periodically break away from the rotor disk. Recovery is made by increasing the helicopter forward speed. More about this hazardous flight condition can be found in (Leishmann, 2006), (Watkinson, 2004), (Wagtendonk, 1996), (Prouty, 1984) or (Brown, 1981).

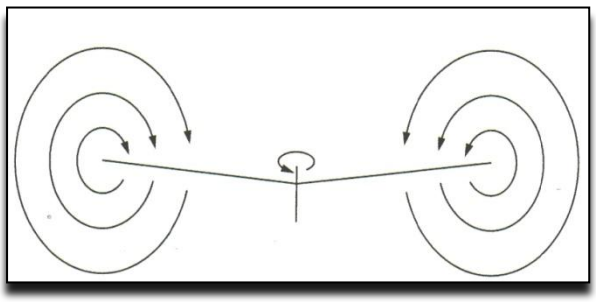

Figure 2. 17 – Schematics of the flow recirculation during vortex ring state (Watkinson, 2004)

(F) Autorotation

Autorotation is defined as a self-sustained rotation of the rotor without the application of any power from the engine; the main rotor is driven only by the action of the relative wind. The power to drive the rotor comes from the airstream upward through the rotor created as the helicopter descends through the air. This capability

is crucial at the time of the loss of engine power and can be used to safely land the helicopter. The helicopter transmission is designed so that the engine, when it stops, is automatically disengaged from the main rotor system, thus allowing the main rotor to rotate freely. In this condition the flow of air is upward through the rotor. Every single engine helicopter needs to respect the predefined "avoid area" (also called "dead man zone") The low speed - low altitude area does not allow sufficient time to make the necessary full transition to autorotative flight in the event of engine failure, so that a heavy landing will be inevitable. This area can normally be avoided by correct piloting procedures, and even if it has to be entered it will only be for a few seconds. (Brown, 1981)

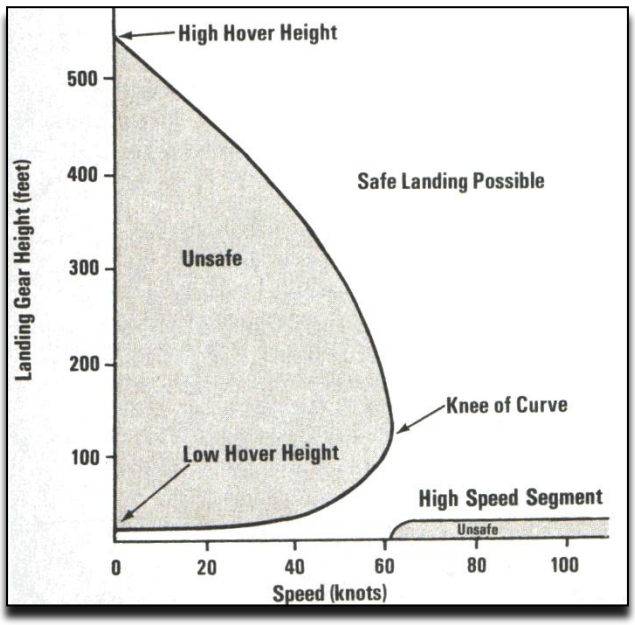

Figure 2. 18 – An example of a "Dead man zone" – an avoid area for a single helicopter (Prouty, 1985)

2.6 Helicopter Performance Analysis

The term helicopter performance engulfs the establishment of the engine power required for a given flight condition, evaluation of the maximum hovering altitude or ceiling (in and out of ground effect), the estimation of the maximum time (endurance) or maximum distance (range) the helicopter can fly for a given amount of fuel or the determination of the maximum forward flight speed (Leishmann, 2006)

2.6.1 The Atmosphere

The helicopter performance is a function of the air density in which it is actually flying. Changes in pressure or temperature will influence the air density which then has a fundamental influence on flight.

This makes it problematic to predict or compare aircraft performance unless the data are corrected to some standard condition. To remedy this problem, the International Standard Atmosphere (ISA) has been established, which gives the height in a standard atmosphere corresponding to the properties of the air in which the aircraft is flying.

The standard atmosphere assumes that:

- Sea level pressure is 101,301 N/m^2 (101.32 kPa, 29.92 inches of mercury)
- Sea level temperature is 15°C (288.16 Kelvin, 59 Fahrenheit)
- Temperature lapse rate is 1.98°C/1000 feet up to 36,090 feet above which temperature is assumed to be constant at -56.5°C. In other words, the temperature varies linearly with altitude according to the expression t = 15-0.001981h, where altitude *h* is expressed in feet and temperature in °C. (Stepniewski & Keys, 1984), (Leishmann, 2006)

2.6.2 Helicopter Power Requirements Breakdown

Helicopter total main rotor power required is a sum of several contributing powers. The main rotor power required can be divided into the following four elements:

Profile Power is the power required to turn the rotor and to overcome blade profile drag (form drag and skin friction). The profile power relates to the maintenance of rotor rotational speed, apart from the factors associated with induced flow and lift coefficient changes which are included in the induced power. The profile power also takes account of the power required to drive the tail rotor, generators and hydraulic systems.

Induced Power is the power required to generate rotor lift and to overcome the induced drag (the portion of rotor drag that is associated with total rotor thrust in its function of supporting weight). It relates to the force opposing weight, and takes into account the changes to induced flow (and the lift coefficient) associated with changes in altitude.

Parasite Power is the power required to provide propulsive thrust for forward (or rearward) flight and to overcome parasite drag (additional rotor drag due to disc tilt). Parasite power deals with the forward thrust component of total rotor thrust proportional to disc tilt and airspeed.

Non-Uniform Downwash Power is the power correction due to non-uniform inflow and downwash effects in forward flight.

Combination of all the power requirements produces a total power required curve for straight and level flight. The curve shows that the power consumption is high at level flight at low speeds, due to the influence of high induced power, and than again at high speeds, due to the influence of parasite and increasing profile power. (Wagtendonk, 1996), (Stanzione et al., 1992)

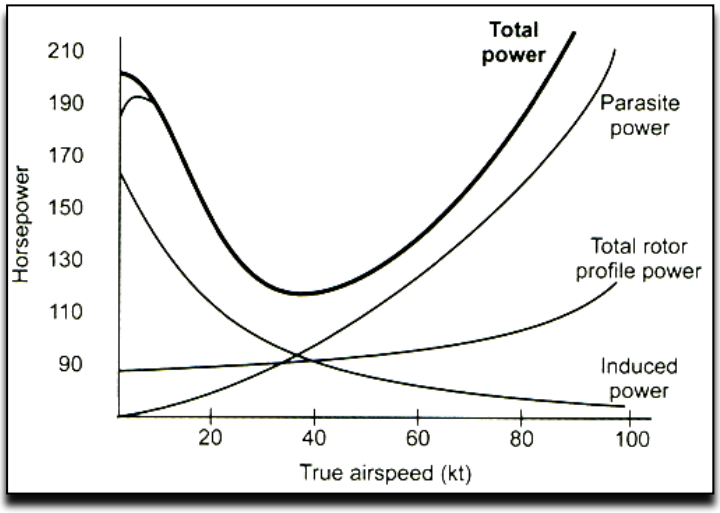

Figure 2. 19 – The example of the total power required curve (Wagtendonk, 1996)

2.6.3 Vertical Flight

Hover

During a hovering flight the main rotor tip path plane is parallel to the ground. Lift acts straight up, the helicopter rotor produces an upward thrust by driving a column of air downwards through the rotor plane, and weight and drag act straight down. For the helicopter to hover the sum of lift and thrust forces must equal the sum of weight and vertical drag (download) on the fuselage. The vertical drag is caused by

the rotor downwash velocity. It is accounted for by using the estimated fuselage vertical drag coefficients derived from wind-tunnel testing. The fluid velocity is increased smoothly as it is entrained into and through the rotor disk plane. There is no sudden change in velocity across the disk; because although a thrust is produced on the rotor, there must be a change in pressure over the rotor disk. The wake boundary or a slipstream forms, outside this boundary the flow velocity is relatively quiescent. The blade tip vortices trail behind and below each blade. Inside the wake boundary, the flow velocities are large and their distribution across the slipstream is not uniform. Below the rotor the stream velocity increases causing a contraction in the diameter of the wake. Since no acceleration takes place during the hover the helicopter is in equilibrium. Many take offs and landings are carried out via hover. (Brown, 1981), (Young, 1978), (Seddon et al., 2002), (Leishmann, 2006), (Stepniewski et al., 1984)

Hovering power required of the main rotor is made up of two elements:

- induced power – during the hover in order for the rotor thrust to equal helicopter weight (plus the download) the pitch angles must be increased over the values required to sustain level flight which leads to an increase in the drag coefficient and an increase in the induced flow. Thus more power needs to be produced to compensate for this. The extra power needed is called induced power.
- profile power – is associated with the energy dissipated by the rotor in the form of direct skin friction

Vertical climb

When the helicopter hovers, the total rotor thrust equals helicopter weight (plus a download). When the total rotor thrust is increased (by increasing the collective pitch) the aircraft can climb vertically at a certain rate of climb. The rate of climb is determined by the amount of surplus power available over that required to maintain an altitude. As an adequate climbing performance is an important operational consideration for a helicopter, sufficient power reserves must be available to ensure

climbing performance is maintained over a wide range of gross weights and operational density altitudes. (Leishmann, 2006), (Wagtendonk, 1996)

Vertical descent

When the collective pitch is lower than the value required to hover the rotor thrust reduces and as a result the helicopter starts to descend. The airflow from below the disc will reduce the induced flow and cause increase in angle of attack and thus increase in rotor thrust. This will lead to a stabilization of the rate of descent. Hence the power required to maintain thrust in vertical descent generally falls as the rate of descent increases, except that in the vortex-ring state an increase is observed. (Seddon et al., 2002)

Caution needs to be exercised during performance calculations of a descending helicopter. The climb flow model cannot be used in a descent, because now the stream velocity is directed upwards and so the slipstream will be above the rotor. Chapter 4 deals with this issue in more detail.

2.6.4 Horizontal Flight

Level Flight

The aerodynamic situation in forward flight is complex. The helicopter rotor must now not only produce a lifting force (to overcome the weight of the helicopter) but also a propulsive force (to propel the helicopter forward). This is achieved by tilting the rotor disk forward at an angle of attack relative to the oncoming flow. The flow through the rotor is no longer axisymmetric. Although the nature of the rotor flow in forward flight is now more complex than in hover, it can still be treated by the momentum theory (see section 2.8.1)

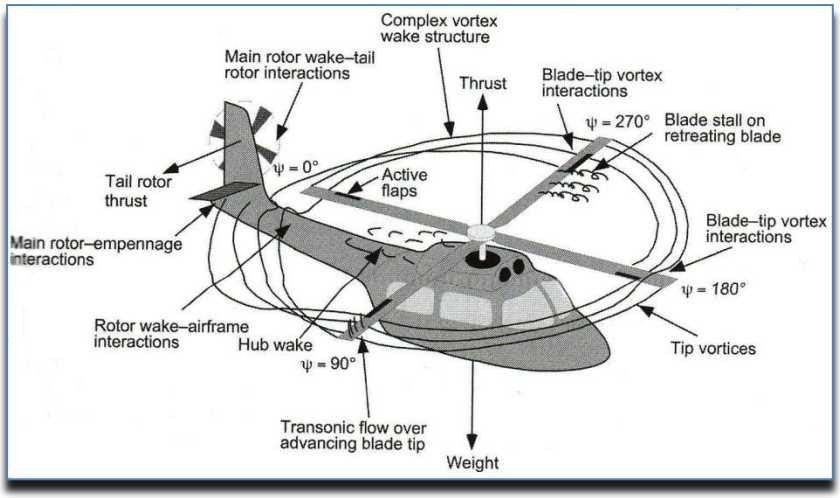

Figure 2. 20 – Flow structure and some aerodynamic problems on a helicopter in forward flight (Leishmann, 2006)

Some of the aerodynamic problems that helicopter rotor encounters during forward flight are depicted in the figure above. The rotor flying edgewise on the stream introduces aerodynamic issues which can be solved by the application of certain mechanical devices. That, however, complicates the aerodynamic situation of forward flight even more.

As mentioned above the level flight speed and manoeuvre capability of a helicopter is usually limited by the amount of power available, the transmission limits, vibration limits or stall inception.

The basic physical origin of the two power elements required in hovering (profile and induced) remains unchanged during forward flight, but the formulas must be modified to account for the effects of translational velocity. Besides that, in forward flight a third factor, parasite power, must be calculated. Parasite power is composed of the power required to overcome the drag of the fuselage, tail rotor and undercarriage and the net drag of the main rotor along the flight path. (Stanzione et al. 1992), (Harris et al., 1952), (Leishmann, 2006)

Forward Climb

The ability of the helicopter to climb is determined by availability of surplus power over and above that required to maintain an altitude, as was the case in hover. Consequently, the rate of climb (which is the gain of altitude per time, expressed in

feet per minute) can be determined from the difference of the power available and the power required to maintain straight and level flight.

Forward Descent

Descent performance is treated as a negative rate-of-climb calculation. In descent the induced velocity term is less than 1.0 and the download and tail rotor power required are lower than in level flight. The situation is similar to the vertical descent, as a result of descent the airflow causes the reduction of the induced flow and the consequent increase of the angle of attack leads to the increase of the total rotor thrust. (Stepniewski et al., 1984), (Leishmann, 2006)

2.6.5 Losses

In the power required calculations it is necessary to account for transmission (gearbox), accessory and engine installation losses. For simplicity it is assumed that the losses represent a fixed percentage of the input power and are then added to the total power required value. The values used for the transmission losses range from 0.5%-3% depending on the type of gears used.

The accessory losses include power extraction for items such as engine and transmission cooling fans, electrical power generation, and hydraulic power supplies. They can be approximated at 1-3%. (Stepniewski & Keys, 1984)

The engine installation losses are associated with the inlet and exhaust pressure losses due to friction, pressure losses due to the inlet particle separator, compressor air bleed or losses associated with the inlet temperature rise due to the exhaust air re-ingestion. Typically a 2% value is assumed. (Prouty, 1984) (Stepniewski et al., 1984), (Harris et al., 1952)

2.6.6 Engine Power Ratings

The helicopter must be capable of flying at various power settings, depending on the flight condition. Typical power settings used when flying the helicopter are:

- maximum continuous power rating – this is the maximum power at which the engine can operate continuously without any time limit.

- take off or 30 minutes power rating – this higher power setting is used for take-off or hover at high altitude and/or ambient temperature. It can be used for short periods of time only, usually one hour, but sometimes half an hour, depending on the situation.
- maximum contingency or 2.5 minute power rating – this even higher power settings is only used in contingency, such as at the time of loss of an engine. This setting should not be used for more than 2-3 minutes. An engine inspection is usually required after this type of use.
- emergency or half-minute power rating – this is the highest and thus the most damaging condition. It is used for situations where there is a real possibility of loss of the aircraft. Typically, the 30-minute power rating is 20% higher than the continuous rating and the short-time rating is another 10% above that. (Newman, 1994), (Stepniewski et al., 1984)

2.7 Anti-Torque Control

The fuselage of the conventional helicopter during a powered flight is subjected to a torque couple that rotates it in a direction opposite to that of main rotor rotation. When the rotor is driven from the central point (the mast), the tendency to yaw occurs, which is caused by the torque couple. The extent of yawing is determined by the amount of power used. The torque couple must be opposed in order to avoid the yaw. That is achieved by implementing a method of anti-torque control. Typically, this is accomplished by installing the anti-torque rotor, producing thrust, which opposes the torque. The anti torque rotor also enables the helicopter to have hover turn capability and balanced forward flight. There are several methods of anti-torque control available and they are discussed below.

2.7.1 The Conventional Tail Rotor

The commonest method of anti-torque control is by mounting the anti-torque rotor at the tail. The weight of machinery at the tail must be balanced and this is achieved by placing the helicopter cabin some way forward of the rotor mast. The large forward area however causes instability in yaw and thus some fin area is necessary to

give directional stability in forward flight. As a result the tail of the conventional helicopter will be a structure supporting a variable pitch tail rotor, its transmission and controls, some fin area and a tail plane. (Watkinson, 2004)

The tail rotor is a structure similar to the main rotor, but positioned at 90 degrees (or other angle at some situations) to the main rotor. From the point of performance calculations, it can still be assessed using a similar approach to the main rotor. However, it is assumed that the tail rotor does not produce any propulsive thrust; therefore there is no tail rotor parasite drag contribution. In a simplified approach the tail rotor power can be taken as a fixed percentage of the total power required. The recommended values range from 5% to 10% (generally 10% is assumed for the case of hovering helicopter and 5% for helicopter in forward flight). (Filippone, 2006), (Leishmann, 2006)

Conventional tail rotors are exposed and therefore operate in difficult airflow conditions. The tail rotor is subjected to the main rotor downwash or disturbances from the fuselage. The position of the tail rotor at the end of the tail boom subjects it to vibration. There is also a risk of damage from foreign objects striking the tail rotor and the potential threat of injury to persons from the exposed blades.

The number of fatal accidents to the ground personnel, caused by interaction with the tail rotor lead to the consideration of the protected environment for the tail rotor blades. The protection can be achieved by mounting a ducted fan (also called Fenestron) at the end of the tail boom of the helicopter. Ducted fans have between eight and eighteen blades arranged with irregular spacing, in order to distribute the noise over different frequencies. The housing allows a high rotational speed, therefore a ducted fan can have a smaller size than a conventional tail rotor. The ducted fans introduce obvious weight penalty and complexity of installation compared to the conventional tail rotor, but the shrouded Fenestron eliminates most of the disturbed airflows on the blades, is quieter and protects the rotor and ground personnel from damage. The Fenestron is also more effective compared to

conventional tail rotors of similar diameter. However, the size of Fenestron brings the risk of ground clearance. (Watkinson, 2004)

Figure 2. 21– Ducted fan (EC 120-B, courtesy of Eurocopter)(www.eurocopter.com)

2.7.2 Other Methods of Anti-Torque Control

While the conventional tail rotor produces the simplest remedy to main rotor torque, the following alternative designs are available:

- The main rotor is driven from the tips rather than the centre using tip-jets (small ramjet engines). Although the principle has some advantages, such as no gearbox is required and no torque reaction but the complications associated with the construction of this type of device, short fatigue life, very high fuel consumption and high noise levels prevent its widespread use.
- Twin-rotor design – such a helicopter has two main rotors that turn in opposite direction, and therefore cancel out each others torque. There is then no need for a separate anti-torque system. The two main rotors may be in tandem, coaxial, side-by-side or intermeshing configuration.
- Sideways tail propulsion through high velocity jet flowing from adjustable nozzles. This principle is incorporated in the NOTAR (NO Tail Rotor) design. A variable pitch fan is enclosed in the aft fuselage section immediately forward of the tail boom and driven by the main rotor transmission. This fan forces low pressure air through two slots on the right side of the tailboom, causing the downwash from the main rotor to encompass the tailboom, producing anti-torque force proportional to the amount of airflow from the rotor. This is augmented by a direct jet thruster (which also provides directional yaw control) and vertical stabilizers.

Figure 2. 22- NOTAR (MD 520N, courtesy of MD Helicopters) (www.notar-helicopters.nl)

The tail boom is cylindrical. On one side of the boom are two downward facing slots fed with air from the interior and pressurized by a variable pitch fan. The air emerging from the slots energizes the boundary layer and delays separation significantly in order to impart a sideways component on the downwash that flows around the boom. As a reaction to this the thrust on the boom is formed. The thrust has a lateral component and a downward component corresponding to the induced drag. However, the slots emit downward jets and this causes some thrust that counteracts the induced drag leaving a side thrust to counteract the torque. About 60% of the anti-torque thrust comes from the boom. The remainder comes from a nozzle at the very end of the boom. Due to the absence of the tail rotor the NOTAR system is considered safer and quieter. The absence of the tail rotor, however, creates the need for a substantial amount of fin area. (Watkinson, 2004)

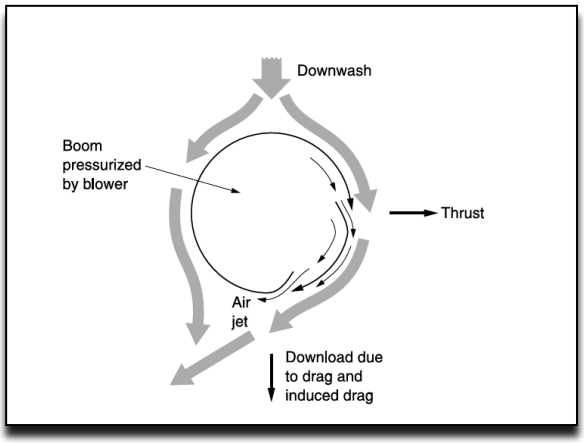

Figure 2. 23 – The NOTAR system (Watkinson, 2004)

2.8 Helicopter Performance Modelling Methodologies

The helicopter performance may be assessed using various approaches ranging from the application of empirical data to the extremely comprehensive theoretical techniques. The more sophisticated analyses are generally used to describe the rotor system aerodynamics (compressibility and blade stall) but can also be applied to the airframe and propulsion systems. (Stanzione et al., 1992)

The empirical sources available, such as the work of (Bailey et al., 1990) typically offer charts that plot the relationship between the rotor profile drag and lift for a helicopter rotor operating in forward flight and having hinged rectangular untwisted blades. The charts are plotted for various combinations of pitch angle, tip-speed ratio, and solidity for a particular value of a parameter representing the shaft power input. The charts are given for a range of power input covering various flight conditions. The data can then be readily used in the estimation of helicopter performance.

Two of the performance assessment theories will be described here. The details on other methods can be obtained from helicopter performance textbooks, such as (Johnson, 1980), (Leishmann, 2006), (Prouty, 1984), (Stepniewski et al., 1984), (Layton, 1984) or (Filippone, 2006)

2.8.1 Momentum Theory

The basic characteristics of the rotor in hover and vertical flight can be obtained from actuator disc theory (momentum theory).

The assumptions made by this model are as follows:

- The rotor is considered as having infinite number of blades of zero thickness, or in other words as an infinitesimally thin actuator disk. The constant pressure difference across the rotor disc is assumed.
- The velocity of the air downward through the disc (downwash) is constant across the disc.
- The vertical velocity is continuous through the rotor disc.

- No rotational velocity is imparted to the air passing through the disc, all flow velocities are axial.
- The airflow is divided into two separate regions, flow that passes through the rotor disc and that which is external to the disc. The division of these two types of flow is done by a stream tube which passes through the perimeter of the disc.

In place of the actual rotor a disc is visualised perpendicular to the generated thrust and capable of imparting axial momentum to the fluid as well as sustaining pressure differential between its upper and lower surface. The disc is assumed stationary while a large mass of fluid flows around it at a velocity. The mechanism of thrust generation is explained as follows: The fluid passing through the disc acquires induced velocity which is uniform over the entire disc and is directed opposite to the thrust. It is assumed that the fluid is ideal. Consequently, rotation of the disc does not encounter any friction or form drag as it imparts purely linear momentum to the passing fluid. The thrust force is generated by the rotation of the rotor blades about the shaft and their action on the air. Power is required to generate this thrust, which is supplied in the form of a torque to the rotor shaft. Work done on the rotor leads to a gain in kinetic energy of the rotor slipstream and this is an unavoidable loss that is called induced power.

The Newtonian conservation laws are applied in a quasi-one-dimensional integral formulation to a control volume surrounding the rotor and its wake. This approach permits to perform an analysis of the rotor performance (e.g. its thrust and power) but without actually having to consider the details of the flow environment local to each blade section.

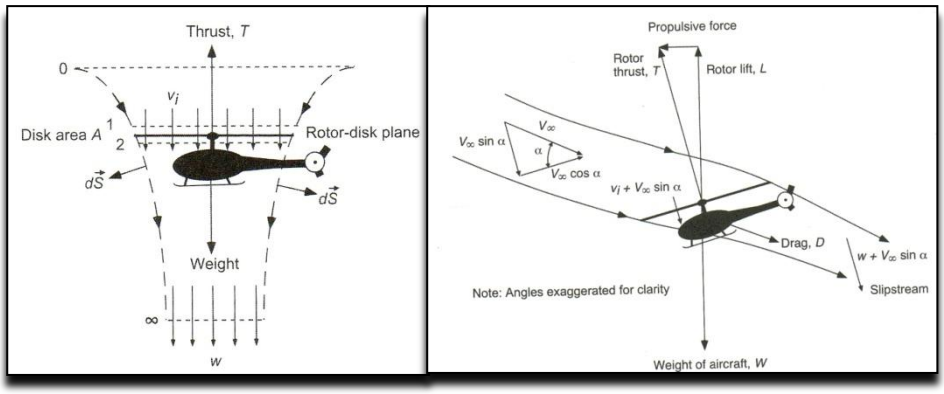

Figure 2. 24 – Flow model for momentum theory analysis of a rotor in hovering and forward flight, adapted from (Leishmann, 2006)

Momentum theory gives a broad understanding of the functioning of the rotor and provides basic relationships for the induced velocity created and the power required in producing a thrust to support the helicopter. It is most suitable for the flight conditions at right angles to its plane.

Should the details of how the thrust is produced by the rotating blades or what design criteria are to be applied to them be needed, the application of a blade element theory, corresponding to aerofoil theory in fixed-wing aerodynamics, will be required. (Seddon et al., 2002), (Leishmann, 2006), (Stepniewski et al, 1984), (Dreier, 2007)

2.8.2 The Blade Element Theory

The blade element theory models the blade geometry and the blade performance in more detail. It proves a necessary tool for the prediction of the aerodynamic forces and moments acting on a rotor blade in forward flight. It provides estimates of the radial and azimuthal distributions of blade aerodynamic loading over the rotor disk. Blade element theory considers each blade section as a quasi two-dimensional airfoil that produces aerodynamic forces and moments. Three- dimensional effects are accounted for by applying tip loss factor and other empirical factors.

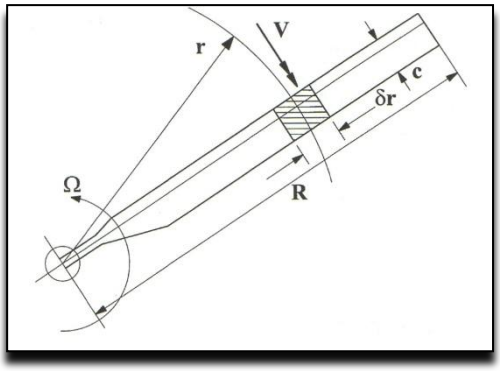

Figure 2. 25 – The blade element definition, adapted from (Cooke & Fitzpatrick, 2002)

Rotor performance can be obtained by integrating the sectional airloads at each blade element over the length of the blade and averaging the result over a rotor revolution. The effects of a nonuniform induced inflow across the blade (from the rotor wake) are accounted for through a modification to the angle of attack at each blade element. The blade element calculation represents a fairy complex task because it must accurately represent the highly nonuniform velocity field induced by the vertical wake trailed from each blade, as well as to account for the influence of all the blades and possibly airframe components. However, if some simplistic analytic assumption for the distribution of the induced velocity can be made, or if the induced velocity can be approximated, then the net thrust and power and other forces acting on the rotor can be readily obtained.

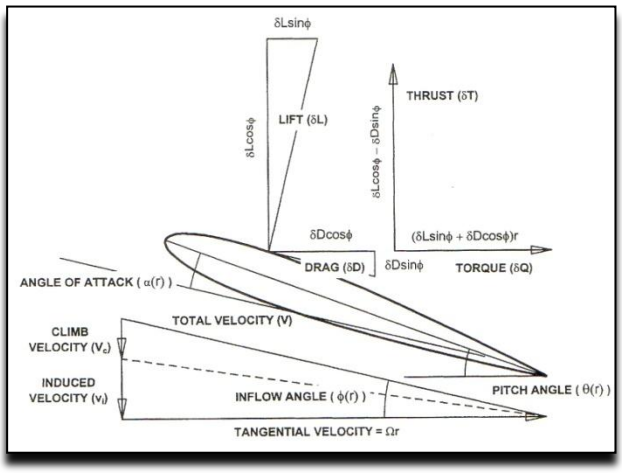

Figure 2. 26 – Conditions at the blade element, adapted from (Cooke & Fitzpatrick, 2002)

As mentioned above, depending on the fidelity of the calculation method used the transmission losses, power off-takes, tail rotor-fin interference effects or drag coefficients can be either calculated or the correction factors derived from flight and wind tunnel tests applied to the power required value. Both the momentum and blade element methods will allow for good estimates of total rotor thrust and power and can be used with confidence to predict overall rotor performance. (Leishmann, 2006), (Seddon, 1990)

2.9 Helicopter Mission Performance

Unlike for a fixed wing aircraft, the helicopter can perform a variety of missions depending on its application. This makes it difficult to define a "typical" helicopter mission. The helicopter can fly range missions, endurance missions, search and rescue missions or accomplish military task such as anti-tank mission or drop of ordnance, etc. The mission performance is explained below on a simple range mission.

Mission performance calculations would start with computing the payload (PAY) (cargo, passengers, equipment, etc.) that can be carried during a given mission. The payload is obtained by subtracting the weight of the fuel required (W_F) plus the weight empty (W_E) and fixed useful load (FUL) (the weight of crew, trapped oil and fuel) from the gross takeoff weight (GTOW):

$$PAY = GTOW - (W_E + FUL + W_F) \quad (3)$$

The maximum GTOW value is used to determine the maximum payload capability of an aircraft. This weight is dependent on the type of takeoff site assumed for the mission. The weight of fuel depends on the type of mission being evaluated. The various segments of the flight profile are:

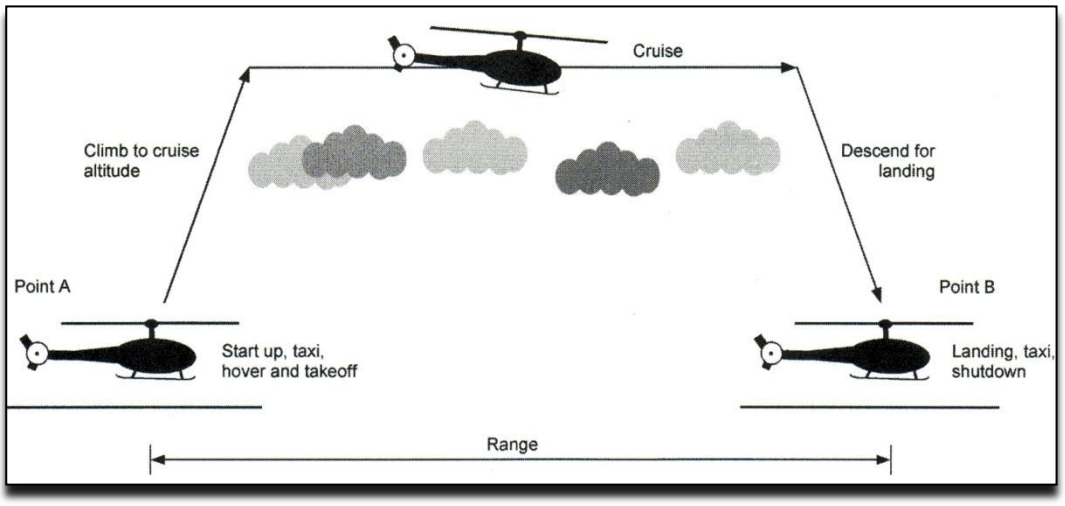

Figure 2. 27 – A representative helicopter mission (Leishmann, 2006)

(1) warm-up – includes fuel consumed to start the helicopter. A fuel allowance of two to five minutes at maximum continuous power is typical.

(2) take off – the fuel required for takeoff and transition to forward flight is generally small enough to be neglected when calculating missions where payload is carried internally.

(3) climb to cruise altitude – for comparative performance calculations and for missions flown 1000-2000 ft above the takeoff site, climb fuel and distance can be neglected. Cruise at higher altitudes will require consideration of the climb effect on fuel.

(4) cruise at constant altitude – the cruise portion of the mission is generally flown at airspeeds which provide the maximum range for a given quantity of fuel. This speed is referred to as the best range speed.

(5) descent to landing site – because of the lower power settings in descent, the fuel used during this stage of the mission is considered negligible. In addition, no allowance is taken for distance travelled in descent, unless the cruise altitude is significant.

(6) landing with fuel reserve – for internal cargo missions where no hover time is required for detaching loads prior to landing, the fuel required to land is negligible. However, it is assumed that the aircraft lands with a specific quantity of fuel reserve, which is typically 10 % of the initial fuel quantity.

At the start and the end of the mission a short period of hover is included to carry out the necessary checks.

During the performance assessment using HELIX (see Chapter 4) the fuel usage during climb and descend were not excluded from the calculations.

The objective of the range mission is to fly the maximum possible distance for given quantity of fuel. These missions are generally computed at constant altitude and optimum airspeed conditions; however, aircraft altitude as well as speed can be optimized to further increase the distance travelled.

Maximum endurance represents another basic mission aimed at maximizing endurance or time on station rather than distance. The mission is typical for search and surveillance or loiter operations and is flown at minimum power speeds where the fuel consumption is the lowest. The cargo for these missions usually consists of electrical equipment or external armament (torpedoes, missiles etc.).

Ferry range capability is the maximum range achievable with zero payload on either internal fuel capacity or with the addition of auxiliary tanks. The delivery of new or refurbished aircraft over extended distances is an example of ferry-range operation. Since there is no payload or cargo, the cabin area can be filled with auxiliary fuel tanks, or external tanks can be added to further increase range capability (Stepniewski et al., 1984), (Leishmann, 2006), (Filippone, 2006)

Chapter 3: Methodology

The tools and methods used during the development of the helicopter performance prediction program (HELIX) are discussed. The Cranfield University in-house engine thermodynamic performance model (TURBOMATCH) is introduced. The description of the emission indices model (HEPHAESTUS) and the JGA optimization toolbox is offered. The discussion on the integration of all the tools within the helicopter performance platform (HECTOR) is provided, outlining its main capabilities and the communication between its models.

The performance of the helicopter as a whole has to be assessed in close cooperation with the helicopter engine model. Moreover, the helicopter performance has to be viewed and analysed in the environment that it is flying, taking into account among other factors the weather conditions, complexity of the terrain or accessibility of landing sites. Such a broad view requires a very complex performance simulation environment. The helicopter performance model developed here (HELIX) in conjunction with the gas turbine engine thermodynamic model (TURBOMATCH), the emission indices prediction tool (HEPHAESTUS) and the optimizer (JGA optimizer), all built into an integrated framework (HECTOR), represent a solid base, which can be built upon to achieve such an objective. The human factors, represented by the pilot and its crew, and their behaviour and skills, however, can never be represented by any model, regardless of its precision, which means that any model could reach the reality only asymptotically. The necessary tools used in cooperation with HELIX are described below. They have been developed over the years in Cranfield University and they are in extensive use not only for the purposes of university research but also in various global research projects.

3.1 Gas Turbine Engine Performance Scheme - TURBOMATCH

The engine performance model (TURBOMATCH) has been developed and refined at Cranfield University over a number of decades. TURBOMATCH is capable of

simulating the performance of an extensive range of aero and industrial gas turbine engines ranging from a simple single shaft turbojet engine to complex multi-spool turbofans as well as novel engine configurations. This tool is capable of simulation the simple steady state performance (design and off-design point) as well as the transient performance computations.

The Turbomatch scheme uses various pre-programmed routines known as “bricks” that can be utilized to simulate the performance of the different components of the engine. The final output is represented by the engine thrust or power, specific fuel consumption, etc. The optional by-products are the details of individual component performance and the gas properties at various stations within the engine.

The scheme has been designed in a way that those with little or no previous experience of computer programming can make use of it comfortably.

The building process of the engine model in Turbomatch consists of assembling the bricks describing particular engine parts in modular fashion. Some bricks correspond to particular components (intake, compressor, combustor, turbine, nozzle, etc.), other bricks serve the arithmetical operations or the final calculation of performance and finally there are bricks to create additional output.

The complete engine model building process does not consist of merely assembling the component bricks, but these bricks need to be linked by some form of an interface. The description of the gas state at the inlet and outlet of the component forms such an interface. These gas states reflect the thermodynamic processes occurring within the engine component and they are described by a number of quantities known collectively as the station vectors of that station. Each station vector consists of the number of quantities including mass flow, velocity, area, static and total pressures and temperatures etc. More details on TURBOMATCH can be obtained from (Palmer, 1990) or (Pachidis, 2008).

TURBOMATCH was used extensively during this research study for the purposes of simulating the performance of the helicopter engines in order to establish a library of

representative helicopter engine models. The results of the simulations are discussed in detail in Chapter 5.

3.2 The Emission Indices Model – HEPHAESTUS

The emission indices (g/kg of fuel burned) can be calculated using the emissions prediction model HEPHAESTUS developed at Cranfield University. It is generally accepted that three broad strategies can be adopted for the purpose of combustor emissions prediction which are the following: 1) empirical correlations, 2) stirred reactor models and 3) comprehensive numerical simulations (CFD) calculations. The use of empirical correlations implies that the fine details of the combustion chemistry and internal flow are degenerated to global expressions, having been established directly from measurements. The deployment of detailed numerical simulations of the turbulent reacting flow inside the combustor (CFD simulations) represents the other extreme of the approaches to gas turbine emissions prediction. However, it is generally acceptable that this approach is both time consuming and requires a high-fidelity definition of the combustor geometry, which may be difficult to obtain for certain combustors designs. Stirred reactor models, in which the turbulent flow is sufficiently idealized and the time-dependent chemistry of pollutant formation is computed with sufficient accuracy, represent an efficient compromise between the two aforementioned extreme approaches and it the method deployed by HEPHAESTUS in order to calculate gas turbine emissions. The critical zones within the combustor are represented by individual stirred reactors, incorporating the processes of mixing, combustion heat release, and pollutant formation. In order to take into account inhomogeneities in gas composition and temperature which influence directly the rates of pollutant formation, a stochastic representation of turbulent mixing in the combustor primary zone is utilized. (Celis et al., 2009), (Goulos et al., 2010)

3.3 The JGA Optimization Toolbox

The JGA optimization toolbox was developed at Cranfield University. Only a brief description of the JGA optimization toolbox is offered here as described in (Celis et al., 2009), the capabilities and the optimization strategies used within the optimization toolbox are discussed in detail in there and also in (Rogero, 2002) or (Celis, 2010). Broad discussion of the trajectory optimization strategies is beyond the scope of this project.

As the first step in the development of the optimization algorithm the track record of optimizers developed by Cranfield University for a range of applications was reviewed and a suitable candidate for the initial optimizer was identified. This led to the decision to use genetic algorithm (GA)-based optimization routines as the basis for the development of the current optimizer. This optimizer, which was developed for carrying out optimization processes of combustor preliminary designs, already includes several algorithms for each of the main phases (selection, crossover, and mutation) involved in the optimization process using this type of technique. However, there are additional enhancements that can be introduced to further improve the quality of the optimizer. These improvements include the use of GA master-slave configurations, which will allow using optimum Gas parameters during the optimization processes, and also the inclusion of the concept of Pareto optimality (Pareto fronts), which will improve its capabilities when performing multi objective optimization processes.

The optimizer has been written in Java as the main programming language. The fact that Java is an independent platform brings a significant advantage when working on a heterogeneous set of computers, especially the advanced support for networking and graphics.

The slower execution time of Java-written programmes (in comparison with fully compiled languages such as C/C++) is compensated by distributed processing. The model was adapted to engineering design optimization problems. Since the application domain considered during the optimizer development was engineering design, the chromosome modules were developed in such a way to support real-

numbered parameter encoding in conjunction with a definition of the allowable range for the parameters (genes). In addition, algorithms for keeping a historical record of all created chromosomes and for preventing the creation of duplicate ones were implemented. The optimization performance improvement phase involved the implementation of more advanced and efficient genetic operators (mutation, crossover, and selection). In addition to the standard random mutation operator, other mutation operators such as creep mutation with and without decay (when used, the decay rate reduces the mutation range as the Gas population ages, resulting in a broad capability to explore during the optimization initial stages and to carry out fine local searches in later stages), and dynamic vectored mutation (which allows mutation in all directions and not only along a dimension axis, and which is able to reach the whole search space and is not biased) have been implemented in the optimizer. Since real code chromosomes were selected as the default encoding for the optimization, several crossover techniques (suitable to this type of encoding) have been implemented in the optimizer, including the weighting averaging crossover (children are a weighted average of two parent points), blend crossover BLX-α (weighting averaging with exploration capabilities), and simulated binary crossover SBX (creation of solutions within the whole search space). All crossover operators implemented include features for consanguinity prevention. Selection operators implemented in the optimizer include among others a modified roulette wheel selection operator (with limitations on the number of instances of a chromosome) and the stochastic universal sampling SUS technique (which minimizes the bias and drift connected with the repeated spinning of the wheel). The tournament replacement and ranked replacement have been improved and implemented in the optimizer as replacement operators. One aspect that characterises the optimization process of practical engineering problems is the large number of parameters that must be accommodated. This is particularly true for the case of the aircraft trajectory optimization problem, where in order to describe properly a given flight path a number of flight segments (each involving several design variables and constraints, e.g., altitude, speed, etc.) will be utilised. Thus, the optimizer uses a unique optimization method. In this method, designers can define,

for each parameter, a target to be attained, a range within which this parameter should remain, and the requirement to maximise or minimise the given parameter. Consequently, the quality of the design is determined from achievement of the targets, the possibility of the violation of ranges, and the optimization of the selected parameters. This approach enables designers to have total control over the optimization process with neither having to know very much about the optimization algorithms nor having to devise a fitness function. (Rogero, 2002), (Celis, 2010), (Celis et al., 2009)

3.4 The Integrated Framework - HECTOR

All the above mentioned tools, including HELIX (described in detail in the following chapter) were integrated into a standalone simulation framework, called HECTOR (HEliCopTer Omni-disciplinary Research) developed by a PhD researcher in Cranfield University.

The HECTOR platform is a complete, integrated, standalone simulation framework for helicopter mission analysis. It is capable of simulating any user-defined helicopter mission profile for a user-specified helicopter configuration, and determining the required operational resources such as fuel consumption and operational time as well as the mission's environmental impact. Having an integrated optimization toolbox, HECTOR is also able to perform multi-disciplinary engine performance optimisation and mission profile optimisation assessments. The three aforementioned simulation tools (HELIX, TURBOMATCH and HEPHAESTUS) have been linked in order to communicate with each other.

The methodology followed for optimising a given helicopter trajectory in terms of sequence of computations is described below.

The mission profile is truncated within a user-specified number of flight segments. The experiment is carried out for each and every flight segment. The segment workflow is illustrated in figure below.

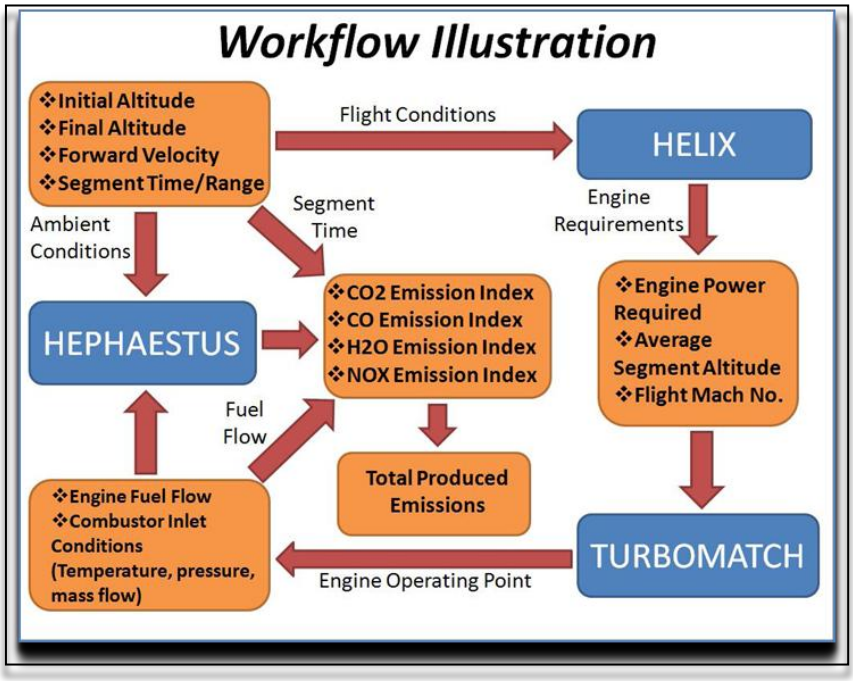

Figure 3. 1 – Workflow Illustration within HECTOR (adapted from (Goulos et al., 2010))

HECTOR performs three separate simulation actions for each flight segment. Each action is performed with the deployment of a simulation model corresponding to the equivalent action. These actions are the following: a) Helicopter aerodynamic performance simulation using HELIX, b) Engine performance simulation using TURBOMATCH, c) Emission indices prediction using HEPHAESTUS.

The experiment is initiated by defining the flight conditions of the segment which are input into the helicopter' aerodynamic performance model - HELIX. The helicopter properties susceptible to user-specification include the geometrical and weight break-down distribution data of the helicopter. The helicopter mission to be assessed in terms of engine power required is defined by the user. The mission profile is truncated in user-specified number of flight segments. The user needs to define the flight conditions occurring for each and every one of the mission profile's segments. The flight conditions are defined in terms of initial and final altitudes, the segment duration/range and the forward velocity of the helicopter.

Having an infinitely small segment range will result in a very smooth and accurate representation of the helicopter trajectory where variations in atmospheric

parameters with altitude can be accurately represented. However in this case, the number of segments which will represent the trajectory will have to be infinitely large resulting in a restrictive increase in computational time. On the other hand, a small number of segments will result in highly finite and discrete altitude steps which will compromise the accurate representation of an actual trajectory. It is therefore realized that the number of segments in which a flight profile is truncated, has to be carefully specified, bearing in mind that a compromise between accurate trajectory representation – accuracy in calculations and computational time is inevitable.

Based on the user-defined helicopter configuration, geometric characteristics and flight conditions, HELIX determines the shaft power required by the engine(s). Having determined the engine shaft power requirement, and with flight conditions defined (altitude and Mach number.) TURBOMATCH determines the engine operating point. Therefore the engine fuel flow and the combustor inlet conditions such as combustor mass flow, inlet temperature and inlet pressure, are established amongst other properties of interest. Based on the engine fuel flow, the combustor inlet conditions and the ambient conditions - required input data for the emissions prediction model, HEPHAESTUS calculates the emission indices for pollutants leaving the engine in chemical equilibrium (CO_2, H_2O), as well as for pollutants in non-chemical equilibrium (UHC, NO_X, CO). Hence, for a given flight segment with user-specified flight time or calculated within the helicopter aerodynamic performance simulation, the segment fuel burn can be calculated as well as the emissions of each pollutant of interest. After the calculations for each mission segment have been completed, the total fuel consumption, the required operational time and the total amount of produced emissions are calculated by adding up the corresponding values of each segment.

The environmental impact of any user-specified mission can be assessed within HECTOR either by means of total emissions produced by the helicopter operation within the defined mission profile, or by evaluating the pollutant's emissions trail of the helicopter. The emissions trail for each pollutant is acquired by evaluating the emissions produced within each flight segment only. Therefore the trail of emissions that the helicopter is leaving behind it during its trajectory is calculated.

The segment's initial altitude, final altitude, horizontal range/operational time at defined and the flight conditions in terms of flight Mach No. and average segment altitude are set. The associated operational resources requirements in terms of fuel burn and operational time are evaluated and the environmental impact in terms of emissions produced is assessed for the given segment. Since all the parameters that can fully define the position of the helicopter are acquired, and the respective properties of interest have been calculated, it is therefore reasonable to say that the problem in hand was defined and solved for the specified flight segment. Having defined and solved the problem within one flight segment, the new flight conditions in terms of final altitude and new helicopter mass are known. The calculations can therefore proceed to the next flight segment using as initial conditions, the previous segment's final conditions in order to ensure flight path continuity. The former segment's final altitude will be input in the new calculations as the new segment's initial altitude and the initial helicopter mass for the new segment will be the former segment's initial mass minus the former segment's total fuel burn. A new final altitude, forward velocity and horizontal range/operational time are defined for the new segment and the previously described calculations are performed for the newly defined flight conditions. The aforementioned process is reiterated for each and every flight segment in which the helicopter trajectory has been truncated.
When all the segments are computed, among other calculations, the total flight time, fuel burned, and gaseous emissions produced during the whole helicopter trajectory are computed. This process is repeated for all the potential solutions, and for the all the generations of potential solutions that the optimizer utilises in order to determine an optimum trajectory according to criteria initially specified by the user.

HECTOR has been developed in standard FORTRAN 90, rendering it compatible with systems ranging from standard WINDOWS OS based personal computers, to LINUX or UNIX based mainframe units. (Goulos et al., 2010)

Chapter 4: Helicopter Performance Model - HELIX

This chapter describes the development of the helicopter performance model (HELIX) to be used for the assessment of the helicopter engine performance. The chapter starts with the definition of the model requirements. The analysis of the performance calculations within the computer program based on the model is offered. The description of program workflow is provided, followed by detailed discussion on the model structure and the specific tasks performed by each part. The model capabilities were further enhanced by accounting for the three-dimensionality of the flight path trajectory and the analysis of this step is offered here. The discussion on the integration of HELIX with HECTOR and the associated alterations of some of the parts of HELIX concludes this chapter.

4.0 Glossary of Used Terms

Aircraft Weight (AW) – operational empty weight + payload + fuel weight

Autorotation – a self-sustained rotation of the rotor without the application of any engine power

Endurance – a maximum time the helicopter can stay airborne for a given gross take-off weight and a given amount of fuel

Equivalent Flat Plate Area - a parameter that accounts for the parasitic drag of the hub, fuselage, landing gear etc.

Gross Take-Off Weight (GTOW) – average value of AW at take-off

Manufacturer's Empty Weight/Dry Weight - the dry weight of the aircraft without crew, mission specific equipment or payload (weight of the aircraft including non-removable items)

Maximum Payload Weight (PAY) - allowable weight that can be carried by the aircraft, i.e. passengers and baggage, bulk cargo, military weapons, equipment for surveillance, etc.

Maximum Take-Off Weight (MTOW) – maximum AW at take-off

Operational Empty Weight (OEW) – the empty weight plus crew, mission specific equipment and no payload or consumable fuel (engine oil, unusable fuel, catering, entertaining, flight manuals, life vests, emergency equipment)

Range – a distance a helicopter can fly for a given GTOW and given amount of fuel

Rotor (Blade) Solidity - the ratio of the lifting area of the blades to the area of the rotor

Useful Load – the sum of payload weight and consumable fuel weight, to include reserve fuel, at take-off or launch (Bauchspies et al., 1985), (Stepniewski et al., 1984) and (Filippone, 2006)

The discussion of previous chapters highlighted the inclination of the aviation industry towards environmentally more efficient air travel concepts born from the realization of unacceptable growth of the gas pollutants and the depletion of the Earth's supply of fossil fuels. These concepts are attempting to remedy the situation by introducing the projects of optimizing the flight paths using current aircraft and also by conceiving new, more efficient aircraft. The economically most efficient way to analyze the performance of existing helicopters for a range of flight conditions but also to assess feasibility of implementing changes to satisfy the growing environmental requirements is the performance modelling using a digital computer.

Thus, in order to provide an insight into detailed challenges and possible gains resulting from the adoption of new technologies and innovative design concepts, a helicopter performance model was developed and integrated into a standalone simulation framework, along with an existing engine performance tool, the emission indices prediction tool and the optimization toolbox (all described in the previous chapter). The model can simulate a mission performance of a given helicopter. The model was built in a manner that allows for current helicopters to be modelled as well as advanced versions to be studied by altering appropriate input data such as

helicopter weight and geometric details, mission specification, aerodynamic characteristics, etc.

Helicopter performance models with a choice of fidelity and with varying capabilities have been developed in the past, however they are typically not available in the public domain. To address this issue a generic helicopter performance simulation tool called HELIX (from Greek *helix*=screw) has been written in the standard FORTRAN 90 language and as such provides a platform for fundamental performance modelling. The model requirements, its structure and the workflow of the computer program are described below.

4.1 HELIX - Model Requirements

The helicopter performance program, HELIX, was developed with the intention to provide fundamental performance information for every step of the flight path or for every flight condition that the helicopter experiences. The following set of requirements was implemented into HELIX:

- The model should calculate the power required by the helicopter at a specified flight condition (i.e. in hover, forward flight, vertical climb or descent and forward flight and descent) from the publicly available data (from the geometric specifications given by the manufacturer)
- The model should calculate the fuel used at each flight segment and then the total fuel usage during the flown mission
- The model should calculate other mission specifications, i.e. the range and endurance, speed for minimum power (recommended forward speed for the minimum fuel consumption), speed for maximum range (recommended forward speed for the maximum distance) and the aerodynamic efficiency (lift/drag ratio) of the rotor and the helicopter as a whole
- The model should compute the performance of the common helicopter configuration (single main rotor/tail rotor), but also be flexible enough to

allow for future enhancements of the model capabilities to account for other helicopter configurations in use.

All these capabilities where subsequently included and are currently part of the code.

4.2 HELIX - Model Description and Structure

The differences in the application of the helicopter over the fixed-wing aircraft and subsequent differences in missions flown by the helicopter are obviously reflected in the mission performance calculation method being different from the one used for fixed-wing aircraft. The versatility of the helicopter machine brings diversity of its mission profile. In order to make the mission performance calculations generic, typically, the mission is divided into segments, each representing fixed flight condition (such as hover, forward flight, vertical climb or descent or forward climb or descent) and the calculations of power required and fuel used are performed separately for each segment.

The helicopter performance program – HELIX – is based on a momentum theory (see section 2.8) and the formulas applied to calculate the helicopter performance are taken from (Filippone, 2006), (Leishmann, 2006), (Newman, 1994), (Stepniewski et al., 1984), (Layton, 1984) and (Prouty, 1984). The computer program was written in standard FORTRAN 90 code, ensuring its compatibility with majority of the computer operating systems. In spite of the extensive use of the imperial units in the above mentioned textbooks, the program employs SI units, rendering it compatible with other performance programs used in Cranfield University and thus avoiding unwanted unit-conversion issues. The program was created with the thought of integrability in mind, and hence it was kept simple, in order to achieve short computational time, while maintaining the desired level of accuracy.

The input into the model was kept as simple as possible, as the model is intended to be used by a general user who has access to the information from the public domain

only. This implies a need for certain number of assumptions and guesses that need to be taken, however.

There are two input files within HELIX, the mission specification input file and the helicopter weight and geometry input file. In the first input file the helicopter mission to be flown is defined by the user, including the helicopter take-off weight, the initial and final altitudes, the duration/distance flown and the forward velocity of the helicopter for each of the segments of the specified mission.

MissionAnalysisInputNEW – The user specifies the helicopter mission here. The mission is divided into segments; each of the segments represents fixed flight condition, such as hover, forward flight, forward climb or descent and vertical climb or descent. For each of the segments the user has to specify initial and final altitudes (the final altitude of the segment represents the initial altitude of the next segment) forward velocity and time or distance flown for each segment of the mission. This method of mission analysis is further described in (Newman, 1994)

GeometryAndWeightInputData - the main geometrical parameters of the helicopters are specified here by the user, such as rotor diameter, number of rotor blades, tail boom length etc. Also the breakdown of the helicopter weights is given here – the MTOW and OEW are specified as fixed input (given by the helicopter manufacturer). The user then has to indicate the fuel carried on board, number of crew members, and the payload in order to supply sufficient information for the GTOW to be determined. The geometrical data of existing helicopters stay fixed as well as the maximum take-off weight and the operating empty weight, which are provided by the manufacturer. What a user can vary, in order to investigate the effect of gross take-off weight on the helicopter performance, are the payload, amount of fuel carried on board or number of crew members. The only obvious limitation in this process is that GTOW< MTOW.

HELIX produces several output files during the run. ***SegmentPowerOutput*** contains the values of powers required for each segment divided by the number of engines. This value then represents the power required per engine and is fed into the Engine

model (TURBOMATCH) in order to attain the value of fuel flow per engine. Two check files are produced during the simulation, namely ***CheckInput*** and ***CheckOutput*** which write the values read by HELIX from the "GeometryAndWeightInput" and "MissionAnalysisInputNEW" respectively. The user then has the option to verify that the input files have been read correctly.

MissionAnalysisFinalOutput is the main output file which contains the breakdown of the helicopter mission flown in terms of the start weight, power required and fuel used for each segment. In addition, for the level forward flight or hover segments the autorotational descent velocity is also outputed. The file also contains the information about the total fuel used during the mission and additional performance parameters such as the range, endurance, speed for minimum power, speed for maximum range, critical autorotational velocity and lift/drag ratios (aerodynamic efficiencies) of the rotor and the helicopter, all as a function of the GTOW.

In summary, the input and output items of HELIX are listed below:

<u>Input:</u>

- Helicopter configuration
- Type of fuselage
- Number of engines
- Blade chord
- Main and tail rotor rotational speeds
- Main and tail rotor radius
- Root chord (if tapered blades are used)
- Airfoil
- Thickness/chord ratio
- Tail boom length
- Weight breakdown (OEW, MTOW, GTOW, Payload, Number of crew members, Standard and Additional fuel weight)

- For each segment of the mission: flight condition (i.e. hover, forward flight etc.), start and finish altitudes, forward speed, time/ distance flown, other weight change over the segment

Output:

- Total fuel used
- Range
- Endurance
- Speed for minimum power
- Speed for maximum range
- Critical descent velocity
- Lift/drag ratio (aerodynamic efficiency) of the rotor
- Lift/drag ratio (aerodynamic efficiency) of the helicopter

In addition, for each segment the following details are produced:

- Helicopter weight change
- Power required
- Fuel used
- Autorotational descent velocity (for hover and forward flight segments only)

Below is a detailed description of the parts of HELIX model in an alphabetical order:

HELIX_AERODYNAMICS

This subroutine receives the values of rotor angle of attack, tip Mach number, helicopter GTOW and fuselage details and returns the value of the average drag coefficient and the equivalent flat plate area. The subroutine implements the performance charts taken from the public domain containing the drag coefficients of various helicopters derived from experiments. The model considers a simplifying assumption of a fixed angle of attack and also one type of airfoil (NACA 0012) which suffices for the desired accuracy of estimation of power required. The allowance for

varying angle of attack and accommodating for the airfoil type would represent useful future enhancement to the model.

Mach number is computed within this subroutine from:

$$M=\Omega R/a_S \qquad (1)$$

where:

Ω - rotor angular speed, R – rotor radius and a_S – speed of sound

From the plot of average drag coefficient against the angle of attack (see below) for various values of Mach number the average drag coefficient is derived. Its value is then supplied for the power required calculations.

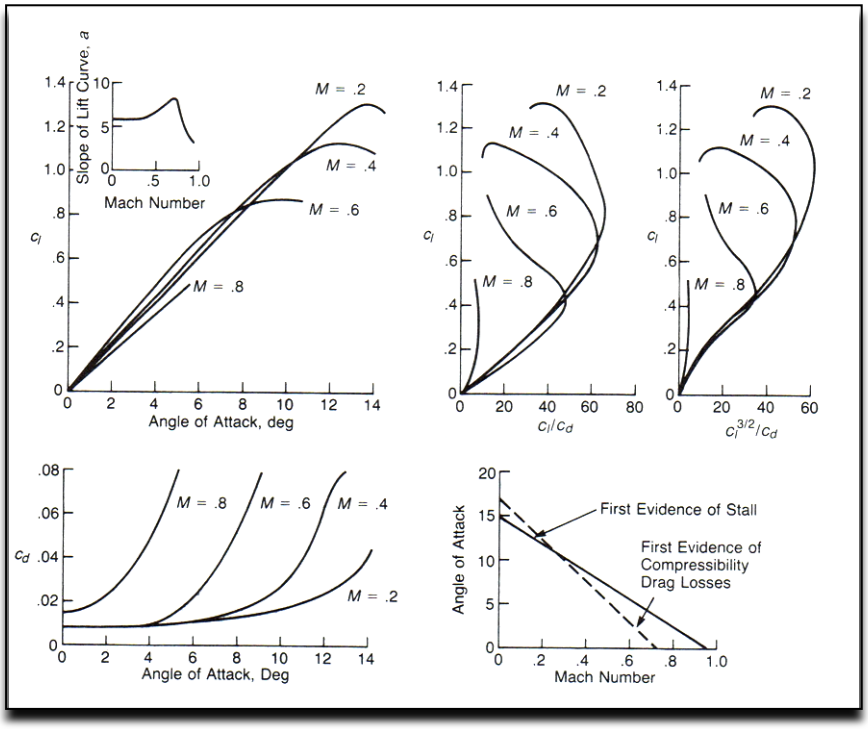

Figure 4. 1– Profile drag characteristics of the NACA 0012 airfoil, adapted from (Prouty, 1984)

A similar approach is taken when deriving a flat plate area used for the determination of parasitic drag: The complicated interaction viscous flows existing over the helicopter fuselages give rise to similarly complicated methods of prediction of the parasitic drag. The large computational times resulting from the use of sophisticated computational fluid dynamic methods for the parasitic drag prediction prevent them

from being in widespread use in the helicopter industry. Instead, semi-empirical drag prediction methods are commonly employed. They are based on component testing in wind tunnels and in combination with certain guesses represent reliable estimates. An estimate of the fuselage parasitic *equivalent flat plate area f* (a parameter that accounts for the drag of the hub, fuselage, landing gear etc) can be determined from knowledge of the drag coefficients of the various components that make up the helicopter using an equation of the form:

$$f=\sum_n C_{Dn} S_n \qquad (2)$$

where

S_n is the area on which the C_D is based.

Based on the helicopter gross weight and the "clean" or "utility" design, the equivalent flat plate area is determined from the plot below:

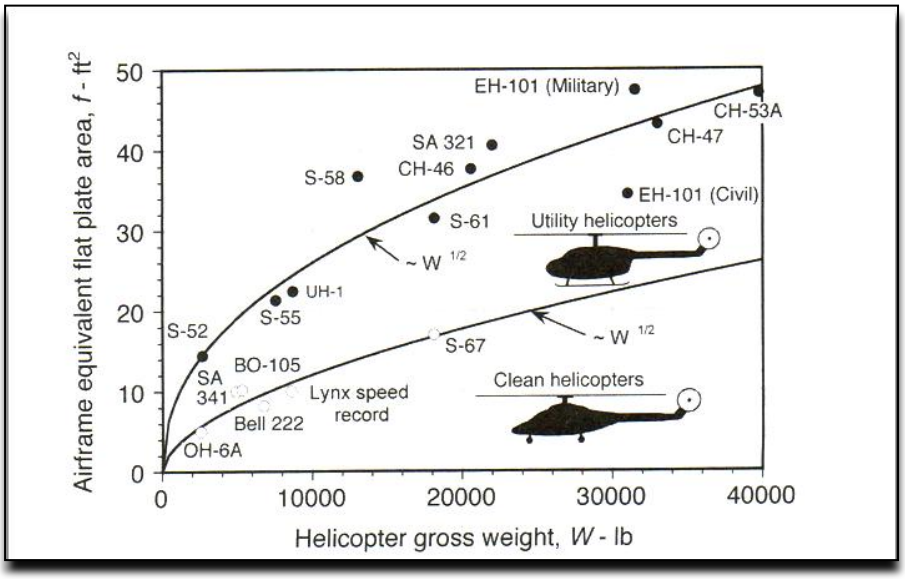

Figure 4. 2 – Helicopter gross weight vs. airframe equivalent flat plate area, adapted from (Leishmann, 2006)

"Clean" design refers to a streamlined helicopter airframe for low parasitic drag. On the contrary, a large rear upsweep angle, exposed rotor mast or fixed skids signify high parasitic drag fuselage used primarily on the utility helicopters. The large

upsweep angle is caused by the inclusion of rear door for cargo loading or passenger access. (Leishmann, 2006), (Prouty, 1984)

HELIX_ATMOSPHERIC

This subroutine computes the values of temperature, pressure, density and sound velocity at a required altitude. The correlations used within the subroutine represent an alternative to obtaining the values from the standard atmospheric charts available in the open literature. While the default values for the sea level altitude are set as the ISA SLS standard values, the user has the option to specify the deviation from the ISA temperature. The *temperature, pressure, density and velocity of sound* are calculated using the respective formulas:

(3)

where:

h- altitude in meters

(4)

(5)

(6)

where:

- ratio of specific heats C_v/C_p, R – gas constant

HELIX_AUTOROTATION

This subroutine computes the steady descent velocities during autorotation in hover and in forward flight. The autorotation is a manoeuvre that can be used to recover the helicopter to the ground in the event of the engine failure, transmission problems, or loss of the tail rotor. It is a self-sustained operating state without the application of any shaft torque from the engine, where the energy to drive the rotor

comes from potential energy converted to kinetic energy from the relative descent velocity (which is upward relative to the rotor). It requires that the pilot let the helicopter descend at a sufficiently high but controlled rate, where the energy to drive the rotor can be obtained by giving up potential energy (altitude) for energy taken from the relative upward flow through the rotor. The ability to autorotate is, therefore, a safety of flight issue. An autorotation at low forward flight speeds will take place in the turbulent wake state where the flow is not smooth and leads to a certain amount of unsteadiness at the rotor. At higher forward speeds the flow through the rotor tends to be smoother in the autorotational condition.

This section of the HELIX model computes *autorotational descent velocity* in hover and forward flight. For the hover case:

(7)

where:

V_{tip} – tip speed, C_D – average drag coefficient, is the hover thrust coefficient given by:

(8)

and

- inflow ratio in hover given by:

(9)

where:

T– helicopter thrust *A* – rotor disk area

And for the forward flight case:

(10)

where:

– total power required to hover, – rotor tip speed and - induced power required in autorotation, where:

(11)

where:

– profile power required in forward flight, - parasite power required in forward flight, - tail rotor power required in forward flight (see equations in HELIX_FORWARD)

HELIX_COMMON_DATA

This is one of the two modules within the programme that specifies parameters frequently used by other parts of the programme during the programme execution, including various correction factors used for the power required calculations, i.e. induced power factor, tail correction factor, forward efficiency factor etc.

HELIX_FORWARD

Power required by the helicopter during forward flight, forward climb and forward descent as a function of helicopter weight is calculated within this subroutine.

As previously discussed, the *power required in forward flight* consists of the induced and profile power as in the hover, but apart from that it contains the parasite power component. The compressibility effects on the overall rotor profile power requirements when the tip of the advancing blade approaches and exceeds the drag divergence Mach number of the airfoil section during forward flight are accounted for by an adequate correction factor. The same applies for the transmission losses. (Leishmann, 2006), (Filippone, 2006), (Stepniewski et al., 1984)

$$P_{level\_FF} = \left(P_{i\_FF\_main} + P_{o\_main} + P_p + P_{i\_FF\_TR} + P_{comp}\right)\tilde{k}_{transmission} \quad (12)$$

where:

$P_{i\_FF\_main}$ – induced power during forward flight, P_{o_main} – profile power, P_p – parasite power, $P_{i\_FF\_main}$ – tail rotor induced power, P_{comp} – factor accounting for compressibility effects, $k_{transmission}$ – transmission losses factor and:

$$P_i = k\frac{T^{\frac{3}{2}}}{\sqrt{2\rho A}} \tag{13}$$

$$P_o = \frac{1}{8}C_D\rho\sigma A V_{tip}^3 \tag{14}$$

$$P_p = \frac{1}{2}\rho A f C_D V_{forw}^3 \tag{15}$$

where:

k – induced power factor	σ – blade solidity
k_{TR} – tail rotor induced power factor	A_{TR} – tail rotor disk area
x_{TR} – main and tail rotor shaft distance	Ω – tail rotor angular speed (or tip speed)

HELIX_GEOMETRY _VAR

Main geometrical parameters frequently used in the calculations are computed here, such as the area of the rotor, rotor tip speed, tip loss factor or *rotor solidity*. The later represents the ratio of the lifting area of the blades to the area of the rotor and is computed using:

$$\sigma = \frac{N_b c}{\pi R} \tag{16}$$

where

N_b is the number of blades, c is blade chord and R is the rotor radius.

The tip loss factor accounts for the effect of the formation of a trailed vortex at the tip of each blade. This produces a high local inflow over the tip region and effectively reduces the lifting capability here. In practice, this reduction is accounted for by employing a tip loss factor based on blade geometry:

— (17)

This can be applied to rectangular blades; for tapered blades, however, the alternative geometric expression is used:

——— (18)

where

- the root chord of the main blade, - blade taper ratio (ratio of the tip chord to the root chord)

HELIX_INFLOW

The main task of this subroutine is to perform an iterative procedure in order to find an *inflow ratio* – a nondimensional parameter used for the calculations of forward power. The iterative solution of the following formula is sought using:

$$\lambda_{n+1} = \mu \tan\alpha + \frac{C_T}{2\sqrt{\mu^2 + \lambda_n^2}} \tag{19}$$

where

λ_n – inflow ratio, α – angle of attack and μ is the advance ratio

——— (20)

The recommended starting value of the iteration is the hover value, i.e.

$$\lambda_0 = \lambda_h = \frac{1}{2}\sqrt{C_T} \tag{21}$$

The error estimator is taken as

$$\varepsilon = \left\| \frac{\lambda_{n+1} - \lambda_n}{\lambda_{n+1}} \right\| \tag{22}$$

and the convergence occurs when ε<0.0005. (Leishmann, 2006)

HELIX_INPUT

The main purpose of this subroutine is to read the input data from the GeometryAndWeightInput file, creating a check file to confirm that the input data was read correctly and in case of the user's typing error printing the error messages to the output file.

HELIX_PERFORMANCE

This subroutine is called by the main program after the power required calculations have been performed in order to obtain the additional performance indicators such

as the helicopter range and endurance, speed for minimum power, speed for maximum range, lift-to-drag ratios (aerodynamic efficiencies) for the rotor and the helicopter. These parameters provide a useful basis for comparisons of the forward flight efficiency with respect to other rotors, helicopters or a fixed-wing aircraft.

There is a number of performance parameters that can be readily obtained from the computed power required and the used fuel flow. Thus, HELIX also calculates the *range and endurance* or the distance and time flown for a given gross take-off weight and given amount of fuel, respectively, using:

——— (23)

and:

——— (24)

where:

W_{GTOW} – initial gross take-off weight and W_F – initial fuel weight, P – power required, SFC – specific fuel consumption

The *aerodynamic efficiencies* or lift-to-drag ratios of the rotor alone and the whole helicopter represent useful parameters that can be used for comparison of the forward flight efficiencies with another rotor, between two helicopters or even between the helicopter and the fixed-wing aircraft. They are determined from:

rotor: $$\frac{L}{D} = \frac{T \times V}{P_i + P_0} \quad (25)$$

helicopter: $$\frac{L}{D} = \frac{T \times V}{P_i + P_0 + P_p} \quad (26)$$

Speed for minimum power is the optimum speed to fly for minimum autorotative rate of descent. In other words, at this speed the power required by the rotor is minimum and thus during the autorotation only the least amount of potential energy has to be used. Also, maximum possible rate of climb is obtained at this speed in level flight.

The best endurance is also achieved at this speed. This proves useful when obtaining maximum time is crucial such as during a search and rescue mission, surveillance, etc. In addition, as the fuel burn is proportional to power at a given altitude and temperature, the speed for minimum power determines the speed for minimum fuel burn as well. *Speed for maximum range* is calculated in a similar fashion using:

$$V_{mp} = \sqrt{\frac{T}{2\rho A}}\left(\frac{4k}{3f/A}\right)^{\frac{1}{4}} \tag{27}$$

$$V_{mr} = \sqrt{\frac{T}{2\rho A}}\left(\frac{4k}{f/A}\right)^{1/4} \tag{28}$$

where:

f – equivalent flat plate area (see HELIX_AERODYNAMICS)

Another helicopter performance parameter that can be readily determined when the power required and power available values are obtained is the *service ceiling* of the helicopter. The absolute ceiling is the altitude at which the power required equals power available and hence represents the maximum altitude the helicopter can climb to. This condition is approached only asymptotically however and thus in practical performance calculations the service ceiling is computed instead, when the rate of climb is arbitrarily set to a low value (typically 1 ft/s ≈0.3m/s) and the service ceiling is obtained when the rate of climb reaches this value. (Filippone, 2006)

HELIX_READ_SEG

The second of the two modules within this code contains the subroutine SEG_NO_READER, which similarly to the HELIX_INPUT reads the input data. The input data is read from the second input file: MissionAnalysisInputNew. This is the file where the helicopter mission is defined by user. The mission is divided into segments, each representing a fixed flight condition (hover, vertical climb or descent, level forward flight and climb or descent) and the user specifies start and finish altitudes, forward velocity and time or distance flown for each segment of the mission.

HELIX_VERTICAL

This subroutine computes the power required during hover, vertical climb or vertical descent. The power required during parts of vertical descent is presented as estimation only as the momentum theory cannot be used beyond certain descent velocity. More details about the limits of the calculation of the power required during powered descent can be found in (Leishmann, 2006) or (Filippone, 2006).

The *power required in hover* is calculated using:

$$P_h = P_i + P_0 + P_{TR} \tag{29}$$

hence:

$$P_h = k\frac{T^{\frac{3}{2}}}{\sqrt{2\rho A}} + \frac{1}{8}\overline{C}_D\rho\sigma A V_{tip}^3 + \frac{k_{TR}}{\sqrt{2\rho A_{TR}}}\sqrt{\left(\frac{P_i + P_o}{\Omega x_{TR}}\right)^3} \tag{30}$$

where:

x_{TR}-the shaft distance between main and tail rotor

In the *vertical climb*, the power required is determined according to:

$$\frac{P_{vert\_climb}}{P_h} = \frac{v_c}{2v_h} + \sqrt{\left(\frac{v_c}{2v_h}\right)^2 + 1} \tag{31}$$

where:

v_c -the climb rate determined from the surplus power available and v_h - the hover induced velocity :

$$v_h = \sqrt{\frac{T}{2\rho A}} \tag{32}$$

In the *vertical descent*, the determination of the power required becomes more complicated. For the situation, when — , the momentum theory becomes invalid, because the well-defined stream of the flow no longer exists and hence the control volume that encompasses the rotor disk cannot be defined. However, the velocity curve can still be defined empirically, even though only approximately, based

on flight tests. In this velocity region the induced velocity is estimated according to the following formula:

— — — — — (33)

where k, $k_1 - k_4$ are appropriate empirical factors.

For the region where —, the momentum theory still applies and the power required is determined by:

$$\frac{P_{vert\_descent}}{P_h} = \frac{v_c}{2v_h} - \sqrt{\left(\frac{v_c}{2v_h}\right)^2 - 1} \quad (34)$$

The power required in forward climb and descent is calculated using similar approach to the vertical climb and descent. More details can be obtained from (Layton, 1984), (Leishmann, 2006) and (Filippone, 2006).

When accounting for *ground effect* on the helicopter performance the empirical corrections to the out-of-ground performance are typically used. The changes in the induced power element required when the helicopter is hovering IGE are determined by:

$$P_i = P_{iOGE}\left[-0.1276\left(\frac{Z}{D}\right)^4 + 0.7080\left(\frac{Z}{D}\right)^3 - 1.4569\left(\frac{Z}{D}\right)^2 + 1.3432\left(\frac{Z}{D}\right) + 0.5147\right] \quad (35)$$

where:

Z – height of the rotor above the ground and D – rotor diameter (Cooke & Fitzpatrick, 2002)

HELIX_WEIGHT_ITER

This subroutine aids the flow of the main programme unit by transferring the control from the main programme unit to one of the HELIX_VERTICAL or HELIX_FORWARD subroutines in order to compute the power required during a particular flight segment and subsequently the control is transferred back to the main programme to compute the fuel used during the segment.

MAIN

The main programme unit transfers the control from and to the above mentioned subroutines and modules in order to obtain the requested performance parameters and information required by the user. The main fuel flow calculation is conducted here as described below:

Once the power required term is calculated the *fuel flow* can be determined according to the schematic below:

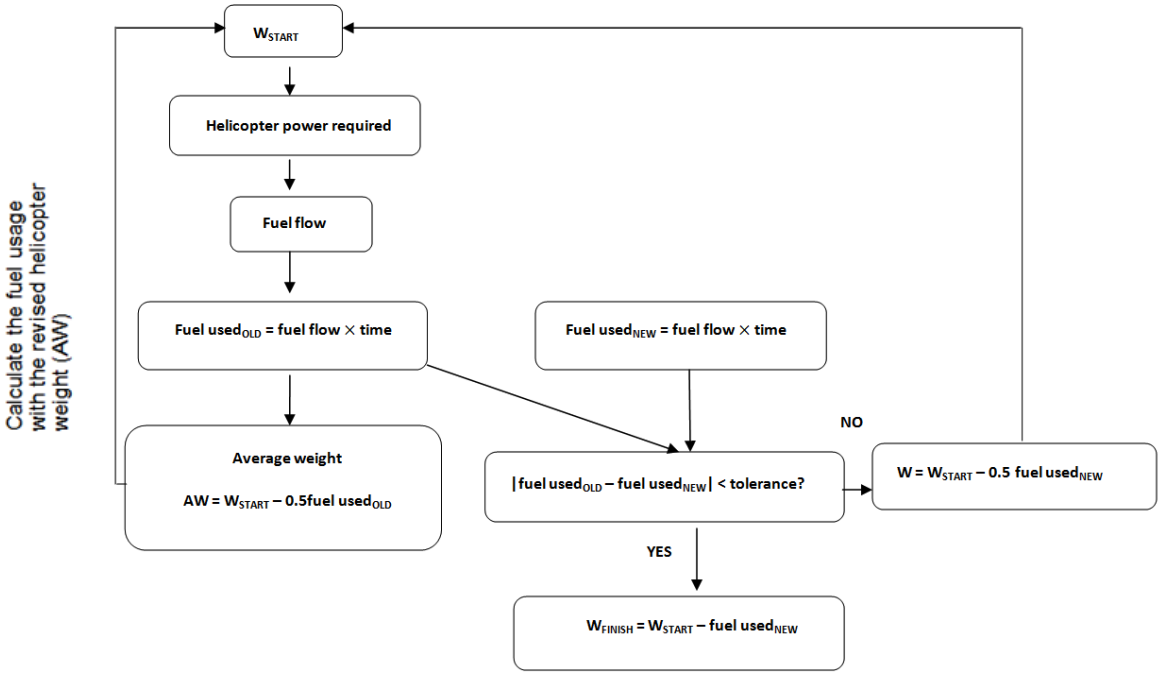

Figure 4. 3 – The schematics of the fuel used calculation algorithm (Newman, 1994)

The power required using the value of gross take-off weight (W_{start}) defined by the user is fed into a suitable helicopter engine performance tool (TURBOMATCH) in order to obtain the fuel flow. This value is subsequently returned to the helicopter model in order to calculate the fuel consumption for that specific segment. Half of the fuel used value is deducted from the initial weight in order to obtain Average weight (AW). The power required is then computed for this weight and the two fuel used values compared. If their difference lies within the specified tolerance, the weight change over the segment can be determined using the new fuel used value. If the tolerance is exceeded, another weight is determined by deducting half the new

fuel used value from the initial weight. The process of calculating the fuel usage is then repeated until the specified tolerance is met and the change of the weight over the segment can be established. In this way the fuel consumed for each segment and subsequently over the whole mission can be determined. The model also takes into account any other helicopter weight changes over the segment, such as a drop of armaments, etc. More information on this algorithm can be obtained from (Newman, 1994).

The computational workflow within HELIX is depicted below.

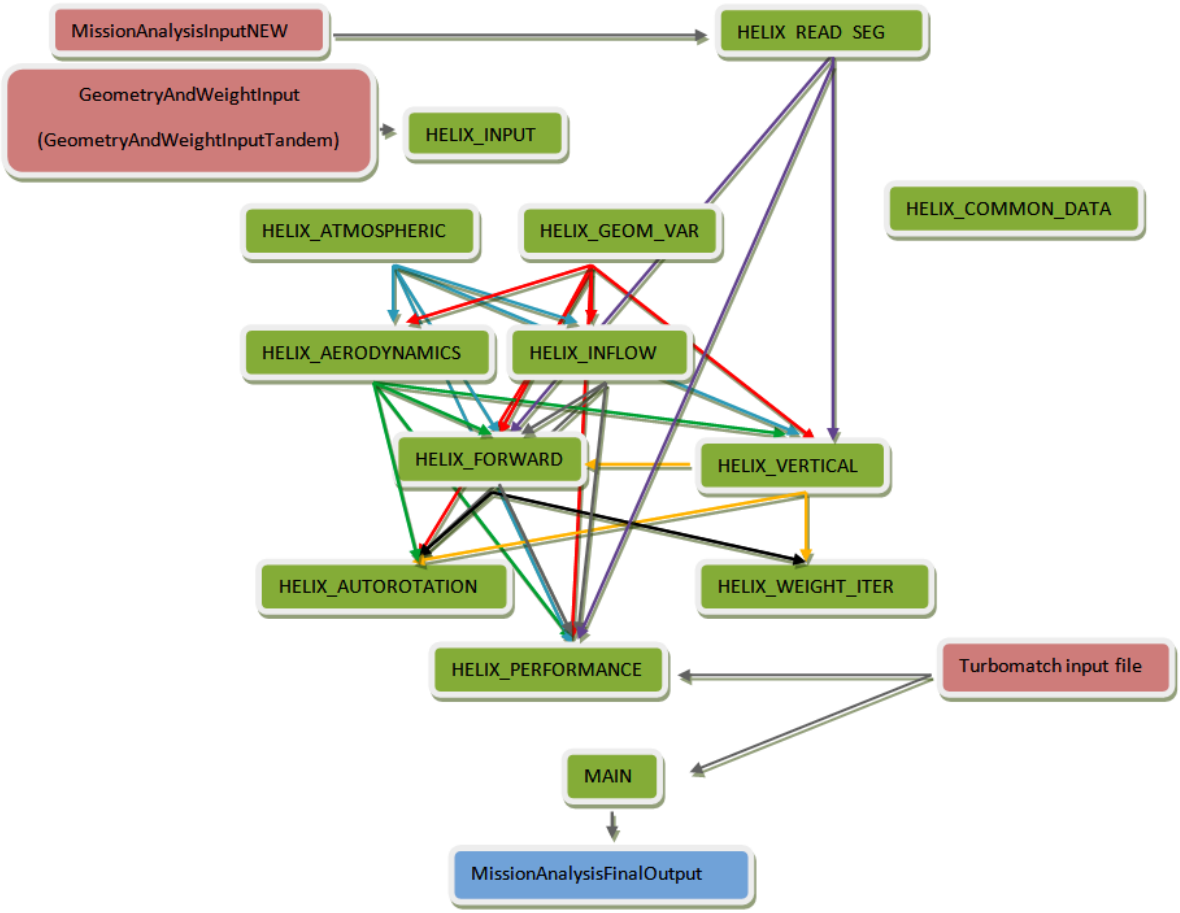

Figure 4. 4 - Schematic diagram of the computational flow within the HELIX programme

4.2.1 Note on the Tandem - Rotor Helicopter Performance Calculations

The performance of the second most commonly used helicopter configuration (tandem rotors) can be adequately estimated using a variation of the momentum theory by accounting for the induced interference effects between the rotors. Tandem rotor designs are often used for heavy-lift helicopters because all of the rotor power can be utilized to provide lift. However, the induced power of partly overlapping tandem rotors is higher than that of two isolated rotors due to the rear rotor operation in the slipstream of the forward rotor, which results in the higher induced power for the same thrust. This effect is accounted for by applying an induced power interference factor, that accounts for the higher power required by the rear rotor due to its operation in the downwash of the forward rotor. Generally, a single value of the interference factor is employed. In order to account for different rotor spacing and rotor overlap, a more sophisticated method of the interference factor determination should be used, that takes into account the geometric data of the helicopter rotors (Filippone, 2006), (Leishmann, 2006). The induced power for the tandem rotor configuration then becomes:

(36)

where:

- thrust of the front rotor, - thrust of the rear rotor, – induced power interference factor,
- induced velocity of the front rotor, - induced velocity of the rear rotor

4.3 Further Development – 3D Trajectory Implementation

HELIX as described above fulfills the main objective and that is to provide the power required and fuel used value at any point during a specified mission and for the mission as a whole. A useful enhancement to the capabilities of this program was seen in the implementation of the spatial definition of the helicopter mission. The mission would no longer be looked at as two-dimensional (function of the altitude only), but the trajectory of the helicopter would be defined by the use of spatial coordinates (latitude, longitude and altitude). This would represent more realistic

approach of defining a mission, it would enable possible terrain-following studies to be conducted and it would more correctly represent the position of the helicopter towards the Earth's surface.

For the purpose of defining the spatial coordinates, the current geodetic system – WGS-84 – was used. This system considers the Earth not as a sphere but as a spheroid (ellipsoid) as a surface of reference for the mathematical reduction of geodetic and cartographic data.

The WGS-84 is not referenced to a single datum point. It represents spheroid whose placement, orientation, and dimensions best fit the Earth's equipotential surface which coincides with the geoid (the actual Earth). The system was developed from a worldwide distribution of terrestrial gravity measurements and geodetic satellite observations. (Stanzione et al., 1992)

The input file of the enhanced version of HELIX (as part of the HECTOR program) includes the specification of the spatial coordinates. The user specifies latitude, longitude and altitude for the fixed points of the helicopter flight trajectory. The fixed points (endpoints of a trajectory segment) typically represent either boundaries between two flight conditions, or a change in the direction which the helicopter is flying. The program then determines what flight condition the helicopter encounters and computes the distance between the endpoints of the flight segment (the segment range) based on the Haversine formula for computing the spherical distance between two points (Sinott, 1984):

(37)

where:

- Earth's radius and

(38)

where:

$$x_1 = [\sin(lat_1 - lat_2/2)]^2 \quad (39)$$

$$x_2 = \cos(lat_1)\cos(lat_2) \quad (40)$$

$$x_3 = [\sin(long_1 - long_2/2)]^2 \quad (41)$$

where:

lat_1, lat_2, $long_1$, $long_2$, – latitude and longitude coordinates of the points

An example of a basic three-dimensional mission profile is shown below. This profile can be taken as a base for many types of missions, including range mission, oil & gas, executive transport etc.

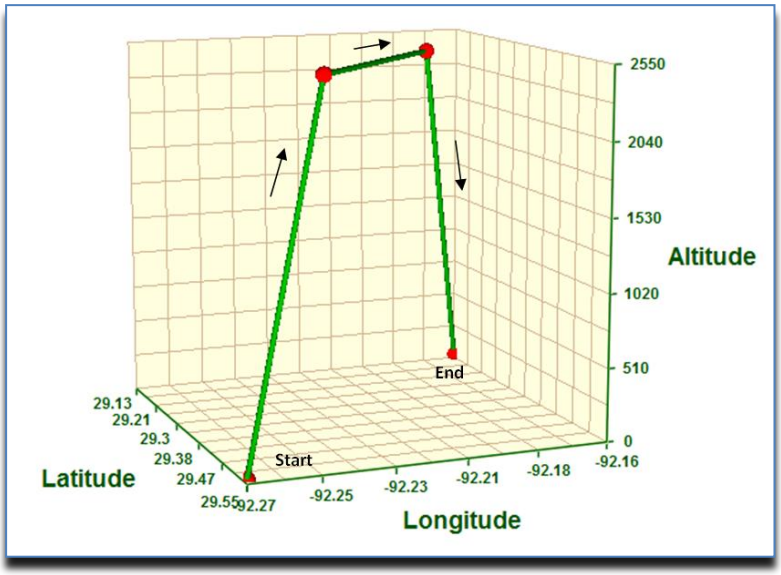

Figure 4. 5 – Basic three-dimensional mission profile example

The mission consists of five segments, three of which are shown in the graph. The first and last segments are take-off and landing segments, respectively, which are generally considered to take place in altitude of 0 meters. Second segment is the forward climb segment, third takes place in cruise and the fourth segment is a vertical descent to the landing site.

Clearly, there is no limit to the number of segments and the variability of the mission depends on the purpose of the mission itself, on the vehicle, weather, pilot and many other factors. One another example of the mission characterization using the three-dimensional trajectory definition is shown below.

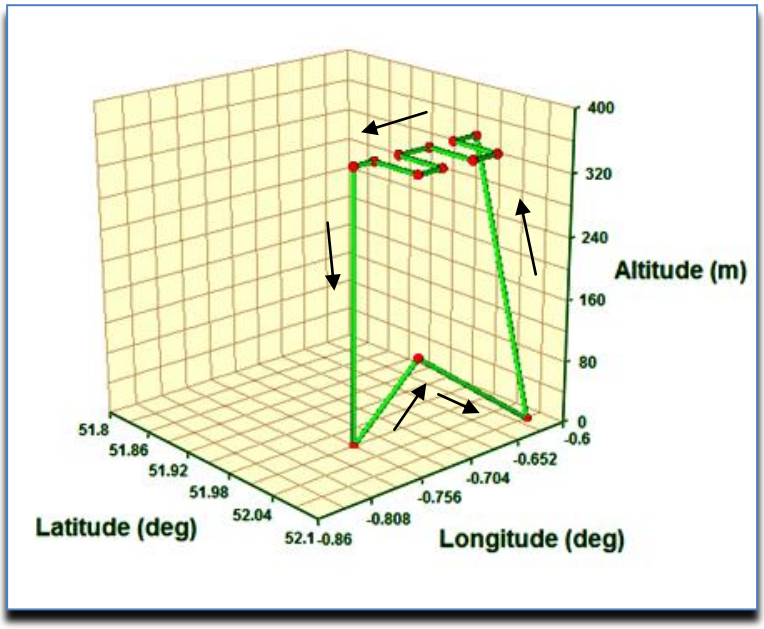

Figure 4. 6 – Example of a search and rescue mission definition

This time a type of search and rescue mission is visualised. The helicopter takes off and climbs in forward flight into the corner of the search area and starts following the creeping line search pattern (see Chapter 6 for details). The length of the individual search tracks represents a distance equal to the sweep width from the side of the rectangular area. After identifying the target the helicopter descends vertically towards it. After target recovery the helicopter gains some altitude while flying forward and finally descends to the base. For more information on the search and rescue patterns and procedures, the reader is referred to (ICAO, 1970).

4.4 Synthesis with HECTOR

The helicopter performance tool needs to be closely coupled with the generic helicopter engine thermodynamic performance prediction model. This coupling has

been done within HECTOR platform (see section 3.4), a complete, standalone simulation framework for helicopter mission analysis. Apart from the helicopter performance prediction tool, HELIX, it contains the engine performance simulation program – TURBOMATCH (see section 3.1), emission indices prediction model – HEPHAESTUS (see section 3.2) and the JGA optimization toolbox (see section 3.3). HECTOR has been designed to ensure a possibility of simulating any user-defined helicopter mission profile for a user-specified helicopter configuration, and determining the required operational resources such as fuel consumption and operational time as well as the mission's environmental impact. Having an integrated optimization toolbox, HECTOR is able to determine optimal mission profiles for any user-specified mission objectives under any user-defined mission constraints. (Goulos, 2009)

After integration with HECTOR the HELIX's input and output files have undergone alterations. The *GeometryAndWeightInputData* input file was retained but the *MissionAnalysisInputNEW* file was merged into HECTOR mission input file called *FullMission*. In this input file the user specifies the following items:

- Profile definition (*2D or WGS-84(3D)*)
- Number of engines
- Maximum allowable engine turbine inlet temperature (TET)
- Minimum allowable engine turbine inlet temperature
- Total fuel reserves
- Power tolerance (*maximum allowable difference between power required and power delivered*)
- Name of the engine model to be used
- Name of the helicopter configuration
- Helicopter configuration
- Number of optimized values
- Type of study (*experiment or optimization*)
- Start latitude
- Start longitude

- Start altitude
- Deviation from ISA temperature

Further, for each of the mission legs (parts) the user needs to specify the following.

For segment (unoptimized part of the mission profile):

- Segment type (*i.e. the flight condition*)
- Latitude
- Longitude
- Segment final altitude
- Segment forward velocity
- Segment range/segment time (optional)

For the profile (optimized part of the mission profile) the following have to be indicated:

- Latitude
- Longitude
- Altitude
- Profile horizontal range (*for 2D analysis only*)
- Forward velocity (*low, high and nominal values*)
- Allowance for intersegmental altitude variation
- Allowance for intersegmental velocity variation
- Allowance for intersegmental altitude variation
- Intersegmental parameter variation (*choose which parameter to vary within segments, time/range*)
- Vertical segment range variation

Latitude is specified in degrees north, the latitude south is identified as negative north. Similarly, the longitude is specified in degrees east and the latitude west is identified as negative east. Finally, if the optimization is desired, the user sets the optimization parameter.

The original output file of HELIX has also been merged with HECTOR output file. The arrays of the following parameters are printed for each segment:

- Total horizontal range

- Total fuel burn
- Total operation time
- Total NO_X emissions
- Total CO emissions
- Total UHC emissions
- Total CO_2 emissions
- Total H_20 emissions

The example of HECTOR input and output file is attached in the Appendix.

The capabilities of HELIX as a part of the HECTOR platform were tested and evaluated. A number of experiments were conducted, generating the performance and fuel consumption of the helicopter during a given mission. The analysis of the results is presented in Chapter 6.

Chapter 5: Helicopter Engine Library Development

This chapter presents a discussion on the choice of the engine for a helicopter and the emphasis of suitable applications of two main helicopter engine representatives. The focus is then directed towards the gas turbine engine and the brief description of its concept is given. The second part of the chapter provides a description of the helicopter engine model library development. The performance simulations of three representative engine models using TURBOMATCH are presented for each helicopter category (light-, medium- and heavy-weight) and the typical performance charts are included.

5.0 Glossary of Used Terms

Gross Thrust (total thrust) - the product of the mass of air passing through the engine and the jet gas velocity at the propelling nozzle

Mach Number – an additional means of measuring speed; ratio of the speed of the body to the local speed of sound; Mach number 1.0 represents a speed equal to the local speed of sound

Momentum Drag – drag due to the momentum of the air passing into the engine relative to the aircraft velocity

Ram ratio – the ratio of the total air pressure at the engine compressor entry to the static air pressure at the air intake entry

5.1 Helicopter Engine Fundamentals

5.1.1 The Choice of Helicopter Engine

The gas turbine engine is being predominantly used in the helicopter market, mainly because of its very high power to weight ratio. The relatively low weight of the gas turbine engine comes from its simplicity. The compression of the air and the extraction of shaft power are both done by rapidly spinning blades. The disadvantage of this concept is that the gas turbine engine uses highly stressed parts and the initial

cost of its development is higher that other engines used on helicopter. Small turbine engines tend to be inefficient because the Reynolds numbers at which small blades must operate will be less favourable.

The other type of engine used on helicopters - piston engine – uses a static compression of the air with a piston in a cylinder. The static compression introduces significantly lower power loss than dynamic compression in a gas turbine. This makes piston engines more efficient at partial throttle settings. The disadvantage is that the piston engine must handle the stresses raised by reciprocating that increase with the square of the rotational speed (RPM). This limits the RPM available as a function of piston size. In piston engines there is a power to weight advantage in using a lot of small cylinders rather than a few big ones. The difficulty arises when a lot of power is required which brings the necessity of having many cylinders and this brings practical issues with cooling, reliability or cost.

An advantage of the gas turbine over the piston engine is also that there are no reciprocating parts thus the RPM can be significantly higher than for a piston engine and hence more power can be produced.

At 400-500 kW of output power, the advantages and disadvantages of using the gas turbine and piston engine are almost equal. For higher powers the gas turbine is typically used, whereas for lower powers the piston engine is the engine of choice. Although the power to weight ratio of piston engine is lower, it is compensated by the saving in fuel load. Consequently, large helicopters are typically equipped with two or three gas turbine engines and they have tendency to use high disc loading because of the availability of large amounts of power. Small helicopters usually utilize piston engines and lower disc loading. (Watkinson, 2004)

5.1.2 Basic Gas Turbine Engine Thermodynamics

The gas turbine engines are continuous gas flow engines. The power available depends on two factors: on the amount of heat energy introduced in the form of fuel per kg of ambient air, and on the rate of air flow through the engine. (Stepniewski & Keys, 1984)

The simplistic explanation of the gas turbine concept is as follows: The air is drawn into the compressor. Here, the air is compressed continuously so that a steady pressure is maintained at the compressor outlet. Compressed air passes to the combustor chamber where it mixes with fuel and burns. The gas temperature consequently increases and it expands. The hot gas enters the turbine, where the energy in the hot gases is converted into shaft power. Some of this energy is used for driving the compressor, and the remainder is available to drive an external load.

There are generally two types of compressors that can be used in the helicopter engine, a centrifugal compressor or an axial compressor. Sometimes, however, a combination of both is utilized. The choice of the compressor depends on the engine requirements. A number of small gas turbine engines widely used in helicopters have axial-centrifugal combination type compressors, as this configuration combines the advantages of both types, bringing moderate pressure ratios and minimizing the length of the engine.

The advantages of centrifugal compressor represent the simplicity of design, lower susceptibility to stalling or surging. Its limit lies in the pressure ratios available for a single stage. This type of compressor is used mostly in the small turbine engines.

When the size of the compressor is of importance, the axial compressor is employed as it produces the same output as the centrifugal one but with smaller diameter. It is also more efficient and thus represents lower fuel consumption. The axial flow through the engine however brings a higher possibility of foreign object damage or the compressor stall. The maintenance costs are also higher due to the blades accumulating fatigue and creep.

The type of the gas turbine engine used in the helicopter is the so called free turbine engine. This configuration employs two turbines. There is no mechanical connection between them. The first part of the engine is essentially a gas generator, and the second part converts the gas energy to the shaft power.

The rotational speeds of the gas generator and the free turbine are typically different. The free turbine should maintain constant speed because it is connected to the helicopter rotor, whereas the gas generator will turn faster if more drive torque is required.

The figure below shows a schematic of a commercial gas turbine engine. Air enters through a multi-stage axial compressor (a) followed by a single-stage centrifugal compressor (b). The flow of compressed air enters two large ducts (c) leading to the combustor (d) where the fuel is injected. The hot gases then enter the gas generator turbine (e) that drives the compressor and then continue through the free turbine (f) that powers the helicopter. The exhaust gases are then turned upwards and exit through the top of the engine compartment (h). Power turbine runs on the outside of the main shaft and transfers power through the gearbox (g) to output shaft.

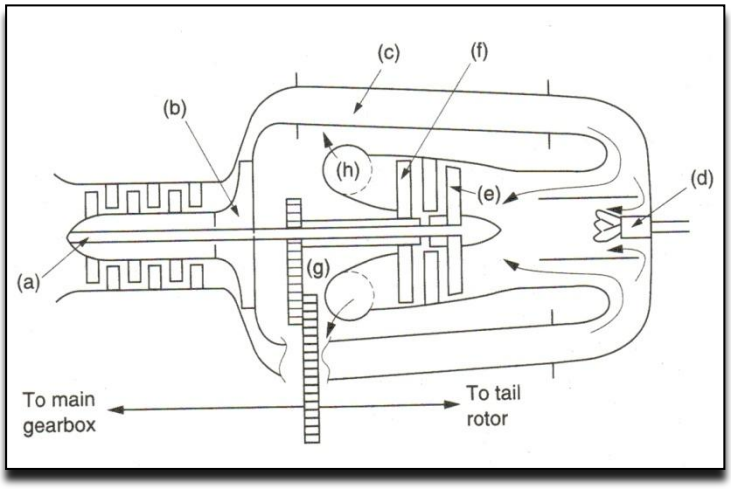

Figure 5. 1 – Schematics of a gas turbine engine, adapted from (Watkinson, 2004)

The engines and transmission are generally placed close together. Gas turbines are typically built into the roof of the hull to maximize internal space. The engine's rotational speed is significantly higher than that of the helicopter rotor and thus a reduction gearing is necessary. The gearbox will generate a large amount of heat and thus requires a cooling system. The gearbox also drives the tail rotor shaft, which runs the length of the tail boom to the tail rotor gearbox, the tail rotor shaft is often

mounted outside the tail cone for ease of inspection and maintenance. It might take some time for the rotors to stop after the engine has been shut down, which can be inconvenient if the passengers need to leave the helicopter quickly, or if the helicopter needs to be camouflaged during a military mission or if it needs to be placed in the hangar on the ship. For this reason a rotor brake is frequently fitted on the transmission. (Watkinson, 2004)

The gas turbine engine is typically started with an electric motor. Once a suitable compressor speed is established the fuel is sprayed through the nozzle and the igniter is operated. This results in hot gas generation that will increase the turbine speed until engine power can take over from the starter motor. (Watkinson, 2004)

At the inlet of the engine typically an inlet particle separator is employed. This application results from the fact that the helicopter, because of the nature of the flow through the rotor system, draws debris up from the ground in the form of dust, small rocks, and grass. This material may stick to the first stages of the compressor and cause the disruption of flow.

Another necessity for the helicopter engine is frequent compressor washing. The helicopter more than a fixed-wing aircraft is affected by the dust erosion due to its frequent operation from small, unprepared landing sites. The major damage occurs to the trailing edge of the tip of the compressor blades. The percentage change in the small blades of the final stages of the compressor is much greater than that of the relatively larger blades of the first stages. The employment of the axial-centrifugal compressor partially remedies this problem as it increases the resistance of an engine to erosion by sand and dust. The centrifugal compressor can be considered essentially insensitive to sand and dust erosion. If the last stages of an axial compressor are replaced by a centrifugal compressor, the engine has been found to become approximately 10 times more resistant to sand and dust erosion. (Saunders, 1975)

Helicopters are limited to low speeds due to the aerodynamic limitations on the rotor blades (approximately 300 km/h) so their engines are designed to produce the maximum available shaft power. (Saravanamuttoo et al., 2001)

The performance of the engine is described in a specification by their manufacturers. These documents present the engine ratings and fuel consumptions under various conditions, based on the engine performance as measured on the test bed and subsequently modified by factors accounting for the effects of altitude, temperature, and forward flight. The engine rating is limited by the maximum allowable turbine entry temperature, torque or fuel flow. The ratings are a function of altitude, temperature and forward speed. The figure below shows the zero forward speed engine ratings for a typical turboshaft engine. (Prouty, 1985)

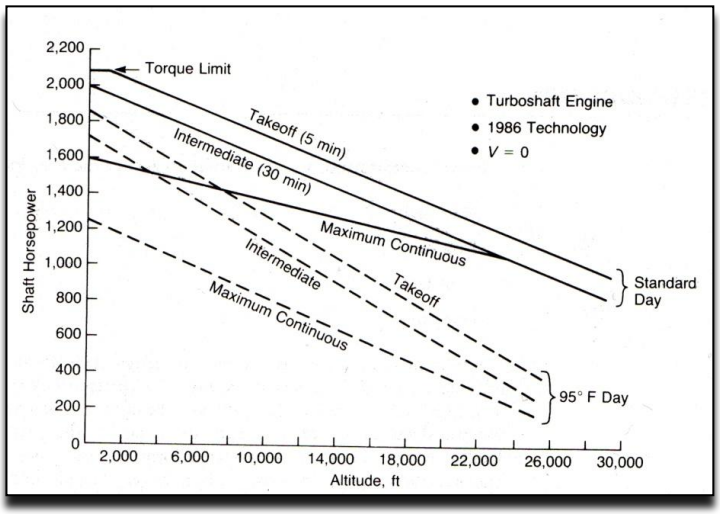

Figure 5. 2 – Typical uninstalled engine ratings as a function of altitude and temperature, adapted from (Prouty, 1985)

5.2 Helicopter Engine Model Library Development

The helicopter performance model (HELIX) requires a thermodynamic engine simulation model. As described in Chapter 3, for this purpose HELIX uses TURBOMATCH, the Cranfield University in-house computational program that facilitates design point and off-design performance calculations for gas turbines engines. In order to verify the functionality of the developed HELIX model and to

assess performance of a variety of existing helicopters, the models of their engines are necessary. A project of developing a library of specifically helicopter engine models commenced at the start of this research. The aim was to develop the models of those helicopter engines that are representatives of their respective categories. Models were developed for light-, medium- and heavy-weight category helicopters. A variety of engine models was built to represent a scale of various engine manufacturers, helicopter applications and purposes.

The work commenced with an upgrade of two existing engine models, the first being the engine model similar to the *RTM 322* engine (collaboratively manufactured by Turbomeca and Rolls-Royce) powering medium-sized helicopters, e.g. the Agusta Westland Apache or NH 90 helicopter with power output of 1,694 kW at take-off. More information on this engine is available from (Vickers, 1995). The second engine model was based on the *Makila 1A2* (manufactured by Turbomeca) powering also medium-sized helicopters, mainly Eurocopter Super Puma with a power output of 1,420 kW at take-off. Further information on this engine can be obtained from (Maythapattana, 1999). The library has been enlarged by the addition of further helicopter engine models and to this day it contains 12 engine models. The available engine models, together with the list of the helicopters that they are used on, their power output at take-off, the category they fall into and the name of their developer are listed in the table below. These models are based on information available in the public domain and some educated assumptions where the information is not available. Consequently, the performance models are similar to but do not completely represent these engines. The development of the engine models was undertaken jointly by MSc Thermal Power and PhD students within the department under the technical leadership of the author.

Engine	Engine manufacturer	Helicopter manufacturer	Helicopter make	Helicopter type	No. of engines	Output - TO	Model developer
Allison 250–C28C	Rolls-Royce	MBB/Eurocopter	Bo105	Light - multipurpose	2	368.4kW	Sergio Caballero[1]
Arrius 2B2	Turbomeca	Eurocopter	EC 135	Light-civil	2	472kW	Thierry Sibilli[2]
Arriel 2C	Turbomeca	Eurocopter	AS 365 N3 Dauphin	Medium-weight multipurpose	2	626kW	Martina Mohseni[2]
			-AS 532 Cougar	Medium-size multipurpose	2		
LHTEC CTS800-4N	LHTEC = RR/Honeywell	Agusta Westland	Super Lynx	Medium size	2	1,015kW	Martina Mohseni
RTM-322-01/12	RR/Turbomeca	Agusta Westland	-WAH-64 Apache	Medium-Size military	2	1,568kW	J.Vickers[3] / Martina Mohseni
		Agusta Westland	-AW101 (EH101) Merlin	Medium-size military	2		
Makila 1A1	Turbomeca	Eurocopter	AS 332 Super Puma AS 532 Cougar	Medium-size multipurpose	2	1,357kW	S. Mathyapattana[4] / Martina Mohseni
Makila 1A2	Turbomeca	Eurocopter	AS 332 Super Puma AS 532 Cougar	Medium-size utility	2	1,376kW	Martina Mohseni
CT7-8A (family of T700)	GE	Sikorsky	S-92	Medium Civil/ military	2	2,043kW	Hamid Varnaseri[1] /Martina Mohseni
PT6C Canada – 67C	Pratt&Whittney	Bell/Agusta	AB139	Medium multi-role	2	1,252kW	Nicholas Bourree[1]
D-136	Lotarev (Inchenko Progress)	Mil	Mi-26	Heavy – Transport/ military	2	7,457kW	Hamid Varnaseri
T-55	Lycoming (Honeywell)	Boeing	CH-47 Chinook	Heavy-lift tandem	2	3,267kW	Thierry Sibilli
GE T64 - 419	GE	Sikorsky	MH-47E Sea Dragon	Heavy-lift	3	3,542kW	Nicholas Bourree

Table 5. 1 – Library of helicopter engine models developed using TURBOMATCH, [1] – MSc Student, [2] – PhD Student, [3] - (Vickers, 1995), [4] - (Maythapattana, 1999)

The engine models were built using the engine information from public sources only, predominantly the manufacturers's websites. The other source of information was the Jane's Encyclopaedia (Gunston, 1996), (Jane's Helicopter Markets and Systems, 1997) and (Jane's All the World's Aircraft, 1993). The following engine specifications were extracted from those sources: types of compressor and its number of stages, engine mass flow, overall pressure ratio, power output, specific fuel consumption (SFC); in some cases also turbine entry temperature (TET) was available. For the construction of the engine model however, a number of other parameters was required, which had to be estimated, based on information from textbooks, or known data of similar engine builds. They were: compressor surge margin, rotational speed and efficiency, turbine rotational speed and efficiency, amount of cooling used throughout the engine, amount of intake pressure loss (due to the presence of inlet particle separator, for instance) and pressure loss and combustion efficiency of the burner. After gathering all the necessary information the engine model was built for the power output specified by the manufacturer (all the engines were built using the take-off power output due to the difficulty of establishing a uniform cruise power output for the helicopter). After running the engine using TURBOMATCH, the SFC was obtained and compared with the SFC specified by the manufacturer. If not matching, the estimated values of certain parameters within the engine were varied iteratively until the match was achieved.

5.3 Results of Turbomatch Engine Simulations

The representative engine models of the three main helicopter categories (light-, medium- and heavy-weight) were selected in order to demonstrate the results of performance simulations using TURBOMATCH.

5.3.1 LWH Engine

The light-weight engine category is represented by LWH (light-weight helicopter) engine, similar to Arrius 2B2, manufactured by Turbomeca. It is the engine of choice for the twin-engine Eurocopter EC-135, with the take-off power output of 472 kW.

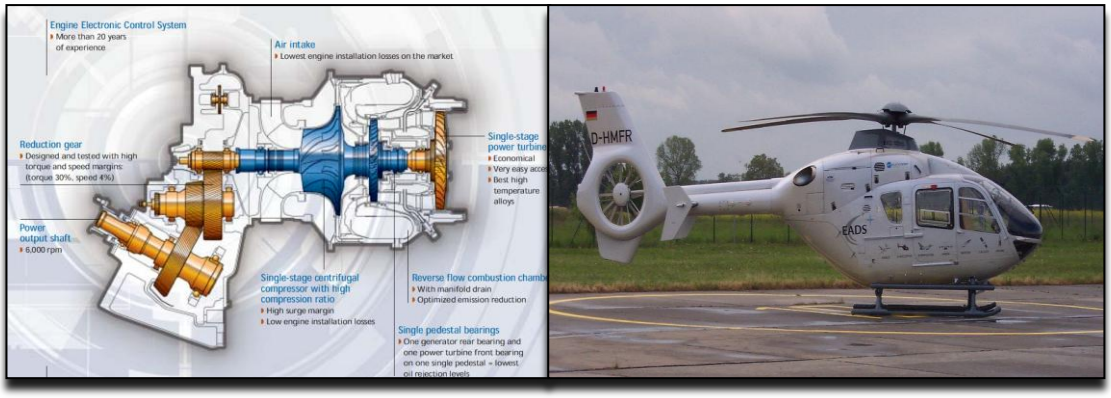

Figure 5. 3 – Arrius 2B2 engine schematic (courtesy of Turbomeca) and Eurocopter EC-135 (courtesy of Eurocopter)

The EC-135 is a lightweight, multi-mission helicopter. It incorporates Fenestron tail rotor. It is used mainly for passenger transportation, for air medical services and for law enforcement operations. (EC-135, 2010)

The engine specifications (some obtained from the manufacturer and the rest assumed) are listed in the table below:

Engine Mass Flow (kg/s)	4.5
Centrifugal Compressor Pressure Ratio (-)	8.4
Centrifugal Compressor Efficiency (-)	0.8
Combustion Efficiency (-)	0.99
Combustion Fractional Pressure Loss $(P_{in} – P_{out})/P_{in}$	0.05
Turbine Entry Temperature (K)	1000
Compressor Turbine Efficiency (-)	0.88
Power Turbine Efficiency (-)	0.85

Table 5. 2 – LWH engine parameters

The results of some of the main parameters obtained through the simulations using TURBOMATCH are listed in the table below:

Parameter	Required (Public Domain)	Achieved (Engine Model)
T-O Shaft Power (W) – 0m and 0 Mach No., ISA	472000	472000
SFC (µg/J) @ 300kW	102.8	102.6
T-O Fuel Flow Rate (kg/s)	not known	0.0506

Table 5. 3 – LWH engine TURBOMATCH simulation results

For each of the selected engine models different performance charts will be shown in order to avoid repetition. It is to be emphasised, however, that the characteristics shown for one engine apply for all of the engines but obviously with different values.

The mass flow through the engine is calculated using the following formula:

(1)

where:

is the density, is the area and is the velocity

The shaft power is calculated using:

(2)

where:

- turbine power, - compressor power, - specific heat constant, - temperature difference across the turbine, - temperature difference across the compressor

The typical variation of the shaft power with flight Mach number across the range of flight altitudes is shown in fig. 5.4.

As the Mach number increases the performance of the engine is affected in three different ways. Firstly by the reduction of the amount of momentum imparted to the fluid due to the momentum drag (the function of mass flow and intake velocity) effect and consequent reduction in the net thrust. This, however, would lead to the increase of the propulsive efficiency, because the flight velocity (air inlet velocity) increases faster than the jet gas velocity relative to the engine. Secondly, the ram ratio effect causes extra air to be taken into the engine and the inlet pressure and subsequently the density and mass flow increase. Finally, the ram temperature rise will generate an increased flow temperature at the inlet to the compressor, which would lead to the reduced thermal efficiency.

With an increase in forward speed the increased mass flow due to the ram ratio effect must be matched by the fuel flow and this results in higher fuel consumption. Although the net jet thrust decreases with increasing forward speed, the shaft power increases due to the ram ratio effect of increased mass flow and also an improvement in the SFC is seen. (The Jet Engine, 1996)

With the increase in altitude the ambient temperature decreases as does the static pressure and density. As the mass flow is the function of density, the drop of mass flow is expected with the increase in altitude. This leads to lower power output at higher altitudes. With the increasing altitude the air ambient temperature is falls and thus the density of the air and subsequently the mass of the air entering the compressor is greater. The combined effect causes the air mass flow to fall off at lower rate and thus to partially compensate for the loss of mass flow due to the drop in pressure.

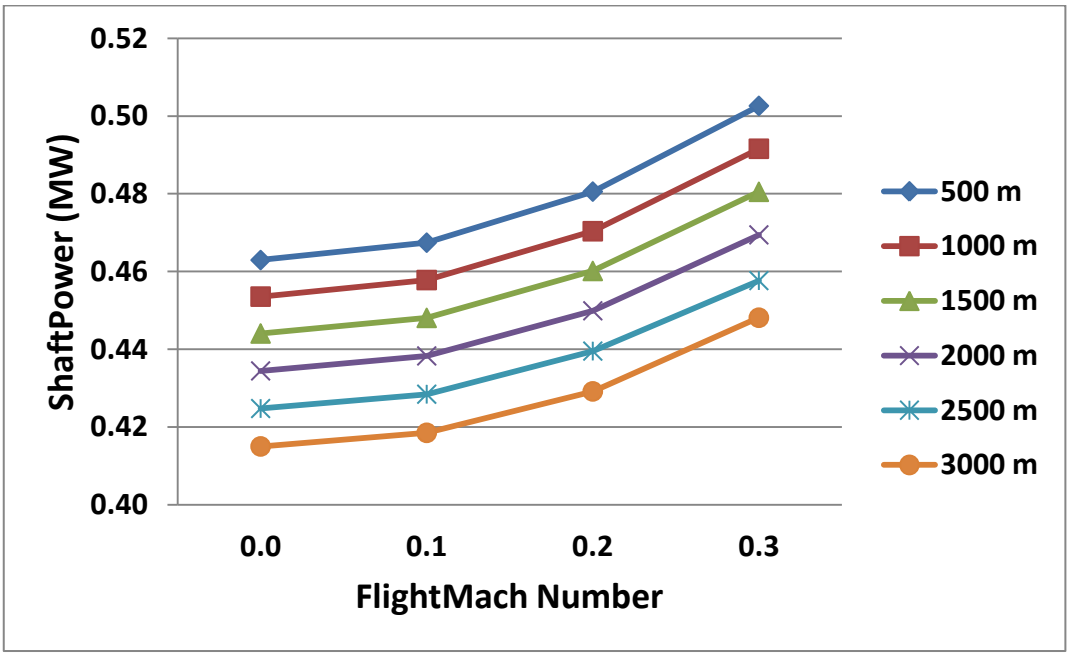

Figure 5. 4– Shaft power output vs. flight Mach number for a range of altitudes for LWH engine

The trend is reverse for the SFC. As the shaft power increases with increasing Mach number, the SFC reduces.

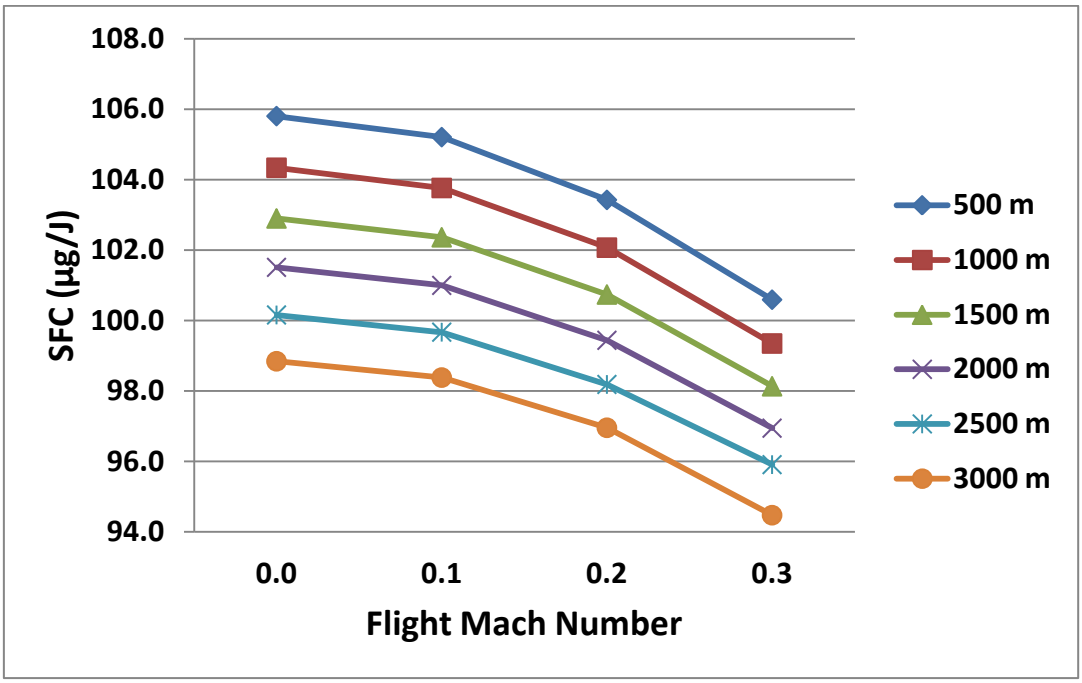

Figure 5. 5– Specific fuel consumption vs. flight Mach number for a range of altitudes for LWH engine

5.3.2 MWH engine

MWH (medium-weight helicopter) engine model is based on the LH TEC CTS800, the representative engine of the medium-weight category, manufactured jointly by Rolls-Royce and Honeywell. This engine powers the twin-engine Agusta Westland Super Lynx, with a take-off power output of 1,015 kW.

Figure 5. 6 – The LH TEC CTS800 engine (courtesy of Rolls-Royce/Honeywell) and the Agusta Westland Super Lynx helicopter (courtesy of Agusta Westland)

The Super Lynx is the latest of the Lynx helicopter family. It is a multi-role military helicopter. It is being operated in a number of roles including maritime surveillance, search and rescue, anti-surface and anti-submarine warfare. The Lynx helicopter is

also the world speed record holder. In 1986 it has achieved 400 km/h and since then it has not been overcome. (Super Lynx, 2010)

The engine specifications as obtained from the manufacturer and the assumptions made are listed below:

Engine Mass Flow (kg/s)	4.5
Centrifugal Compressor Pressure Ratio (-)	15.5
Centrifugal Compressor Efficiency (-)	0.81
Combustion Efficiency (-)	0.99
Combustion Fractional Pressure Loss $(P_{in} – P_{out})/P_{in}$	0.05
Turbine Entry Temperature (K)	1465
Compressor Turbine Efficiency (-)	0.89
Power Turbine Efficiency (-)	0.86

Table 5. 4 - MWH engine parameters

Parameter	Required (Public Domain)	Achieved (Engine Model)
T-O Shaft Power (W) – 0m and 0 Mach No., ISA	1015000	115000
SFC (µg/J) @ 300kW	78.6	78.42
T-O Fuel Flow Rate (kg/s)	not known	0.0796

Table 5. 5 – MWH engine TURBOMATCH simulation results

During the engine design process the main performance parameters are established in order for the engine to be designed and built. This in practice leads to defining fixed engine geometry. The engine is said to be designed to achieve its design-point performance. Clearly, the engine is expected to operate in a wide range of flight and atmospheric conditions (or off-design). In order to understand the behaviour of the engine at off-design conditions a computer model is built consisting of the performance characteristics of different engine components. (Pilidis, 2008)

One such characteristic is used in TURBOMATCH simulations - a compressor characteristic or *compressor map*. TURBOMATCH program includes a number of standard compressor maps. The user can select any of these maps according to the design point conditions of the compressor. If the design point of the standard map in terms of pressure ratio or mass flow does not coincide with those defined for the compressor in the user's model, the program will scale its standard map to match it to the one in the user's data file (Palmer, 1990). In the compressor map the

compressor pressure ratio is plotted against a compressor mass flow across a range of compressor rotational speeds (PCN). At each value of PCN as pressure ratio is increased (which represents a change in the geometry of the engine, such as closing the nozzle), the mass flow will decrease and up to a point where the compressor cannot produce more pressure ratio. The engine will enter a limiting condition - either stall or surge (depending on the geometry of the engine and other factors)- accompanied by the breakdown of the flow. This situation is to be avoided because it can lead to severe damage to the compression system. An increase in the temperature of blades and change in distribution of stresses through aerodynamic pulsations at high frequencies may result. The stall/surge points on the PCN lines when joined together form a so called *surge line* (it is called surge line regardless of whether surge or stall will appear). The points close to the surge line are also points where the engine is operating most efficiently, however in order to avoid this dangerous condition a certain margin (called *surge margin*) has to be set. This surge margin will then define an operating point where the engine can operate the most efficiently, but also in a safe distance from surge/stall. These operating points when joined together will form a *running line*. The surge line and the running line are shown in fig. 5.7 in the compressor notional map in TURBOMATCH.

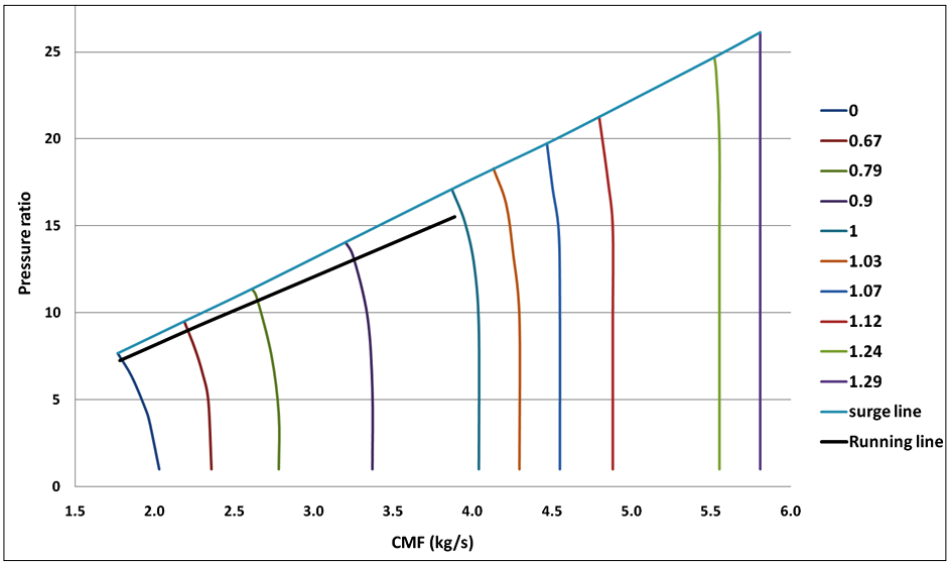

Figure 5. 7 – The compressor notional map in TURBOMATCH

The plot below shows the variation of the shaft power with thermal efficiency across the range of flight altitudes. The efficiency is a function of the shaft power (and also the heat input and component efficiencies). For the range of TETs examined, as the efficiency increases, the shaft power increases linearly. The detrimental effect of altitude is similar to the previous case.

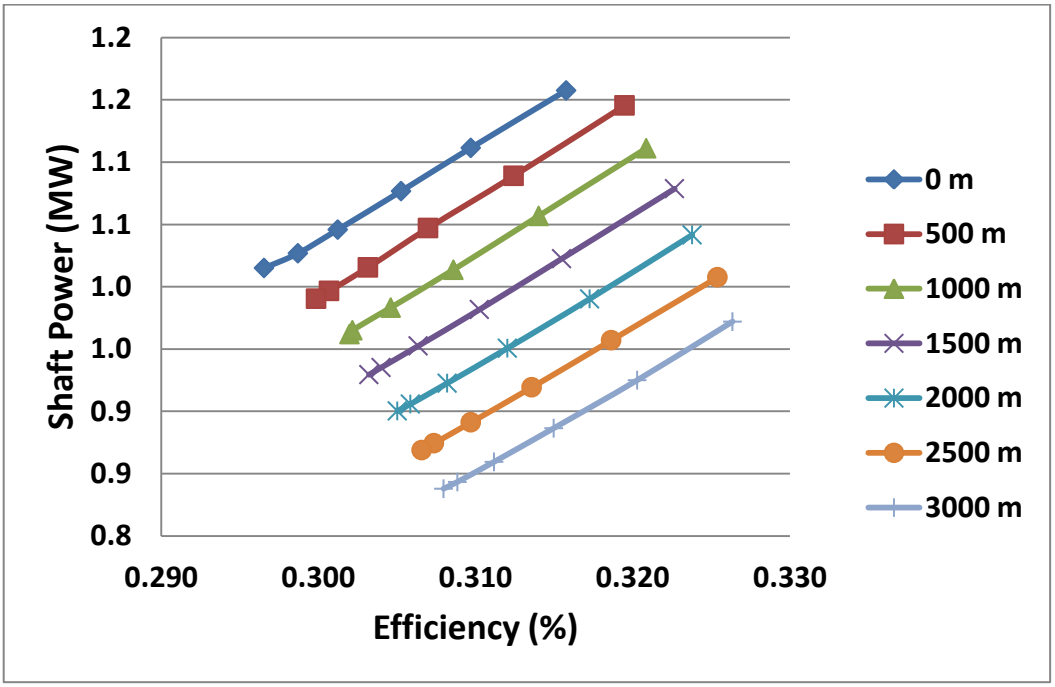

Figure 5. 8 – The variation of shaft power with efficiency for range of altitudes for the MWH engine

5.3.3 HWH engine

Finally, the heavy-weight category is represented by the HWH (heavy-weight helicopter) engine, similar to the GE T64-419 engine, manufactured by General Electric. With the take-off power output of 3,542kW it is the engine of the MH-47E Sea Dragon built by Sikorsky. The MH-47E helicopter is a three-engine utility machine primarily used for vertical on-board delivery, including the transport of cargo, personnel and supplies to shore facilities. The military version is then used mainly for mine sweeping, neutralization and mine hunting operations. (MH-47, 2010)

Figure 5. 9 – GE T64-419 engine (courtesy of GE) and the MH-47 Sea Dragon (courtesy of Sikorsky)

The engine specifications as obtained from the manufacturer and the assumptions made are listed below:

Engine Mass Flow (kg/s)	13.4
Centrifugal Compressor Pressure Ratio (-)	14
Centrifugal Compressor Efficiency (-)	0.85
Combustion Efficiency (-)	0.99
Combustion Fractional Pressure Loss $(P_{in} - P_{out})/P_{in}$	0.01
Turbine Entry Temperature (K)	1328
Compressor Turbine Efficiency (-)	0.89
Power Turbine Efficiency (-)	0.86

Table 5. 6 – HWH engine parameters

Parameter	Required (Public Domain)	Achieved (Engine Model)
T-O Shaft Power (W) – 0m and 0 Mach No., ISA	3542000	3542000
SFC (µg/J) @ 300kW	70.5	69.84
T-O Fuel Flow Rate (kg/s)	not known	0.2474

Table 5. 7 – HWH engine TURBOMATCH simulation results

The influence of increasing the TET on the shaft power output is shown in the plot below. The shaft power is the difference of the turbine work and the compressor work (or in other words the excess power available over that which is needed to drive the compressor). The ΔT in the equation (2) is increased with increasing value of TET while the rest of the parameters remain unchanged. Thus the increased shaft power results.

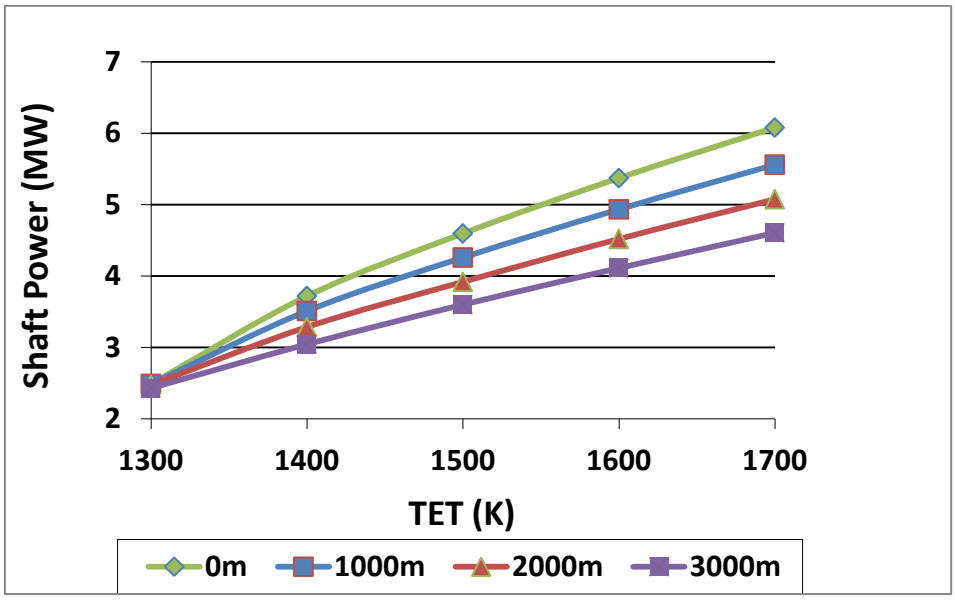

Figure 5. 10 – Variation of shaft power with TET for the range of altitudes for the HWH engine (graph developed by N.Bourree (MSc Thermal Power, 2009-2010))

The reverse is seen for the SFC due to the inverse relationship of the power and SFC as explained above.

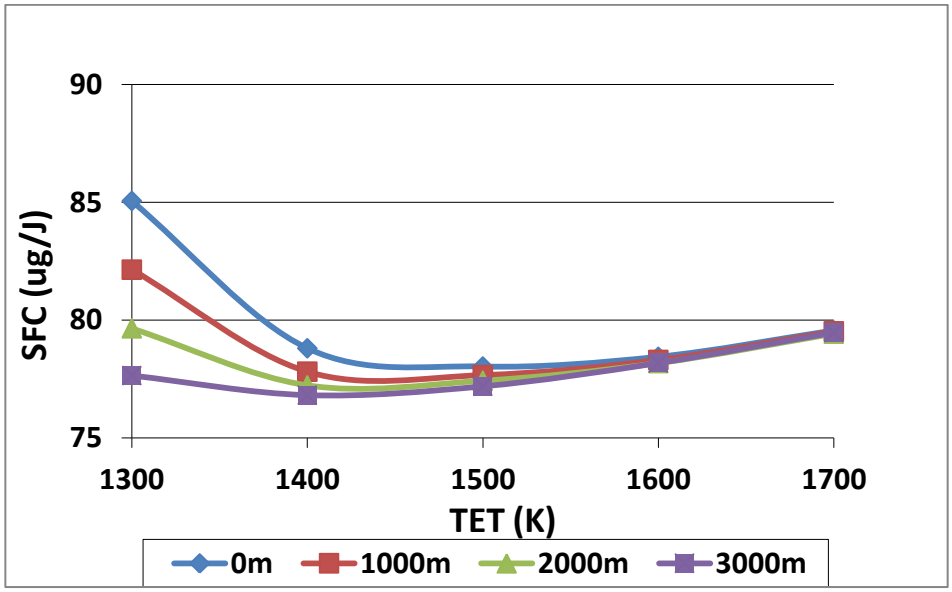

Figure 5. 11 - Variation of SFC with TET for the range of altitudes for the HWH engine, (graph developed by N.Bourree (MSc Thermal Power, 2009-2010))

The helicopter engine simulations using TURBOMATCH show good agreement with the data supplied by the manufacturers and thus give the confidence that they can be used for the purposes of the helicopter engine simulation.

Chapter 6: Results

This chapter presents the results of simulations using HELIX as part of the integrated simulation platform HECTOR. Several scenarios are presented: Firstly, the effect of a change in cruise altitude and gross take-off weight on the fuel burn and the emissions is investigated during the forward flight. In addition, a representative distribution of the helicopter engine emissions (CO_2 and NO_X) during a mission fragment (cruise conditions) is shown for a range of airspeeds and gross take-off weights. Secondly, the search and rescue mission is conducted and the effect of the choice of the search pattern on the fuel burn and emissions is examined. Finally, the executive transport mission is simulated, where the comparison between the performances of two typical helicopters used for this purpose is carried out along with the discussion on the effect of the change of the climb and descent angle and cruise forward speed on the fuel burn and emissions.

6.1 Effect of the Change in Altitude and Gross Take-Off Weight

The effect of altitude on overall helicopter performance is an important operational consideration. There are two dominant effects of increasing the altitude. The air static pressure and density decrease and hence the mass flow decreases, lowering the power available from the engine. The ambient temperature also decreases with altitude which helps to keep the turbine temperature low. Increasing the altitude increases the power required in hover and at lower airspeeds. At higher airspeeds, the lower air density results in a lower parasitic drag and consequently smaller power requirement.

The results below were generated using the simulation model of one of the commercially used helicopters during forward flight. The main helicopter characteristics and the input for the simulation are listed in the tables below:

Rotor Parameters	Main Rotor	Tail Rotor
Radius(m)	7.79	1.525
Chord(m)	0.6	0.2
Solidity	0.098	0.209
No. of blades	4	5
Shaft distance(m)	10.15 (assumption)	
Tip speed(m/s)	217	204

Table 6. 1 - Geometrical specification of the example helicopter (Prouty, 1984)

Weights (kg)		Other specifications	
Empty weight	4420	Engine output at take-off	1300 kW
MTOW	8600	Number of engines	2
Fuel capacity	1620	Max. TO rating	2712 kW
Useful load	4100	Max. usable power	2133 kW

Table 6. 2 - Weight and engine specification for the example helicopter (from manufacturer's website)

General characteristics	
Crew	2
Capacity	19
Length (m) – blades folded	69
Height (m)	4.8
Never exceed speed (km/h) at 8,600 kg GTOW	278
Maximum speed (km/h) At 8,600 kg GTOW	262
Cruise speed (km/h) at 8,600 kg GTOW	252

Table 6. 3 - General characteristics of the example helicopter (from manufacturer's website)

Engine specification	
Engine Mass Flow (kg/s)	5.5
Overall Pressure Ratio (-)	10.4
Axial Compressor Pressure Ratio (-)	3.4
Centrifugal Pressure Ratio (-)	3.05
Axial Compressor Efficiency (-)	0.79
Centrifugal Compressor Efficiency (-)	0.79
Compressor Turbine Cooling Flow (%)	12.5
Combustion Efficiency (-)	0.99
Combustion Fractional Pressure Loss $(P_{in} - P_{out})/P_{in}$	0.05
Turbine Entry Temperature (K)	1453
Compressor Turbine Efficiency (-)	0.88
Power Turbine Efficiency (-)	0.86

Table 6. 4 – The engine characteristics (Jane's Helicopter Markets and Systems, 1997)

The simulations were carried out for the range of forward speeds and cruise altitudes. As can be seen from the graph the helicopter power requirements initially drop with increasing forward speed reaching a minimum. Then they start increasing again as the rotor disk is progressively tilted forward to meet greater propulsion requirements causing the induced and propulsive part of the power to increase. The rotor is required to do more work in order to overcome rotor profile and airframe parasitic losses. In high forward flight speeds the power required increases significantly due to the parasitic losses, which are proportional to μ^3 (see section 4.2, equation 20). With the increase in altitude and consequent fall in air density, however, the parasitic drag reduces. Therefore, as the altitude is increased, after reaching a certain forward speed, the power requirements will be lower than at sea level altitude.

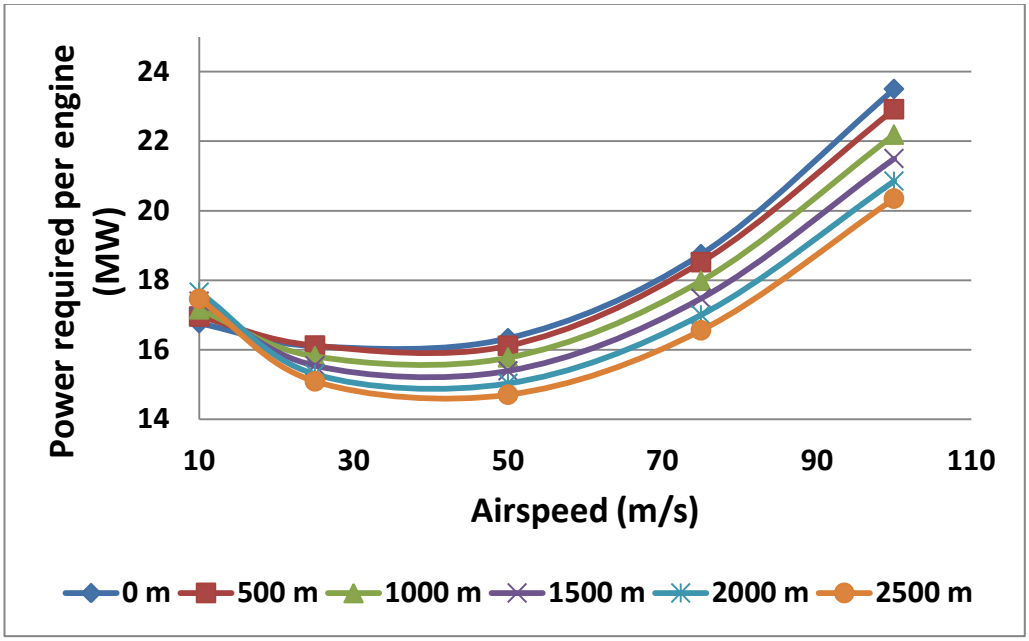

Figure 6. 1 – The effect of cruise altitude on the power required for the range of forward velocities

For comparison, the prediction of the main rotor power required in forward flight at different altitudes as adapted from (Leishmann, 2006) is shown.

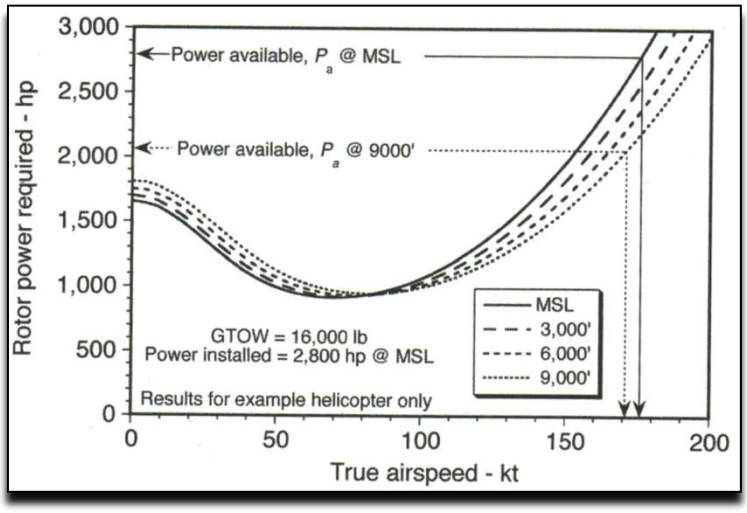

Figure 6. 2 – Predictions of main rotor power in forward flight at different altitudes, adapted from (Leishmann, 2006)

The engine specific fuel consumption (SFC) curve is almost flat over the range of power settings where the helicopter engines operate in practice (as seen in the plot below), therefore the fuel flow is proportional to the power required at a given altitude and temperature. (Leishmann, 2006)

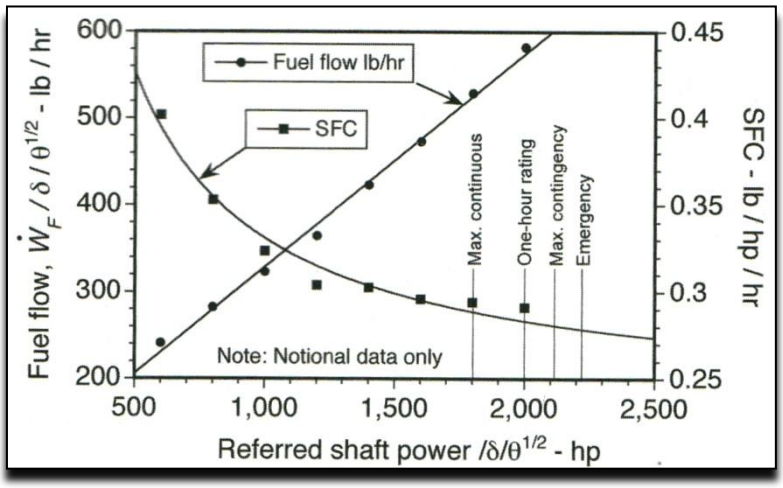

Figure 6. 3 – Normalized SFC and fuel flow for a notional turboshaft engine, adapted from (Leishmann, 2006)

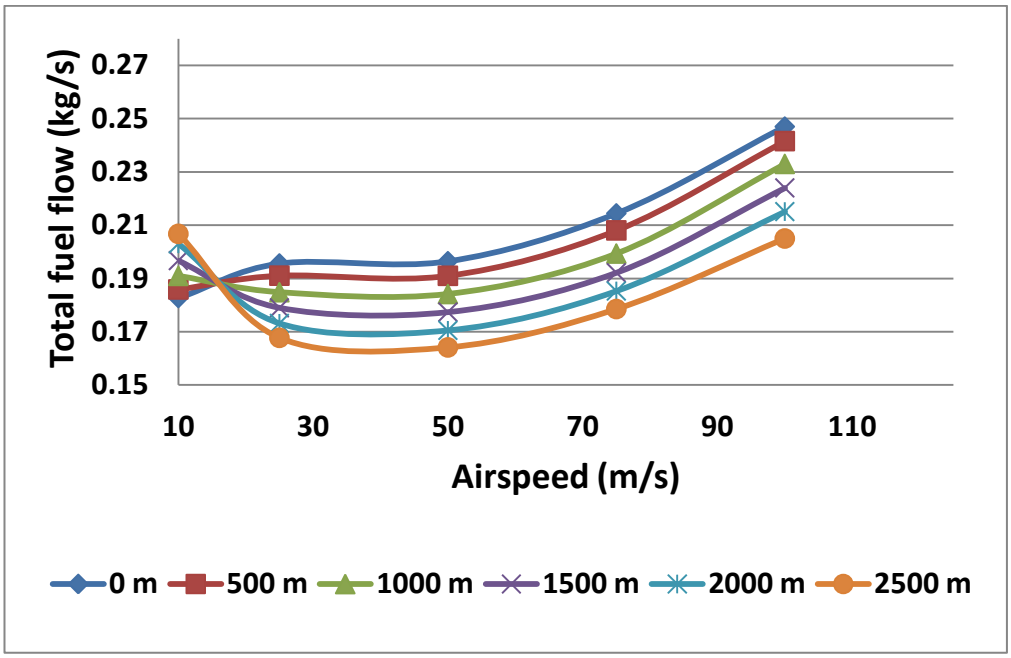

Figure 6. 4 – The effect of cruise altitude on the engine fuel flow for the range of forward velocities

From this curve it is possible to determine the speed for maximum range and the speed for maximum endurance. The range of the helicopter is a function of the velocity and time. Therefore, the speed to fly for the best range is obtained when the ratio of velocity/power is a maximum, or when the power/velocity ratio is a minimum. This speed is graphically obtained from a line drawn through the origin and tangent to the power (or fuel flow) versus speed curve at SLS conditions as can be seen in the graph below. It can be observed that this airspeed is at a higher value than that required for maximum endurance.

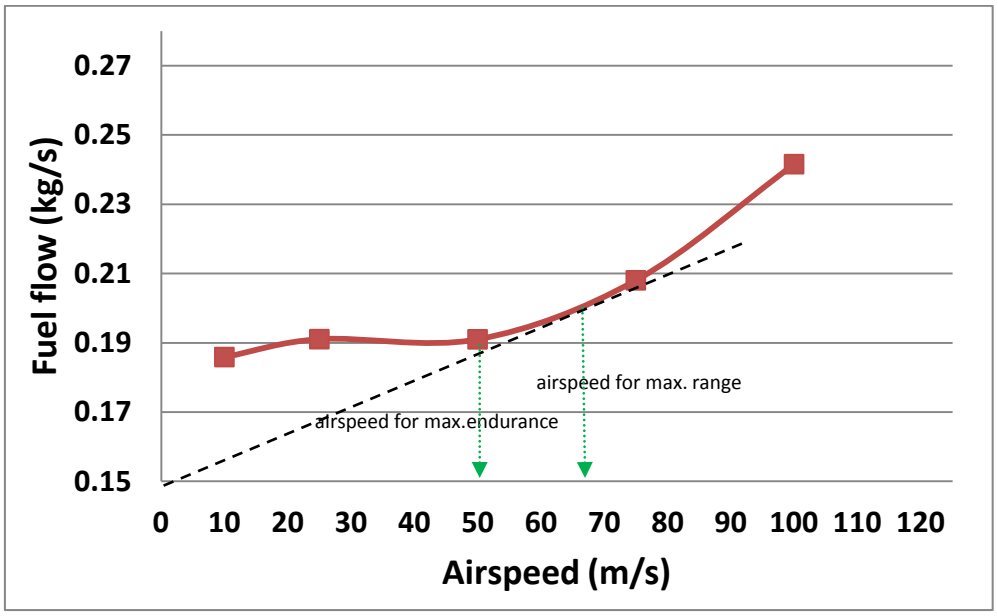

Figure 6. 5 – Fuel flow versus airspeed for the example helicopter at SLS conditions

The power required in forward flight is a function of gross take-off weight (GTOW). With increasing GTOW the power required increases, especially at low airspeeds where the induced power requirement forms a greater fraction of the total power and then again at high airspeeds due to the dominant effect of parasitic power. Below are the results of the simulations showing the effect of GTOW on the power required and fuel flow over the range of forward speeds.

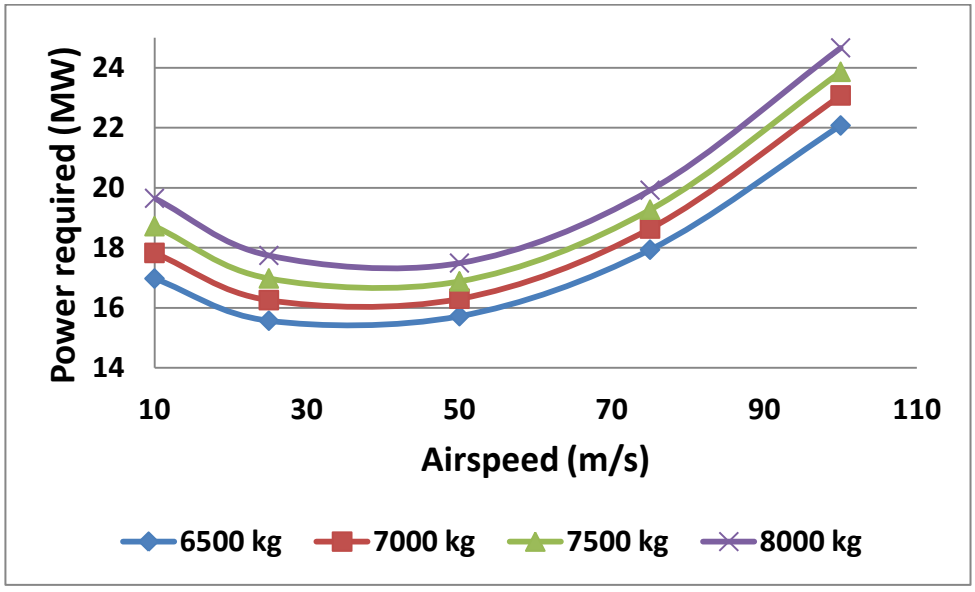

Figure 6. 6 – The effect of GTOW variation on the power required for the example helicopter

For comparison, the prediction of the main rotor power required in forward flight at different GTOWs as adapted from (Leishmann, 2006) is shown.

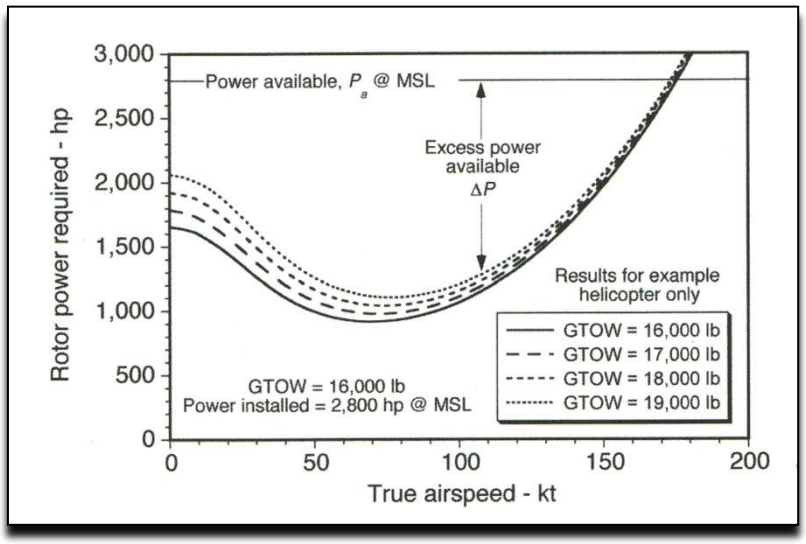

Figure 6. 7 – Predictions of main rotor power in forward flight at different GTOWs, adapted from (Leishmann, 2006)

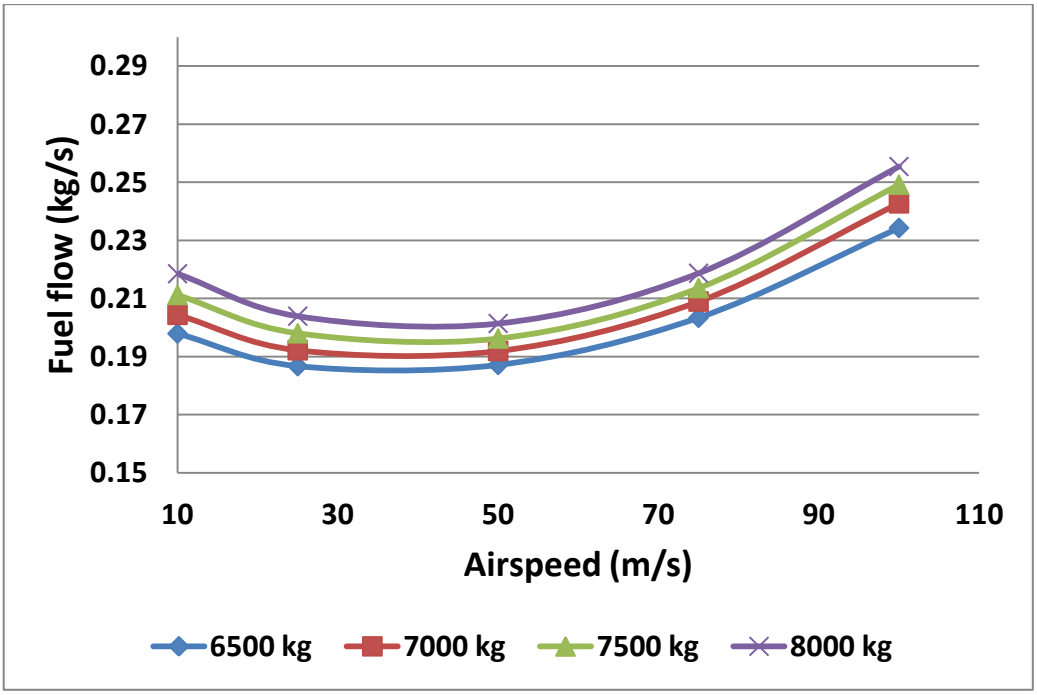

Figure 6. 8 - The effect of GTOW variation on the fuel flow for the example helicopter

It is also possible to obtain the distribution of emissions over the mission trajectory or its part.

As emphasised in Chapter 2, aero engine emissions are the main concern due to their effect in airport environments and also at altitude. The ones affecting the airport environments the most are the CO and unburnt hydrocarbons, during take-off and climb out at high power the nitrogen oxides contribute significantly, carbon dioxide (CO_2) and water vapour have an effect throughout the whole flight envelope. (Goodger, 2008)The quantities of CO_2 emitted from the engines are proportional to the amount of fuel used. NOx emissions from engines reach their maximum value during take-off and climb out, but also at high altitudes the long range aircraft are the main if not the only ones responsible for the emission of this type of pollutant. (Celis, 2010)

The graph below shows the NO_X and CO_2 emissions for a mission segment (cruise). The mission segment in this case was flown at the altitude of 500 m, varying the airspeed and the simulations were performed across the range of GTOWs.

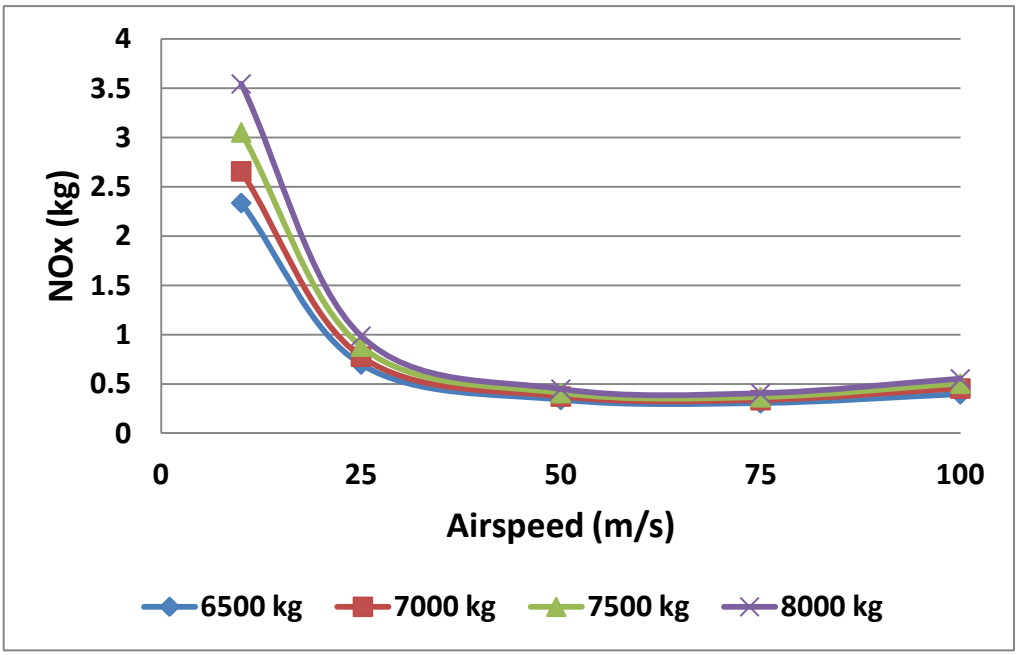

Figure 6. 9 – NO_x variation with airspeed over the range of GTOW for the example helicopter

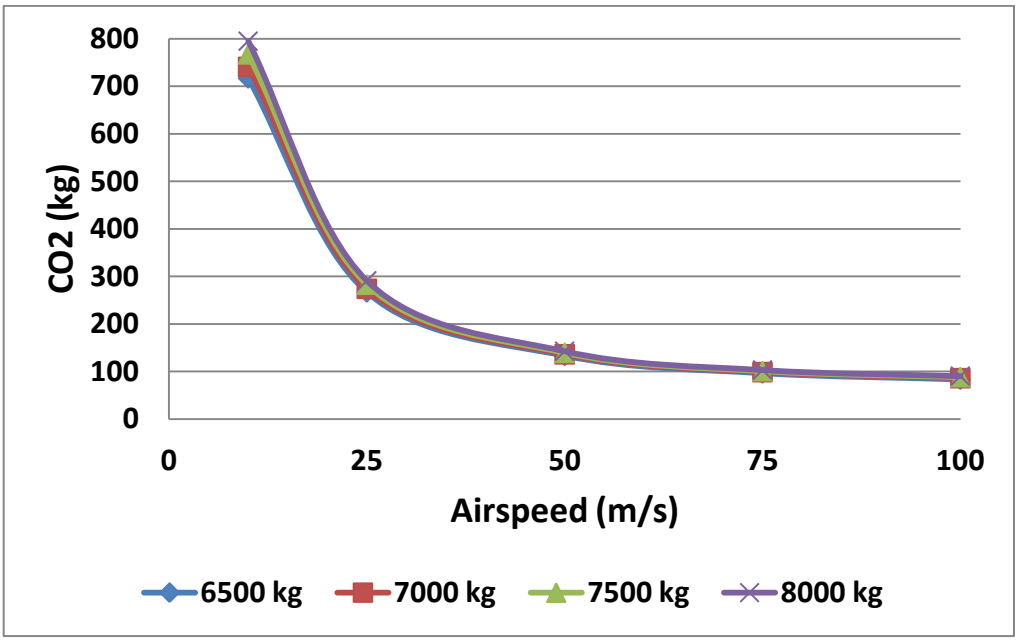

Figure 6. 10 – CO_2 variation with airspeed over the range of GTOW for the example helicopter

6.2 Effect of the Choice of Search Pattern during the Search and Rescue Operation

The next evaluation study represents a hypothetical search and rescue (SAR) operation. The helicopter is irreplaceable in this type of mission due to its versatility, ability to fly at very low altitudes, hover and take-off and land from almost any type of terrain. While the fixed-wing aircraft has also been successfully used during SAR operations, it can only identify the target and possibly drop survival kit but its ability to actually rescue the survivors depends on the terrain and the possibility of landing and take-off in the vicinity of the survivors.

Despite being typically an emergency type of mission, the SAR operation needs careful planning in advance. Before the commencement of the SAR mission the approximate location of the target/survivor and the extent of a search area need to be determined. The success of the SAR operation depends on many factors, such as the weather conditions, the size of the target, visibility conditions, time available for search, search altitude, etc. The search area coverage is determined by the number of helicopters available, the width of the area (or sweep width) depends on the

search visibility. The search area is explored in search tracks which are spaced from each other in a way that ensures adequate coverage of the whole area. The picture below explains the search area terminology.

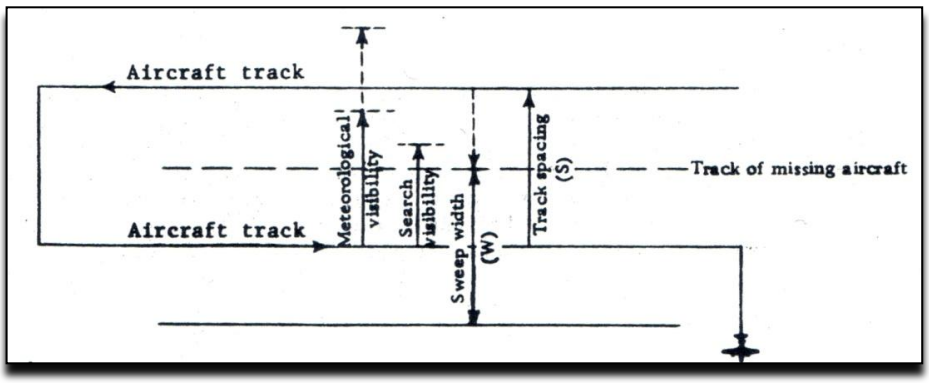

Figure 6. 11 - The search area terminology during the SAR mission, adapted from (ICAO, 1970)

The search area is scanned following a certain search pattern. The choice of the search pattern is again a function of a number of factors, such as the time of the day, the terrain of the search area, the time available, the possession of any radio equipment by the survivor, etc. Detailed information about the SAR operations can be obtain from (ICAO, 1970)

Two choices of the search pattern are considered. It is assumed that the position of the target is approximately known (within a certain radius). At first the parallel track search is assumed. This type of search is applied when the search area is large and fairly level, when a uniform coverage is desired and when only the approximate location of the target is known.

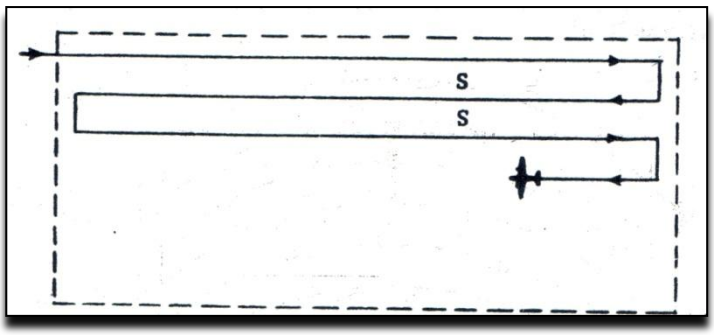

Figure 6. 12 – Parallel track search pattern using one aircraft, adapted from (ICAO, 1970)

The parallel track search and rescue trajectory is depicted below:

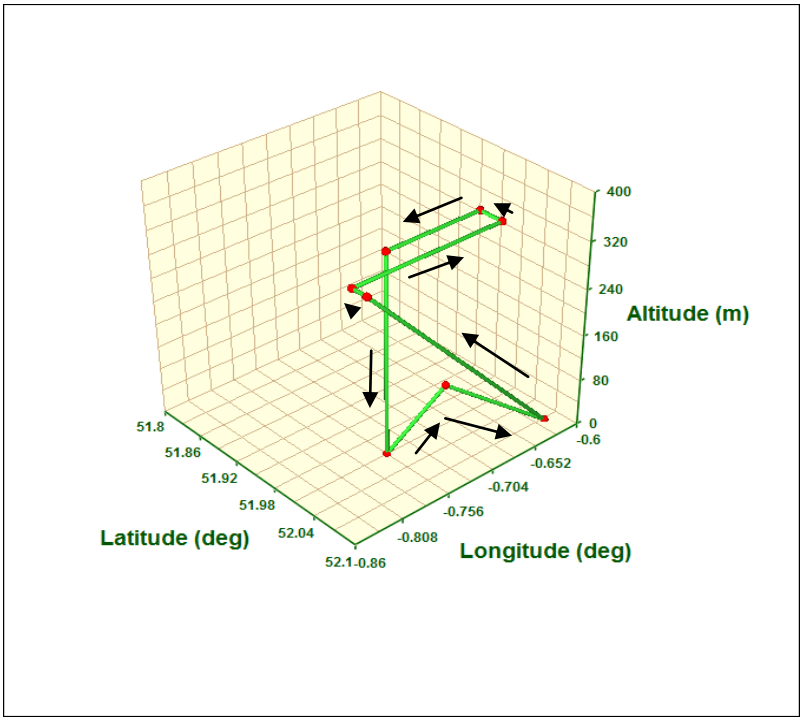

Figure 6. 13 - Hypothetical search and rescue mission trajectory – parallel track

The second search pattern of choice is the creeping line search. This search can be used in similar type of situation as the parallel track search. The search area remains unchanged. Depending on the position of the target the choice of the search pattern will dominate the fuel burn and the amount of emissions.

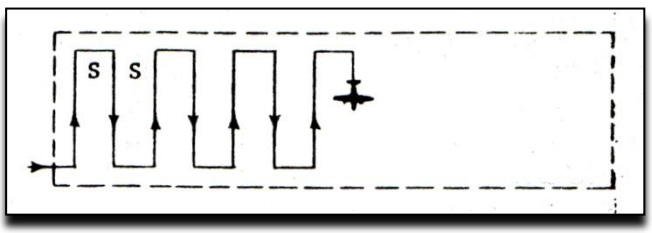

Figure 6. 14 – Creeping line search pattern using one aircraft, adapted from (ICAO, 1970)

The hypothetical creeping line search trajectory is depicted below.

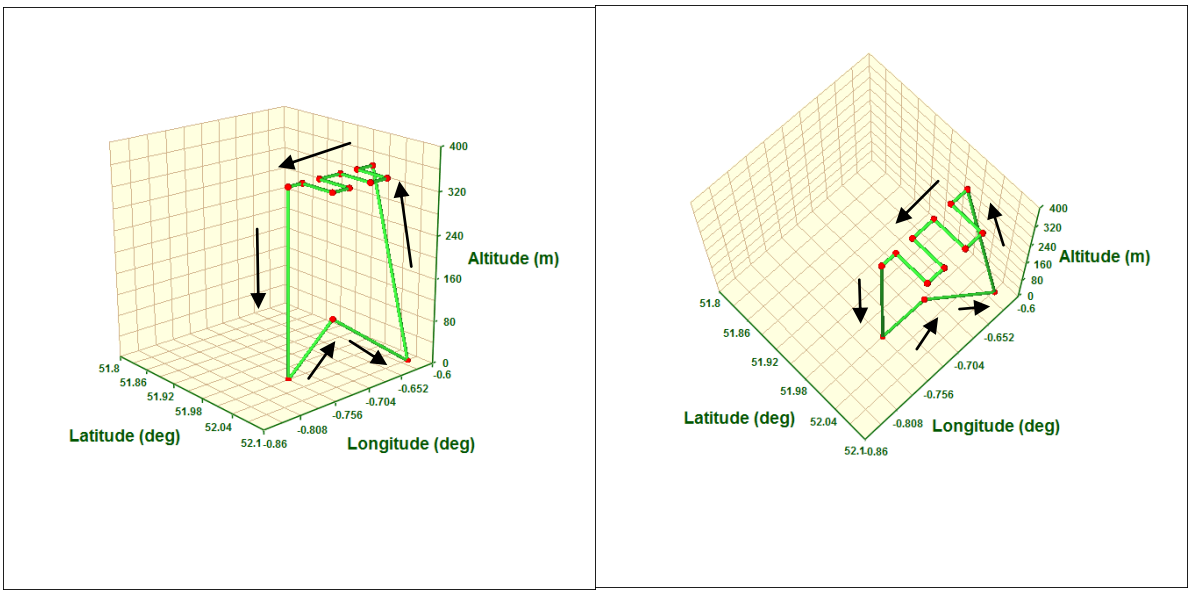

Figure 6. 15 - Hypothetical search and rescue mission trajectory– creeping line search, side and top view

The simulation input information for the SAR mission specified by the user consists of the following:

- *Mission leg number*: The mission is truncated into number of parts (typically called segments, but also mission legs; here for clarity the term *mission legs* will be used).
- *Segment/ Profile*: For each of the mission legs the user specifies whether it is a segment or a profile. *Segment* signifies that part of the mission which is kept fixed, i.e. is not subjected to optimization. *Profile*, is the part of the mission which is to be optimized. During a single experiment only the nominal values of each variable are used (see below), the rest is ignored.
- *Flight Condition*: For each segment the user specifies the flight condition. For the profile part the flight condition is being determined by the programme from comparing the initial and final altitudes and forward velocities.
- *Latitude, Longitude and Altitude*: The coordinates of the initial and final point of each mission leg, along with the initial and final altitudes need to be specified (in fact, the start coordinates and start altitude needs to be specified and then for every mission leg only the final altitude and final coordinates as

they are identical to the initial coordinates and initial altitude of the following mission leg).

- *Forward velocity*: three values of forward velocity can be specified: low-high and nominal values; low and high values representing the boundary values during optimization. Clearly, in case of a segment, only the nominal values are specified.

The same helicopter was used for the purposes of this simulation as in the previous scenario.

The helicopter takes off and climbs up to the search altitude, until it reaches the probability area. The search altitude is typically 300-600m during the day and 600-900m at night (ICAO, 1970). The helicopter then follows the prescribed search pattern. After identifying the target the helicopter descends, recovers the survivor, climbs out to a cruise flight altitude and descends back to the base.

The creeping line search pattern resulted in longer total range and hence larger amount of fuel burn and emissions.

The effect of the forward velocity on the fuel burn and emissions for both search patterns was also investigated and the results are presented in the graphs below.

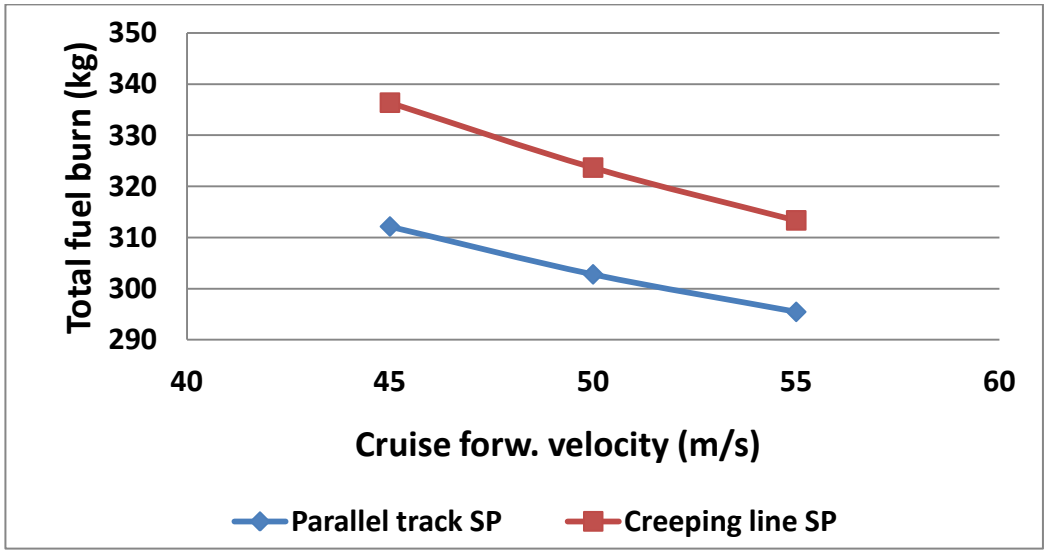

Figure 6. 16 – Comparison of the total fuel burn during the SAR mission between the parallel and creeping line search patterns for the range of helicopter forward velocities

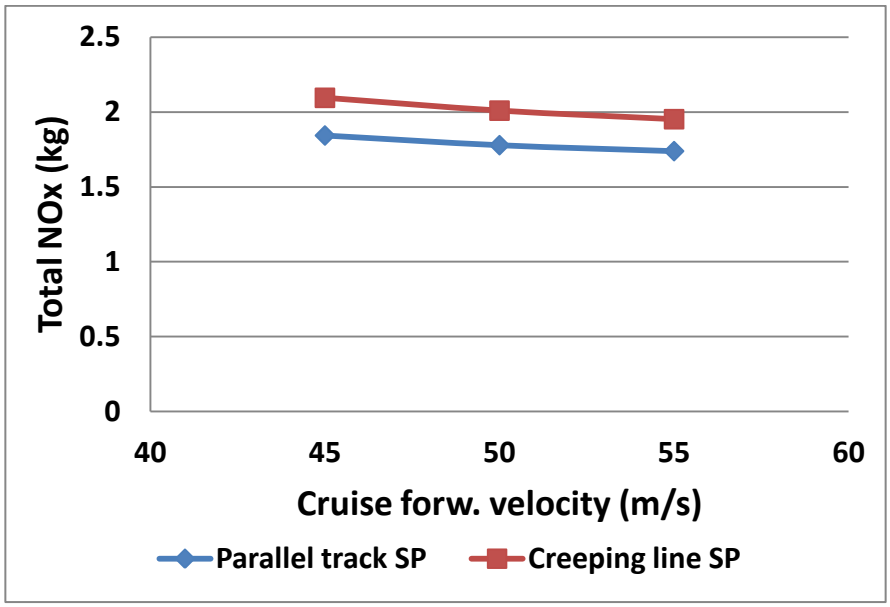

Figure 6. 17 - Comparison of the total NO_X emissions during the SAR mission between the parallel and creeping line search patterns for the range of helicopter forward velocities

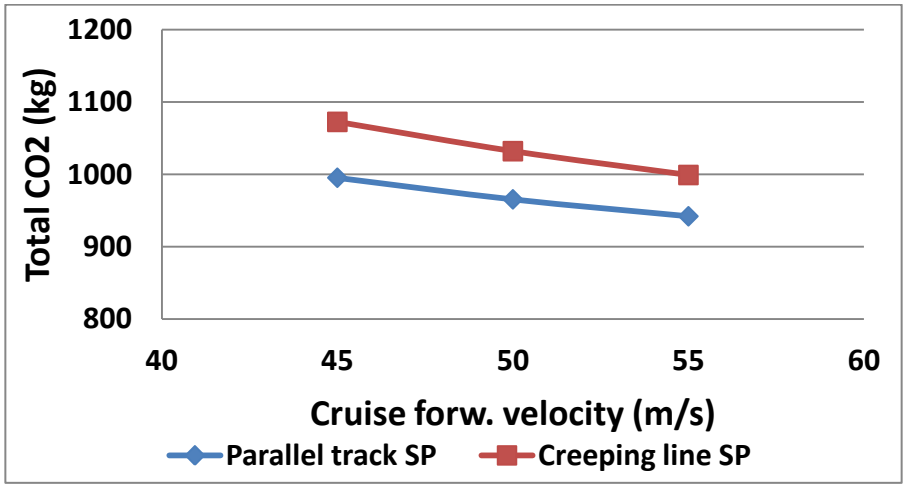

Figure 6. 18 - Comparison of the total CO_2 emissions during the SAR mission between the parallel and creeping line search patterns for the range of helicopter forward velocities

6.3 Executive Transport Mission

6.3.1 Fuel Burn and Emissions Comparison

The final simulation scenario involves a comparison between two helicopters typically used for the purposes of business and executive transport. Both helicopters are included in the medium-weight helicopter category, their size, weight and passenger transport capacity varies, however. For both helicopters the same number of the

crew members was assumed. The main helicopter specifications are listed in the table below:

	Helicopter A	Helicopter B
Engine output at take-off (kW)	626	1,252
MTOW (kg)	4,300	6,400
Max.forw.speed (km/h)	306	310
Max.number of seats	9	15

Table 6. 5 – Executive transport helicopter specifications

The fuel burn and the amount of emissions during the given mission were subsequently compared, along with the fuel cost per passenger seat. Such a comparison may be beneficial for the customer wishing to buy a helicopter specifically for the purpose of executive business transport and evaluating the options in terms of the cost of fuel per passenger.

During the simulations, the mission profiles of both helicopters were kept the same, the resulting fuel burn and emissions were compared. From the results listed below it can be observed that the helicopter B despite having higher fuel consumption during the flown mission, because it can carry larger number of passengers, the actual fuel burn per passenger is lower than helicopter A.

Should the largest possible number of passengers transported be the objective of the flown mission, the obvious choice would be the helicopter B. If the number of passengers is small, the more economic choice would be the helicopter A.

	Helicopter A	Helicopter B
Total horizontal range (m)	341117	341117
Total fuel burn (kg)	1149.2	1335.5
Total operational time (sec)	7034	7034
Total NOx emissions (kg)	2.22	4.06
Total CO emissions (kg)	0.038	0.007
Total CO2 emissions (kg)	3662	4280
Total H2O emissions (kg)	1426	1658
Fuel burn per passenger seat (kg)	127.7	89.0

Table 6. 6 – The results of the executive transport mission simulations

6.3.2 Effect of Forward Velocity

The next step was to examine the performance of the two helicopters in terms of the increase of cruise forward velocity. The plot of total fuel burn against the increase in cruise forward velocity shows decrease in fuel burn with rising forward speed. It needs to be considered, however, that with the increasing forward velocity the mission flight time decreases, the mission range is kept constant. As the fuel burn is a function of the fuel flow and time, despite the slight increase in the fuel flow, because the time is dropping faster, the actual total mission fuel burn decreases.

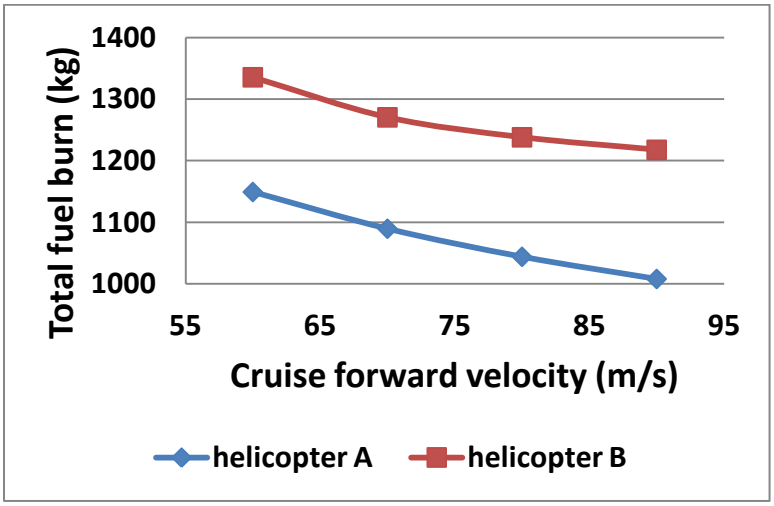

Figure 6. 19– Effect of change in cruise forward velocity on the total fuel burn

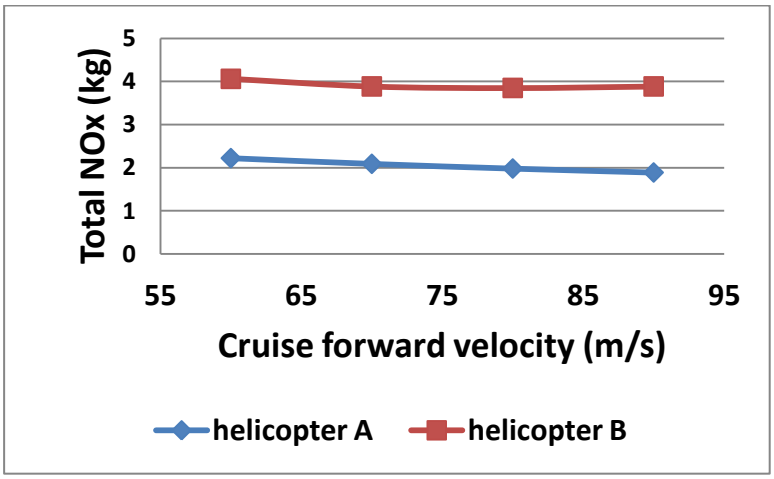

Figure 6. 20 - Effect of change in cruise forward velocity on the total NO_X emissions

Again, the cost of fuel burn per passenger seat is shown for both helicopters with the increase in forward cruise speed.

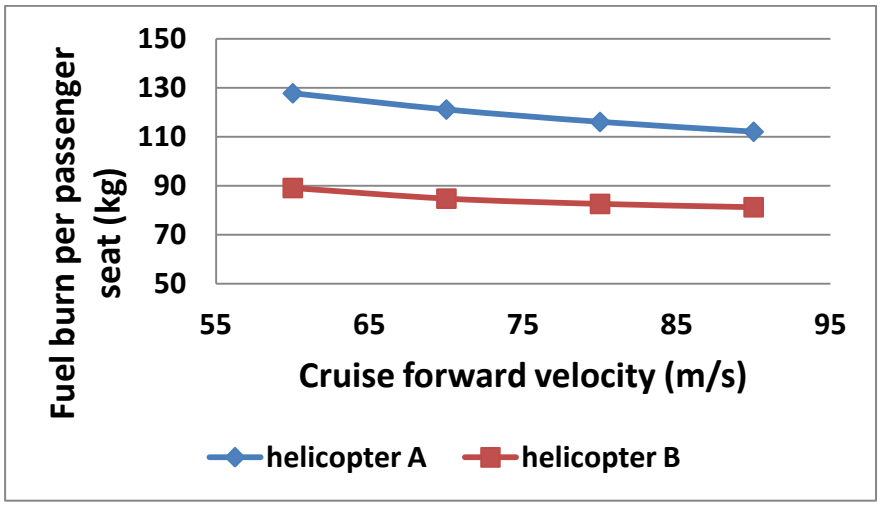

Figure 6. 21 - Effect of change in cruise forward velocity on the fuel burn per passenger seat

6.3.3 Climb and Descent Angle Variation

The next step to be examined is effect of changing the climb and descent angle during the flown mission. Three simulations were carried out: the change in the climb angle, the change in descent angle and the change of both climb and descent angle were investigated. The respective flight trajectories are visualised below:

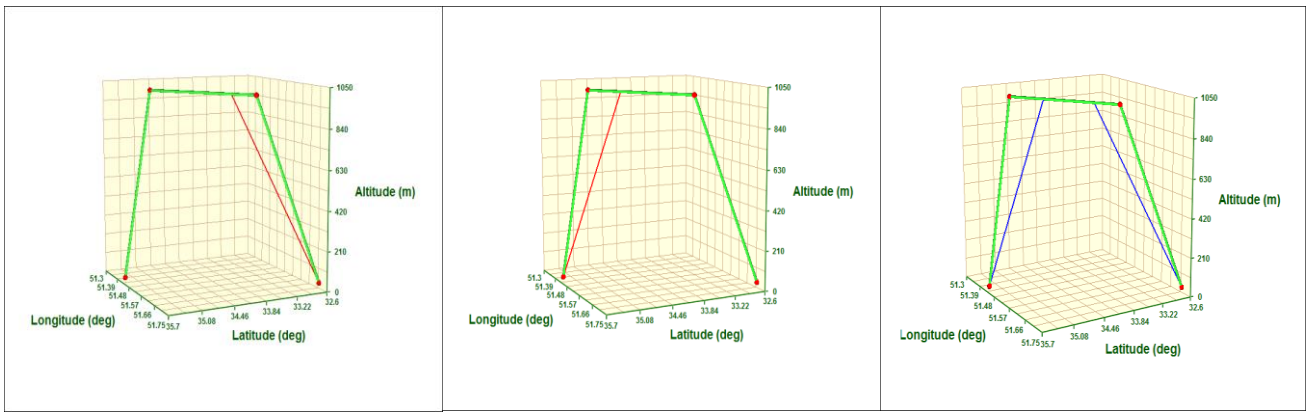

Figure 6. 22 – Trajectories - effect of change in climb angle, descent angle and both climb and descent angle

The change in flight angle will affect the range and time of the mission and consequently the fuel flow, total fuel burn and emissions. The four different simulation scenarios are listed below in terms of their range, time and fuel flow.

Case study	Mission type	Range (km)	Time (hr)	fuel burn helicopter A (kg)	fuel burn helicopter B (kg)
1	baseline	341.117	1.95	1149	1335
2	climb angle variation	341.014	1.90	1119	1306
3	descent angle variation	340.388	1.93	1136	1327
4	climb and descent angle variation	340.274	1.98	1166	1363

Table 6. 7 – Range, time and fuel flow for both helicopters during the simulation scenarios

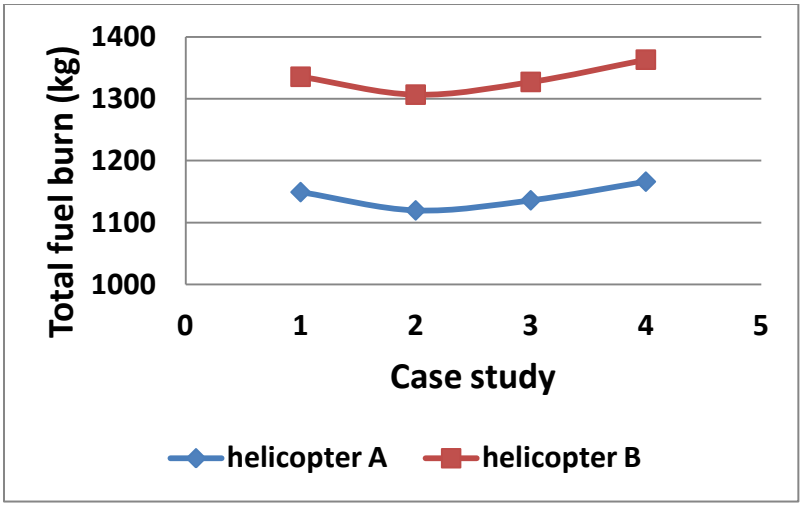

Figure 6. 23 – The effect of the climb and descent angle variation on total fuel burn during the mission

The change in climb and descent angles alters the range and time of the respective missions and that is reflected in the total fuel burn and emissions (the variation in the total amount of NO_X emissions is shown in fig. 6.24 as an example). As can be observed from the graphs below as in the previous simulation scenario, although the total fuel burn was higher for helicopter B in all four cases, the actual total fuel burn per passenger seat was lower than helicopter A.

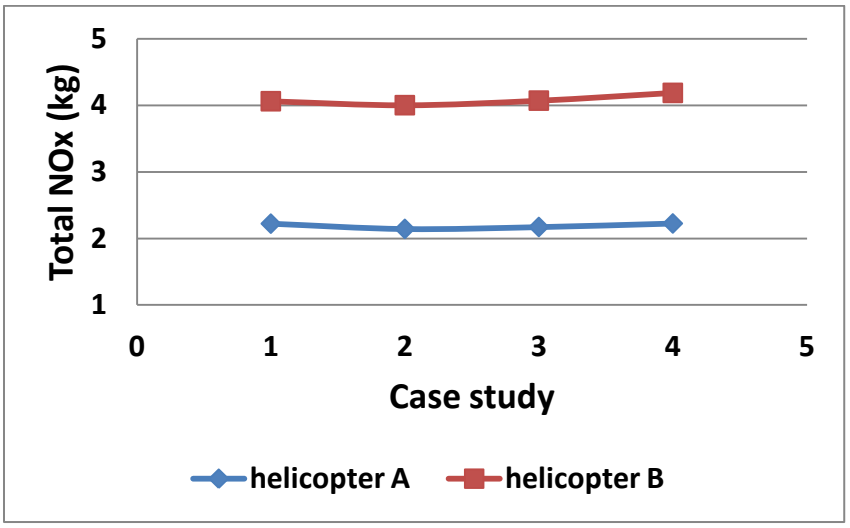

Figure 6. 24 - The effect of the climb and descent angle variation on total NO_X emissions during the mission

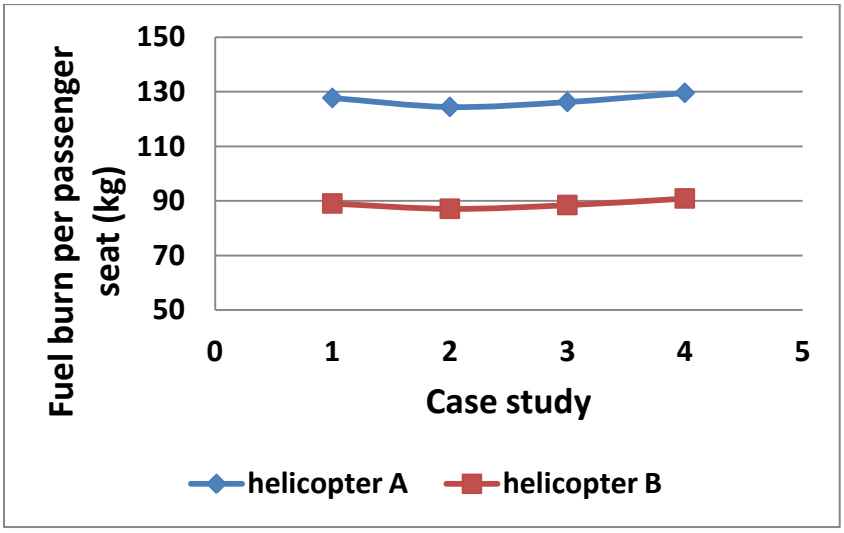

Figure 6. 25 - The effect of the climb and descent angle variation on total fuel burn per passenger seat during the mission

6.3.4 Range Variation

Finally, the effect of variation in length (and time spent) in the cruise on the total fuel burn and emissions was examined. The expected consequence of shortening the length of the cruise was shortening the time spent in this flight condition and lowering the total fuel burn and emissions. Helicopter B still represents the more economic option.

The respective trajectories are depicted below. Case study 1 represents the baseline trajectory (in green colour), case study 2 is the shorter cruise- and case study 3 the longer cruise- trajectory.

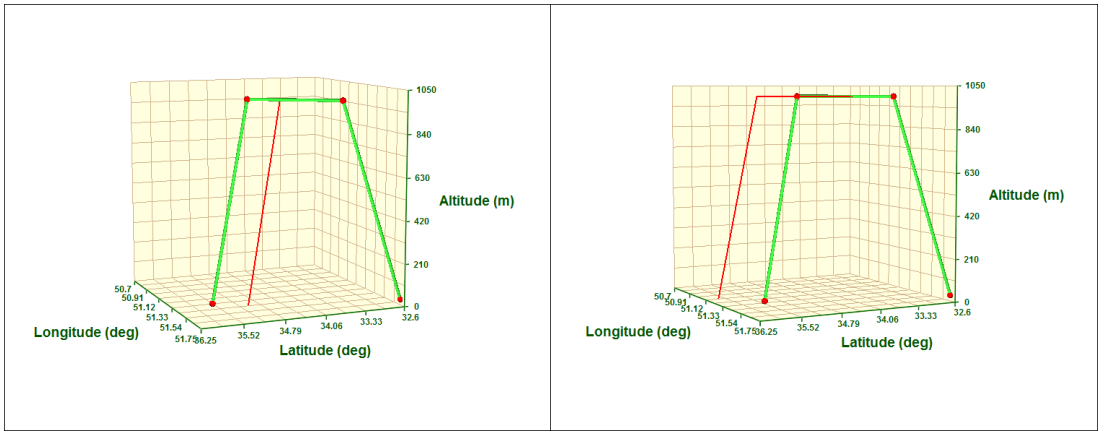

Figure 6. 26 – Short and long cruise trajectories

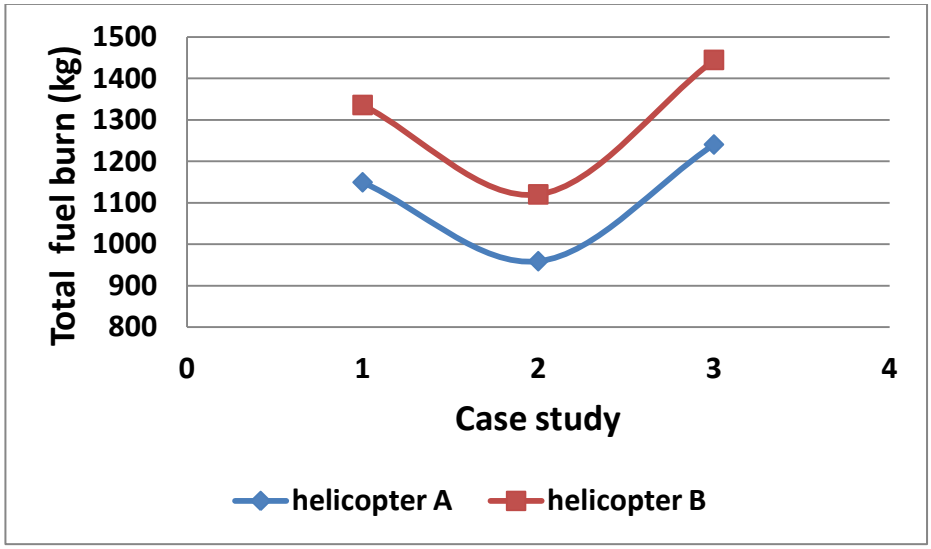

Figure 6. 27 – The effect of cruise length variation on total fuel burn during the mission

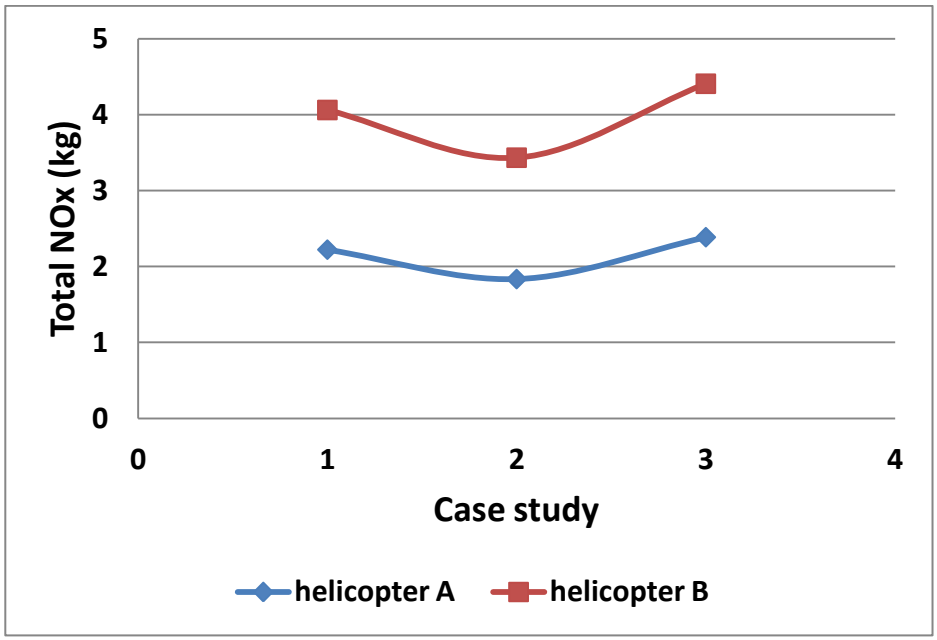

Figure 6. 28 - The effect of cruise length variation on total NO_X during the mission

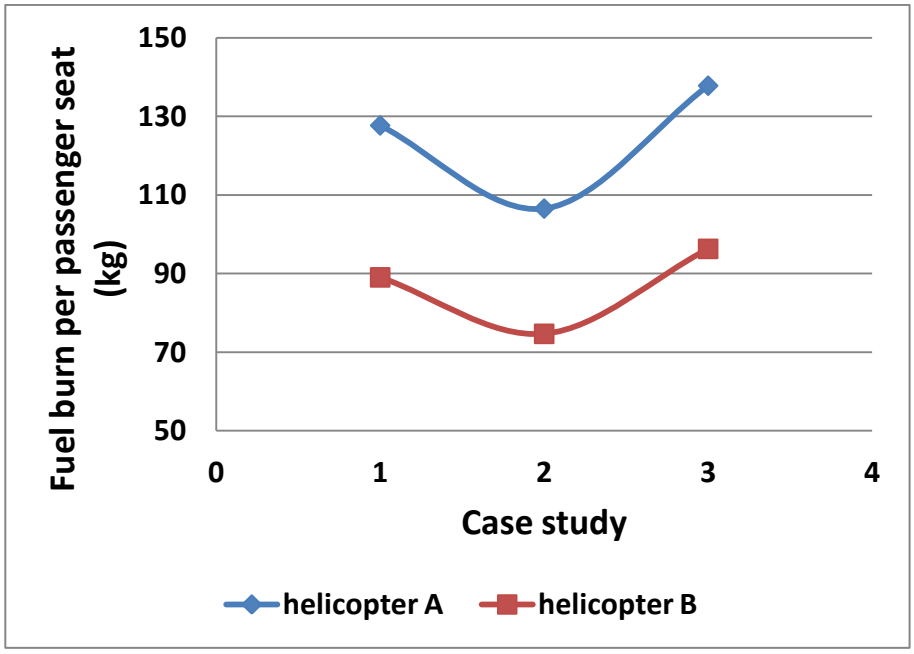

Figure 6. 29 - The effect of cruise length variation on total fuel burn per passenger seat during the mission

Chapter 7: Conclusions and Further Work

The conclusions of the presented research and recommendation for further work are offered in this chapter. The summary of HELIX development, its capabilities and results are presented. The limitations of HELIX capabilities are recognized and suggestions for their enhancement are offered in detailed steps.

7.1 Conclusions

The main objective of this research project was to develop a computational model capable of assessing helicopter thermodynamic performance at any given point during the flight path. This tool was then expected to be included into a larger optimization platform in order to ensure availability for potential evaluation and optimization studies for various helicopter missions. The need for such a tool stems from considering this approach to be one of the mitigation strategies of an increasing problem of deteriorating air quality and the rise of greenhouse emissions resulting from the continuing growth of air traffic.

A number of strategies to solve the problem of unsustainable growth of gaseous emissions have emerged in the past few decades. Some involve the design of new, more environmentally friendly aircraft, including employment of new materials, some focus on the change in aircraft operational procedures and regulations, but perhaps the least costly solution corresponds to the optimization of the helicopter flight paths using existing types of aircraft. It has been recognized that the helicopter, despite playing an irreplaceable role in certain operations where the environmental concerns are not priority (medical or police services, etc.), still represents an object of those studies as it is also being employed for non-urgent operations, such as executive business travel, transportation of personnel to and from oil rigs, surveillance, etc.

The main contributions of this research are summarized below:

- Development of a tool (HELIX) with the capabilities to simulate the performance of the most common helicopter configuration. The tool

computes basic performance parameters along the user-specified helicopter flight path. The performance prediction program is generic, i.e. it possesses the capability to assess current helicopter designs as well as novel concepts. Design of this tool was carried out in mind with the potential of integration with the optimizer and also with the TERA environment. It has been recognized that although the helicopter companies typically make use of their own helicopter performance tools or the commercial ones, these are generally not available in public domain.

- Further enhancement of HELIX's capabilities was carried out to enable a more realistic (three-dimensional) definition of a helicopter mission trajectory. In other words, the position of the helicopter at any given time is expressed by using the recognized geodetic system – WGS84.
- Evaluation and analysis of the results of the developed helicopter performance model and performing mission profile analyses.
- Development of a library of thermodynamic helicopter engine models that are used for the purpose of helicopter performance simulation studies: active role (development of four engine models) and passive role (advisory approach over several MSc projects).

At the start of this research project an initial literature review was carried out. This literature review was oriented towards familiarization with the works relating to the environmental issues of aviation, specifically the ones focused on the topic of the helicopter mission analysis and emission reduction. A number of approaches was identified that aim to solve this problem, including the technology developments, such as optimization of the design of rotor blades or air intakes to reduce the external noise generated by the helicopter or improvements to the helicopter airframe for the reduction of aerodynamic drag. These approaches, however, do not represent immediate solutions. More readily applicable solutions are seen in the development of environmentally friendly flight paths, i.e. in optimization of take-off and landing procedures (especially in densely populated areas) or optimizations of mission profiles for lower fuel burn and gaseous emissions.

The second part of the literature review was focused on the helicopter theory in general and particularly on the helicopter performance modelling. Studies in this area were reviewed and a number of commonly used methodologies was examined. Subsequently, for the purposes of the development of the computational model the momentum theory was chosen, considered to offer sufficient accuracy while keeping the computational time to minimum.

The process of evaluation of the helicopter performance included the use of an engine performance simulation tool (TURBOMATCH) developed at Cranfield University. As a part of familiarization process with this tool and also for the purposes of development of the engine models employed during helicopter performance simulations, a number of helicopter engine models was created and then simulation processes using TURBOMATCH were performed. The developed engine models now form a part of an engine library. This library includes several representative engine models for each of the three helicopter categories, based on the helicopter weight. The process of forming this library was a joint effort of the author and a number of MSc and PhD students.

In order to establish a base for conducting the helicopter engine performance studies and investigating its effects on the helicopter mission to fulfil the objectives laid out for this research a helicopter performance simulation scheme (HELIX) was developed. The intention was to lay a foundation for an integrated tool that would encompasses several models, predicting not only the performance of the helicopter but also the environmental impact and possibly including models for prediction of the cost of design and maintenance, economics and lifing model etc; in a similar fashion to the framework already existing in Cranfield University for the aircraft modelling (TERA). The methodology used for this purposes was adapted from several helicopter performance studies. The choice of the methodology was governed by the requirement to keep the computational time to minimum while ensuring a sufficient accuracy. The computer program based on this methodology was then written in standard FORTRAN 90. In this way a compatibility with a majority computer operating systems currently used. The methodology applied within HELIX with the mathematics behind it is described in detail in Chapter 4.

In addition, in order to represent the helicopter mission trajectory more realistically (three-dimensionally), the trajectory definition was enhanced to include the spherical coordinates of the key trajectory points (latitude and longitude) on the top of the current altitude-only point definition. In this way, the user needs to specify the coordinates of the key mission points and the distance between these points is then computed from the calculation of the distance between two points on Earth. HELIX employs the currently used WGS-84 world geodetic system, considering the Earth as spheroid (ellipsoid). This enhancement of HELIX's capabilities enables more realistic and versatile definition on mission trajectory and is especially of use during simulation of already existing mission scenarios as well as evaluations of the potential ones.

During the performance simulations using HELIX a frequent interaction with TURBOMATCH is necessary. The interlinking of these two tools was achieved within HECTOR, a standalone simulation platform for helicopter mission analysis, developed by a Cranfield university researcher. This platform apart from the two above mentioned tools contains also an emission indices prediction model and an optimization toolbox, both also developed by Cranfield University researchers. HECTOR is capable of simulating any user-defined helicopter mission profile for a user-specified helicopter configuration. The outcome of the simulations is evaluated in terms of the required operational resources such as fuel consumption or the mission's environmental impact. The user wishing to perform optimization studies can take advantage of the in-built optimization toolbox in order to obtain optimum mission profiles for any user-specified mission objectives under any user-defined mission constraints. All the tools that are incorporated in HELIX and their capabilities were briefly described in Chapter 3.

In order to increase the flexibility of the tool, HELIX's input was kept simple and requires only the information easily accessible from the public domain, i.e. the helicopter main geometrical specifications and weight specifications.

Several performance studies were carried out in order to compare the results with available data from public domain. While the exact data for validation was not available, a comparison with the general performance curves was performed. The similarity of the trends of the simulation results with the available performance curves is encouraging and verifies the accuracy of HELIX calculations.

Firstly, a parametric study was carried out, investigating the effect of change in cruise altitude and the helicopter gross take-off weight on helicopter performance, specifically on the power required, fuel burn and emissions. The simulations were carried out using the simulation model of one of the commercial helicopters. In addition, a representative distribution of the helicopter engine emissions (CO_2 and NO_X) during a mission fragment (cruise conditions) was shown for a range of airspeeds and gross take-off weights.

Secondly, a hypothetical search and rescue mission (SAR) simulation was performed, comparing the performance of the helicopter following two possible search patterns, again using the existing helicopter simulation model. The conditions of the SAR mission were kept as real as possible, adapting the typically used search patterns, search altitude or definition of search area. Despite being a type of an emergency mission, the SAR mission still needs careful planning in advance. It was shown that if the approximate location of the target is known and the choice of two or more search patterns is available, a brief simulation study before the commencement of the mission would determine the most appropriate search pattern in terms of shortest time, or if time is not crucial, in terms of lowest environmental impact or possibly both.

Finally, the versatility of application of HELIX was demonstrated on another real-life example. This time a comparative study was carried out between two currently used helicopters for executive transport or business purposes. Both helicopters belong to the medium-weight category although they differ in size, weight and passenger capacity. A number of mission scenarios was simulated and the performance of the helicopters in terms of power required, fuel burn, fuel flow and environmental

impact was obtained. The results were then analyzed in terms of the actual fuel burn per passenger. It was then demonstrated that the choice of the helicopter for the executive transport purposes is not straight forward and depends on the mission requirements. The effect of the forward velocity, climb and descent angle and cruise length on the fuel burn and emissions was also investigated.

Reviewing the results of the simulations using HELIX, the following conclusions were drawn:

- HELIX is a generic performance simulation tool, capable of simulating any user-defined helicopter mission profile for a user-specified helicopter configuration, both for the existing configurations and possible novel concepts. In connection with the integrated HECTOR platform it is possible to determine the required operational resources such as fuel consumption and operational time as well as the mission's environmental impact.
- The input into HELIX is simple and consists of the helicopter geometrical and weight parameters that are easily obtained from the public domain.
- The results of the parametric analyses performed using HELIX display satisfactory similarity with the available typical helicopter engine performance charts. Despite the inability to perform verification studies, due to the lack of appropriate data in the public domain, the trends obtained from simulations are correct.
- The methodology used (momentum theory) proves to give sufficiently accurate results, while being computationally inexpensive. The computational times of running a basic helicopter mission study, consisting of take-off, climb out, cruise, descent and landing, in HELIX, within the integrated HECTOR platform (including the computation of emissions) is of the order of minutes.
- The potential uses of HELIX are numerous: it can be employed to investigate the helicopter engine performance and its effects on the helicopter mission including comparative studies assessing the best choice of helicopter for a certain purpose, comparing the performance of two or more engines for a selected helicopter in terms of fuel burn and emissions, fuel cost per

passenger, etc. The short simulation computational time can be of advantage for a beforehand brief assessment of flying patterns during certain emergency missions and their environmental impact. The three-dimensional definition of the mission trajectory broadens the HELIX capabilities even further, including possible terrain following studies. The optimization option included in HECTOR suggests potential future use for optimization of take-off or landing procedures, or flying "greener" trajectories.

7.2 Further Work

As mentioned above, the developed helicopter performance simulation scheme allows for the reliable calculation of the helicopter performance during a given mission. The results of the simulations follow the correct trends. Nonetheless, as certain simplifying approaches were employed during its development, it is possible to improve its capabilities by employing the following enhancements:

- *Accounting for variable angle of attack during flight*. Currently, a constant angle of attack is assumed, which does not reflect the real in-flight situation, it is however sufficient as the first assumption. The user should have the option to specify the initial angle of attack and the programme should subsequently iterate on the correct angle of attack at specific flight conditions.
- *Airfoil specification*. At present, NACA0012 is being taken as a default airfoil. It is recommended to enhance the capability of the model in a way that user can specify the airfoil used and the model will automatically allocate the appropriate Mach divergence number of the airfoil and the thickness/chord ratio.
- *Drag determination*. In order to simplify the input into the model, charts of average drag coefficient distribution for fixed angle of attack derived from wind-tunnel tests were implemented in this version of HELIX. More accurate expressions of the average drag coefficient can be considered as one of the future enhancements of the capabilities of the model. The same applies for

the determination of the equivalent flat plate area for the prediction of the parasitic drag of the fuselage. Possible use of standalone models for the prediction of the helicopter drag coefficient (using computational fluid dynamics, or other high-fidelity modelling) can be considered. Nonetheless, a care has to be exercised, not to increase substantially the computational run time of the model, the complication which would far outweigh the potential benefits of obtaining more accurate drag coefficient representation.

- *Calculation of the vertical download* (vertical drag) – currently 5% of GTOW penalty is assumed for the thrust of the helicopter in hover which is a value recommended in Prouty (Prouty, Helicopter Performance, Stability and Control, 1984). More accurate representation can be derived using the projected area of the helicopter. More geometrical details will be required and hence the number of necessary input items will grow.
- *Accounting for other helicopter configurations* – the single main rotor – tail rotor configuration is by far the most commonly used helicopter design today; however it would enhance the versatility of the performance tool to account for the second most commonly used configuration - the tandem (two overlapping main rotors). The tandem helicopters are used primarily within the military sector and as this research study directs its main focus on the non-military use of helicopters, the algorithms for the performance calculations using tandem helicopter have not been implemented within HELIX.
- *Verification studies* – More extensive verification studies are needed. For this purpose the helicopter mission analysis data need to be obtained, possibly from the helicopter manufacturers or other entities from helicopter industry.

References

ACARE (2007), *Second ACARE Opinion on the Proposal for the Joint Technology Initiative CLEAN SKY.*

ATAG (2010), *Clearer vision, cleaner skies*, available at: http:// www.enviro.aero, accessed 18th October 2009).

Bailey, F. and Gustafson, F (1990), *Charts for Estimation of the Characterstics of a Helicopter Rotor in Forward Flight; I- Profile drag-Lift Ratio for Untwisted Rectangular Blades.* NACA - ACR L4H07.

Bauchspies, J., Bryant, W. and Simpson, W. (1985), *Trade-off Analysis of Technology Needs for Public Service Helicopters.* NASA CR-3927.

Berghoff, R. (2007), J*TI and Technology Evaluator overview*, Presentation to Cranfield University at DLR ,Cologne.

Betts, J. (1998), "Survey of Numerical Methods for Trajectory Optimization", *Journal of Guidance, Control, and Dynamics* , vol. 21, no.2, p.193-206.

Bree, H. and Backmann, G. (1981), *Future Requirements for Helicopter Propulsion Systems,* AGARD - CP - 302.

Brown, E. (1981), *The Helicopter in Civil Operation,* Granada Publishing, London.

Carlson, R. (2002), "Helicopter Performance - Transportation's Latest Chromosome: The 21st Annual Alexander A. Nikolsky Lecture", *Journal of the American Helicopter Society , vol.47* , no.1, p.3-17.

Celis, C. (2010), *Evaluation and Optimization of Environmentally Friendly Aircraft Propulsion Systems,* PhD Thesis, Cranfield University, Cranfield.

Celis, C., Moss, B., and Pilidis, P. (2009), Emissions Modelling for the Optimisation of Greener Aircraft Operations. *Proceedings of GT 2009,ASME Turbo Expo 2009, Power for Land, Sea and Air,* Orlando.

Celis, C., Sethi, V. and Zammit-Mangion, D. (2009), *On Trajectory Optimization for Reducing the Impact of Commercial Aircraft Operations on the Environment,* ISABE - 2009-1118.

Clean Sky JTI (2009), available at: http://www.cleansky.eu (accessed 10th November 2009).

Cooke, A. and Fitzpatrick, E. (2002), *Helicopter Test and Evaluation,* Blackwell Publishing, Oxford.

Crouch, P. and Cook, M. (1994), *The development of a computer model of a helicopter for flight dynamics applications,* MSc. thesis. Cranfield University, Cranfield.

Done, G. and Balmford, D. (2001), *Bramwell's Helicopter Dynamics,* Bath Press, Avon.

Dreier, M. (2007), *Introduction to Helicopter and Tiltrotor Flight Simulation.* AIAA, New York.

EC-135 (2010), available at :www.eurocopter.com (accessed 25th January 2010).

Eurocopter AS 332 (2009), available at: http://www.eurocopter.co.uk (accessed 26th January 2009).

Eurocopter AS332. (2009), available at :http://en.wikipedia.org/wiki/Eurocopter AS 332, (accessed 26th January 2009).

Filippone, A. (2006), *Flight Performance of fixed and rotary wing aircraft,* Elsevier, Oxford.

Fradenburgh, E. (1973), *Aerodynamic Factors Influencing Overall Hover Performance,* AGARD - CP - 111.

Gmelin, B. and Pausder, H. (1985), *Mission Requirements and Handling Qualities,* AGARD LS-139.

Goodger, E. (2008), *Transport, Fuel, Technology,* Landfall Press, Norwich.

Goulos, I. (2009), private communication.

Goulos, I., Mohseni, M., Pachidis, V., D'Ippolito, R. and Stevens, J. (2010). Simulation Framework Development for Helicopter Mission Analysis, *Proceedings of Asme Turbo Expo 2010: Power for Land, Sea and Air,* Glasgow.

Gunston, B. (1984), *Helicopters of the World,* Temple Press, London.

Gunston, B. (1996), *Jane's Aero Engines,* Jane's Information Group, London.

Harris, R., Sloan, L. and Ulrich, K. (1952), *Typical Helicopter Performance Calculation,* Rotorcraft Puublishing Committee, Morton.

ICAO(2008), *Environmental Protection.* Annex 16 to the Convention on International Civil Aviation, Volume II, Montrea.

ICAO (1970), *Search and Rescue Manual, Part 2 - Search and Rescue Procedures,* ICAO/DOC - 7333.

Jacobson, S., McLay, L., Hall, S., Henderson, D. and Vaughan, D. (2006), "Optimal Search Strategies Using Simulateneous Generalized Hill Climbing Algorithms", *Mathematical and Computer Modelling* , p. 1061-1073.

Jane's All the World's Aircraft (1993), Jane's Information Group, London.

Jane's Helicopter Markets and Systems (1997), Jane's Information Group, London.

Johnson, W. (1980), *Helicopter Theory,* Dover Publications, New York.

Keys, C. (1979), *Rotary wing aerodynamics – volume II – Performance prediction of helicopter,.* NASA -3083.

Kumar, N. (2007), "What will accelerate a step change performance - Regulation, Market based options or Incentives?" *Greener by Design Group conference.Aviation and the Environment: State of Play,* RAes*,* London.

Laskaridis, P. and Pilidis, P. (2005), *An Integrated Engine – Aircraft Performance Platform for Assessing New Technologies in Aeronautic,* ISABE - 2005-1165.

Layton, D. (1984), *Helicopter Performance,* Matrix Publishers, New York.

Leishmann, J. (2006), *Principles of Helicopter Aerodynamics,* Cambridge University Press, New York.

Marzal Espi, R. (2010), *Benchmarking and Testing of Different Genetic Algorithms for Multidisciplinary Aircraft Trajectory Optimization Studies,* MSc Thesis, Cranfield University, Cranfield.

Maythapattana, S. (1999), *The Growth Potential of a Helicopter Engine,* MSc. Thesis, Cranfield University, Cranfield.

McCormick, B. (1995), *Aerodynamics, Aeronautics and Flight Dynamics,* Wiley & Sons, New York.

MH-47. (2010), available at: www.deagel.com (accessed 23rd November 2010).

Newman, S. (1994), *The foundations of helicopter flight,* Edward Arnold, London.

Noppel,F. and Singh,R. (2008), "Contrail Avoidance in the Aircraft Design Process",

The Aeronautical Journal, vol.112, no.1138, December 2008

Ogaji, S., Pilidis, P. and Hales, R. (2007), "TERA – A tool for aero-engine modelling and management", *Second world congress on engineering asset management and fourth international conference on condition monitoring.*

Ogaji, S., Pilidis, P., & Hales, R. (2007). TERA – A tool for aero-engine modelling and management. *Second world congress on engineering asset management and fourth international conference on condition monitoring.* Harrogate, UK.

Pachidis, V. (2008), *Gas Turbine Performance Simulation,* Lecture notes, Cranfield University, Cranfield, UK.

Padfield, G. (1996), *Helicopter Flight Dynamics,* Blackwell Science, Oxford.

Palmer, J. (1990), *The Turbomatch Scheme For Aero/Industrial Gas Turbine Engine Design Point/Off Design Performance Calculation,* Cranfield University, Cranfield.

Paramour, M. and Jennings, P. (1993), "Operational Requirements for Helicopter Engines for UK Services", *AGARD meeting on Technoloty Requirements for Small Gas Turbines*, (pp. 1-1 to 1-9), France.

Pascovici, D., Colmenares, F., Ogaji, S. and Pilidis, P. (2007), "An Economic and Risk Analusis Model for Aircrafts and Engines", *Proceedings of GT2007 ASME Turbo Expo 2007: Power for Land, Sea and Air,* Montreal.

Payne, P. (1959), *Helicopter dynamics and aerodynamics,* London.

Pilidis, P. (2008), *Gas Turbine Theory,* Lecture Notes, Cranfield University, Cranfield.

POST. (2010), *Aircaft Engine Emissions - Report Summary*, available at: www.parliament.uk/post, Parliamentary Office of Science and Technology, (accessed 18th October 2010).

Prouty, R. (1985), *Helicopter Aerodynamics,* PJS Publications, Peoria.

Prouty, R. (1984), *Helicopter Performance, Stability and Control,* Krieger Publishing, Florida.

Quentin, F. (2009), *ACARE: The EuropeanTechnology Platform for Aeronautics,* available at*:* www.acare4europe.org, (accessed 26th October 2009).

Rogero, J. (2002), *A Genetic Algorithms-based Optimization Tool for the PReliminary Design of Gas Turbine Combustors,* PhD thesis, Cranfield University, Cranfield.

Rozhdestvenskiy, M. and Tarasov, N. (2002), "Impact of Helicopter Vertical Fin on Tail Rotor Performance in Hover", *Proceedings of 28th European rotorcraft forum*, vol.*1*, pp. 22.1-22.8, Bristol.

Sadiq, M. (2007), *The Effects of Aircraft Emissions and Global Warming,* MSc. Thesis, Cranfield University, Cranfield.

Saravanamuttoo, H., Rogers, G., & Cohen, H. (2001), *Gas Turbine Theory,* London.

Saunders, G. (1975), *Dynamics of Helicopter Flight,* Willey& sons, New York.

Seddon, J. (1990), *Basic Helicopter Aerodynamics,* AIAA, New York.

Seddon, J. and Newman, S. (2002), *Basic Helicopter Aerodynamics,* Blackwell Science,

London.

Sinott, R. (1984), "Virtues of the Haversine", *Sky and Telescope , vol.68, no.*2.

Slater, G. and Erzberger, H. (1982), *Optimal Short-Range Trajectories for Helicopters,* NASA - TM - 84303.

Slater, G. and Stoughton, M. (1987), "On-Line Determination of Optimal Flight Paths for Helicopters", *Journal of the American Helicopter Society ,* vol.32, no.3, p.54-61.

Sonneborn, W. (2003), "Vision 2025 for Rotorcraft", *AIAA/ICAS International Air and Space Symposium and Exposititon: The next 100 years,* Dayton.

Stanzione, K., Smith, R. and Oliver, L. (1992), *Application of Generic Helicopter Performance Methodology to Mission Analyses,* AIAA-92-4281.

Stepniewski, W. and Keys, C. (1984), *Rotary-Wing Aerodynamics,* Dover Publications, Inc., New York.

Super Lynx. (2010), available at: www.agustawestland.com, (accessed 24th February 2010).

The Jet Engine (1996), Rolls-Royce, Derby.

Thompson, A., Friedl, R. and Wesoky, H. (1996), *Atmospheric Effects of Aviation: First Report of the Subsonic,* NASA - RP-1385.

Turbomeca. (2009), available at: http://www.turbomeca.com, (accessed 28th August 2009).

Varnaseri, H. (2009), *Performance Simulation of Helicopter and Rotorcraft/Engine Simulation,* MSc. Thesis, Cranfield University, Cranfield.

Vickers, J. (1995), *The growth potential of a helicopter engine,* MSc. Thesis, Cranfield University, Cranfield.

Wagtendonk, W. (1996), *Principles of helicopter flight.* Aviation Supplies & Academics, New York.

Wahab, A. and Ismail, M. (2006), "Estimating Vertical Drag on Helicopter During Hovering", *1st Regional Conference on Vehicle Engineering & Technology,* Kuala Lumpur.

Wall, R. (2009), "Healthier Helicopters", *Aviation Week & Space Technology ,*vol. 170, no 7, p. 46-47.

Watkinson, J. (2004), *The Art of the Helicopter,* Elsevier, Oxford.

Wildi, J. (2008), *Clean Sky - EU Joint Technology Initiative,* available at: www.cleansky.eu, (accessed 12th October 2008).

Turbomeca (2009), available at: www.turbomeca.com, (accessed 15th December 2009).

Young, C. (1978), *A User's Guide to Some Computer Programs for Predicting Helicopter and Rotor Performance,* NASA TM-924.

Appendix

1. Example of the HECTOR input file

```
---------------------------------------------------------------------------------------------
**************!SETUP FILE FOR HELICOPTER MISSION ANALYSIS SIMULATION FRAMEWORK*******************
---------------------------------------------------------------------------------------------
**********************Created by John Goulos, Cranfield University 2009**************************
****************************Input_Data_for_All_Flight_Segments***********************************
---------------------------------------------------------------------------------------------
!Use this file to setup the mission type you want to simulate-optimize.
---------------------------------------------------------------------------------------------
***********************************Rotorcraft Technical Data***********************************
---------------------------------------------------------------------------------------------
!AW139                !HELICOPTER
!PT6C_67C_CANADA      !ENGINE
!SAR                  !MISSION TYPE
!NOTE: For each segment please specify flight condition as one of the following:
!Hover, ForwClimb, ForwDesc, ForwFlight, VertClimb, VertDesc
---------------------------------------------------------------------------------------------
***********************************PROBLEM SETTINGS************************************************
---------------------------------------------------------------------------------------------
PROBLEM_TYPE: OPTIMIZATION STUDY
AERODYNAMIC_MODEL_TO_BE_USED HELIX              !SELECT "HECTOR" FOR HECTOR BUILT IN AERODYNAMICS OR SELECT "HELIX"
PROFILE_DEFINITION   WGS84                      !SELECT WGS84 FOR WSG84 PROFILE DEFINITION AND 2D FOR 2D-PROFILE
NO_OF_ENGINES        2                          !NUMBER OF ENGINES
MAXIMUM_ENGINE_TET   1630                       !MAXIMUM ALLOWABLE ENGINE TURBINE INLET TEMPERATURE
MINIMUM_ENGINE_TET   1050                       !MINIMUM ALLOWABLE ENGINE TURBINE INLET TEMPERATURES
TOTAL_FUEL_RESERVES  1620                       !IN KILOGRAMS
POWER_TOLERANCE      5000                       !MAX ALLOWABLE DIFFERENCE BETWEEN POWER REQUIRED AND POWER DELIVERED
ENGINE_MODEL_FILENAME     PT6C-67C-ODP.dat      !NAME OF ENGINE MODEL FILE TO BE USED (NO BLANKS IN BETWEEN THE FILENAME)
HELIX_CONFIG_FILENAME     AW139.DAT             !NAME OF HELICOPTER CONFIGURATION FILE (NO BLANKS IN BETWEEN THE FILENAME FOR HELIX)
HELIX_HELICOPTER_CONFIG   CONVENTIONAL          !SELECT 'TANDEM' OR CONVENTIONAL - HELIX
HECTOR_ROTOR_FILENAME     ROTOR.DAT             !HELICOPTER ROTOR INPUT FILE (NO BLANKS IN BETWEEN THE FILENAME - FOR HECTOR)
HECTOR_HELI_CONFIG_FILENAME  AS_332.DAT         !NAME OF HELICOPTER CONFIGURATION FILE (NO BLANKS IN BETWEEN THE FILENAME - FOR HECTOR
NO_OF_OPTIMIZED_VALUES 1                        !NUMBER OF VALUES TO BE OPTIMIZED
EXPERIMENT_CONSOLE_OUTPUT  YES                  !SELECT WHETHER THE FRAMEWORK WILL SHOW THE EXPERIMENTS IN THE CONSOLE (YES OR NO)
---------------------------------------------------------------------------------------------
```

```
*****************************LOW-HIGH-NOMINAL RANGES FOR VARIABLES*****************************
-----------------------------------------------------------------------------------------------
!Set the low-high values for 4 main variables of each segment being: Final Altitude(meters),
!Forward Velocity (M/SEC) and segment time (hours). The values are set in LOW, HIGH and nominal order.
!Between the 3 of forward velocity, segment time and segment range, only 2 can be used and the third-one
!should be set to -1.0 to avoid inconsistency in the flight profile. The final altitude must always be set
!as a variable.If it is desired to keep a value constant then the LOW limit must be set equal to the HIGH limit of
!each variable.STARTALT is the value of the starting altitude which by default is zero but needs to be set up.
In order to determine which values are to be concidered as variables and which ones are concidered to be
constants, 2 strings can be used which are the following:
CONSTANT:If you wish a value to remain constant during an optimization, then set it as such,
REALVARIABLE:Set the value as such if it is a variable.
***********************************************************************************************
-----------------------------------------------------------------------------------------------
MISSION ANALYSIS ----- AUTOMATIC PROFILE TRUNCATION AND SEGMENT DETERMINATION----------------------
-----------------------------------------------------------------------------------------------
START_LATIT:              32.61161640317
START_LONGIT:             51.71264648
START_ALT:                30
ISA_DEVIATION:            0
-----------------------------------------------------------------------------------------------
PART_NUMBER               1            !INCREASING NUMBER OF MISSION PART (TAKE-OFF)
SEGMENT                          !PART TYPE (SEGMENT OR PROFILE)
SEGMENT_TYPE              Hover        !IN CASE A SEGMENT IS SELECTED,DEFINE THE SEGMENT CHARACTERISTICS AS ABOVE
LATITUDE                  32.61161640317        !PROFILE END POINT,LATITUDE IN DEG. NORTH, LATITUDE SOUTH IS NEGATIVE
NORTH
LONGITUDE                 51.71264648       !LONGITUDE IN DEG EAST, DEGREES WEST ARE NEGATIVE EAST
CONSTANT LOW-HIGH-NOMINAL    30 30 30       !SEGMENT FINAL ALT
CONSTANT LOW-HIGH-NOMINAL    0 0 0          !SEGMENT FORWVEL
CONSTANT LOW-HIGH-NOMINAL    0.03 0.25 0.1    !SEGMENT TIME
CONSTANT LOW-HIGH-NOMINAL   -1.0 -1.0 0      !SEGMENT RANGE
-----------------------------------------------------------------------------------------------
PART_NUMBER                                  2                !INCREASING NUMBER OF MISSION PART (CLIMB OUT)
PROFILE                                  !PART TYPE (SEGMENT OR PROFILE)
SEGMENT_NUMBER                                                          10                       !NUMBER   OF   SEGMENTS
IN WHICH THE PROFILE IS TRUNCATED
LATITUDE                  33.5597    !PROFILE END POINT,LATITUDE IN DEG. NORTH, LATITUDE SOUTH IS NEGATIVE NORTH
LONGITUDE                   51.613769    !LONGITUDE IN DEG EAST, DEGREES WEST ARE NEGATIVE EAST
ALTITUDE                  1000.0     !ALTITUDE IN METERS
PROFILE_HORIZONTAL_RANGE          4120      !PROFILE HORIZONTAL RANGE IN CASE OF 2D ANALYSIS (IN METERS)
FORWARD_VELOCITY LOW-HIGH-NOMINAL   30 70 50   !LOW,NOMINAL AND HIGH VALUES OF FORWARD VELOCITY
INTERSEGMENTAL_ALTITUDE_VARIATION   YES       !ALLOW FOR INTERSEGMENTAL ALTITUDE VARIATIONS
INTERSEGMENTAL_VELOCITY_VARIATION   YES       !ALLOW FOR INTERSEGMENTAL VELOCITY VARIATIONS
INTERSEGMENTAL_PARAMETER_VARIATION   TIME        !CHOOSE WHICH PARAMETER TO VARY WITHIN SEGMENTS (TIME OR
RANGE)
VERTICAL_SEGMENT_RANGE            500       !VERTICAL SEGMENT RANGE VARIATION (IN METERS)
```

```
---------------------------------------------------------------------------------------------
PART_NUMBER                                3                    !INCREASING NUMBER OF MISSION PART (FORWARD FLIGHT)
PROFILE                                !PART TYPE (SEGMENT OR PROFILE)
SEGMENT_NUMBER                                                  10                    !NUMBER OF SEGMENTS
IN WHICH THE PROFILE IS TRUNCATED
LATITUDE                35.52    !PROFILE END POINT,LATITUDE IN DEG. NORTH, LATITUDE SOUTH IS NEGATIVE NORTH
LONGITUDE                51.2775    !LONGITUDE IN DEG EAST, DEGREES WEST ARE NEGATIVE EAST
ALTITUDE                1000.0    !ALTITUDE IN METERS
PROFILE_HORIZONTAL_RANGE        4120      !PROFILE HORIZONTAL RANGE IN CASE OF 2D ANALYSIS (IN METERS)
FORWARD_VELOCITY LOW-HIGH-NOMINAL   30 70 70   !LOW,NOMINAL AND HIGH VALUES OF FORWARD VELOCITY
INTERSEGMENTAL_ALTITUDE_VARIATION   YES       !ALLOW FOR INTERSEGMENTAL ALTITUDE VARIATIONS
INTERSEGMENTAL_VELOCITY_VARIATION   YES       !ALLOW FOR INTERSEGMENTAL VELOCITY VARIATIONS
INTERSEGMENTAL_PARAMETER_VARIATION   TIME        !CHOOSE WHICH PARAMETER TO VARY WITHIN SEGMENTS (TIME OR
RANGE)
VERTICAL_SEGMENT_RANGE          500       !VERTICAL SEGMENT RANGE VARIATION (IN METERS)
---------------------------------------------------------------------------------------------
PART_NUMBER                                4                !INCREASING NUMBER OF MISSION PART (FORWARD DESCENT)
PROFILE                                !PART TYPE (SEGMENT OR PROFILE)
SEGMENT_NUMBER                                                  10                    !NUMBER OF SEGMENTS
IN WHICH THE PROFILE IS TRUNCATED
LATITUDE                36.25    !PROFILE END POINT,LATITUDE IN DEG. NORTH, LATITUDE SOUTH IS NEGATIVE NORTH
LONGITUDE                51.2775     !LONGITUDE IN DEG EAST, DEGREES WEST ARE NEGATIVE EAST
ALTITUDE                30.0     !ALTITUDE IN METERS
PROFILE_HORIZONTAL_RANGE        4120      !PROFILE HORIZONTAL RANGE IN CASE OF 2D ANALYSIS (IN METERS)
FORWARD_VELOCITY LOW-HIGH-NOMINAL   30 70 50   !LOW,NOMINAL AND HIGH VALUES OF FORWARD VELOCITY
INTERSEGMENTAL_ALTITUDE_VARIATION   YES       !ALLOW FOR INTERSEGMENTAL ALTITUDE VARIATIONS
INTERSEGMENTAL_VELOCITY_VARIATION   YES       !ALLOW FOR INTERSEGMENTAL VELOCITY VARIATIONS
INTERSEGMENTAL_PARAMETER_VARIATION   TIME        !CHOOSE WHICH PARAMETER TO VARY WITHIN SEGMENTS (TIME OR
RANGE)
VERTICAL_SEGMENT_RANGE          500       !VERTICAL SEGMENT RANGE VARIATION (IN METERS)
---------------------------------------------------------------------------------------------
PART_NUMBER            5            !INCREASING NUMBER OF MISSION PART (LANDING)
SEGMENT                        !PART TYPE (SEGMENT OR PROFILE)
SEGMENT_TYPE            Hover         !IN CASE A SEGMENT IS SELECTED,DEFINE THE SEGMENT CHARACTERISTICS AS ABOVE
LATITUDE              36.25        !PROFILE END POINT,LATITUDE IN DEG. NORTH, LATITUDE SOUTH IS NEGATIVE NORTH
LONGITUDE              51.2775        !LONGITUDE IN DEG EAST, DEGREES WEST ARE NEGATIVE EAST
CONSTANT LOW-HIGH-NOMINAL    1350 1350 30    !SEGMENT FINAL ALT
CONSTANT LOW-HIGH-NOMINAL    0 0 0         !SEGMENT FORWVEL
CONSTANT LOW-HIGH-NOMINAL    0.03 0.25 0.1    !SEGMENT TIME
CONSTANT LOW-HIGH-NOMINAL   -1.0 -1.0 0     !SEGMENT RANGE
---------------------------------------------------------------------------------------------
END_PART
************************************PARAMETER-CONSTRAINTS************************************
---------------------------------------------------------------------------------------------
!Set various contraints regarding the outputs of each experiment. The Parameters are outputted as
!shown below. It is reminded that thhe framework will automatically penalize a chromosome if the
```

!experiment fails and its fitness will be set to zero.

PARAMETERS:

PARAMETER1 1 LOW 0 !TOTAL HORIZONTAL RANGE LOW LIMIT

PARAMETER2 2 HIGH 1000000000 !TOTAL HORIZONTAL RANGE HIGH LIMIT

PARAMETER3 3 LOW 0 !TOTAL FUEL BURN

PARAMETER4 4 LOW 0 !TOTAL OPERATIONAL TIME

PARAMETER5 5 LOW 0 !TOTAL NOX PRODUCTION

PARAMETER6 6 LOW 0 !TOTAL CO PRODUCTION

PARAMETER7 7 LOW 0 !TOTAL UHC PRODUCTIOM

PARAMETER8 8 LOW 0 !TOTAL CO2 PRODUCTION

PARAMETER9 9 LOW 0 !TOTAL H2O PRODUCTION

END_PARAM 10 DUMMY 0

**********OPTIMIZED-VALUES**********

!The optimizer within this framework can be used for single or multi-optimization purposes. Select

!which of the 9 above parameters you wish to optimize here by setting. It is reminded that the number

!of optimized values has been set above. Select "3" for FUEL BURN, "4" for OPERATIONAL TIME and so on.

OBJECTIVES:

OBJECTIVE 2

**********END OF SETUP FILE**********

2. Example of HECTOR output file

2.1 Main results

CompModels Output file

========== OUPUT DATA ==========

OR ---------- Overall Results ----------

Elem PARAMETER1 PARAMETER2 PARAMETER3 PARAMETER4 PARAMETER5 PARAMETER6 PARAMETER7 PARAMETER8 PARAMETER9

[--]

1 407129.44 Meters, TOTAL HORIZONTAL RANGE

2 407129.44 Meters, TOTAL HORIZONTAL RANGE

3 1444.3257 KG, TOTAL FUEL BURN

4 7604.6157 SEC, TOTAL OPERATIONAL TIME

5 4.4068537 KG, TOTAL NOX EMISSIONS

6 0.008438787 KG, TOTAL CO EMISSIONS

7 0. KG, TOTAL UHC EMISSIONS

8 4628.7363 KG, TOTAL CO2 EMISSIONS

9 1793.197 KG, TOTAL H2O EMISSIONS

2.2 Breakdown of segment results

THESE_ARE_THE_RESULTS_FOR_EXPERIMENT_NO: 1

****

SEGMENT_NO: 1

SEGMENT_CONDITION:Hover

SEGMENT_FINAL_LONGITUDE: 51.712646 DEGREES

SEGMENT_FINAL_LATITUDE: 32.611618 DEGREES

SEGMENT_INITIAL_ALT: 30.

SEGMENT_FINAL_ALT: 30.

SEGMENT_CLIMB_RATE: 0. METERS/SECOND

SEGMENT_FORWARD_VELOCITY: 0. METERS/SECOND

SEGMENT_POWER_REQUIRED_PER_ENGINE: 683517.8 WATTS

SEGMENT_RANGE: 0. METERS

TOTAL_FUEL_BURNED_ALL_ENGINES: 70.56 KG

SEGMENT_TIME: 360. SECOND

TOTAL_NOX_ALL_ENGINES: 0.2188242 KG

TOTAL_CO_ALL_ENGINES: 0.00034743742 KG

TOTAL_UHC_ALL_ENGINES: 0. KG

TOTAL_CO2_ALL_ENGINES: 226.23146 KG

TOTAL_H2O_ALL_ENGINES: 87.6454 KG

TOTAL_SEGMENT_TET: 1050. KELVIN

TOTAL_SEGMENT_ESFC: 84.3019 KG/KWATT

****

SEGMENT_NO: 2

SEGMENT_CONDITION:ForwClimb

SEGMENT_FINAL_LONGITUDE: 51.712646 DEGREES

SEGMENT_FINAL_LATITUDE: 32.611618 DEGREES

SEGMENT_INITIAL_ALT: 30.

SEGMENT_FINAL_ALT: 127.

SEGMENT_CLIMB_RATE: 0.4583978 METERS/SECOND

SEGMENT_FORWARD_VELOCITY: 50. METERS/SECOND

SEGMENT_POWER_REQUIRED_PER_ENGINE: 821529.5 WATTS

SEGMENT_RANGE: 10580.33 METERS

TOTAL_FUEL_BURNED_ALL_ENGINES: 41.771145 KG

SEGMENT_TIME: 211.6066 SECOND

TOTAL_NOX_ALL_ENGINES: 0.13403438 KG

TOTAL_CO_ALL_ENGINES: 0.00021357587 KG

TOTAL_UHC_ALL_ENGINES: 0. KG

TOTAL_CO2_ALL_ENGINES: 133.93336 KG

TOTAL_H2O_ALL_ENGINES: 51.88365 KG

TOTAL_SEGMENT_TET: 1050. KELVIN

TOTAL_SEGMENT_ESFC: 85.2232 KG/KWATT

****

SEGMENT_NO: 3

SEGMENT_CONDITION:ForwClimb

SEGMENT_FINAL_LONGITUDE: 51.720932 DEGREES

SEGMENT_FINAL_LATITUDE: 32.706436 DEGREES

SEGMENT_INITIAL_ALT: 127.

SEGMENT_FINAL_ALT: 224.

SEGMENT_CLIMB_RATE: 0.4583978 METERS/SECOND

SEGMENT_FORWARD_VELOCITY: 50. METERS/SECOND

SEGMENT_POWER_REQUIRED_PER_ENGINE: 814017.1 WATTS

SEGMENT_RANGE: 10580.33 METERS

TOTAL_FUEL_BURNED_ALL_ENGINES: 41.517216 KG

SEGMENT_TIME: 211.6066 SECOND

TOTAL_NOX_ALL_ENGINES: 0.13188101 KG

TOTAL_CO_ALL_ENGINES: 0.00021402125 KG

TOTAL_UHC_ALL_ENGINES: 0. KG

TOTAL_CO2_ALL_ENGINES: 133.10686 KG

TOTAL_H2O_ALL_ENGINES: 51.56432 KG

TOTAL_SEGMENT_TET: 1050. KELVIN

TOTAL_SEGMENT_ESFC: 85.0508 KG/KWATT

****

SEGMENT_NO: 4

SEGMENT_CONDITION:ForwClimb

SEGMENT_FINAL_LONGITUDE: 51.729218 DEGREES

SEGMENT_FINAL_LATITUDE: 32.801254 DEGREES

SEGMENT_INITIAL_ALT: 224.

SEGMENT_FINAL_ALT: 321.

SEGMENT_CLIMB_RATE: 0.4583978 METERS/SECOND

SEGMENT_FORWARD_VELOCITY: 50. METERS/SECOND

SEGMENT_POWER_REQUIRED_PER_ENGINE: 806561. WATTS

SEGMENT_RANGE: 10580.33 METERS

TOTAL_FUEL_BURNED_ALL_ENGINES: 41.220966 KG

SEGMENT_TIME: 211.6066 SECOND

TOTAL_NOX_ALL_ENGINES: 0.12984885 KG

TOTAL_CO_ALL_ENGINES: 0.00022011997 KG

TOTAL_UHC_ALL_ENGINES: 0. KG

TOTAL_CO2_ALL_ENGINES: 132.14664 KG

TOTAL_H2O_ALL_ENGINES: 51.192535 KG

TOTAL_SEGMENT_TET: 1050. KELVIN

TOTAL_SEGMENT_ESFC: 84.8783 KG/KWATT

****

SEGMENT_NO: 5

SEGMENT_CONDITION:ForwClimb

SEGMENT_FINAL_LONGITUDE: 51.737503 DEGREES

SEGMENT_FINAL_LATITUDE: 32.89607 DEGREES

SEGMENT_INITIAL_ALT: 321.

SEGMENT_FINAL_ALT: 418.

SEGMENT_CLIMB_RATE: 0.4583978 METERS/SECOND

SEGMENT_FORWARD_VELOCITY: 50. METERS/SECOND

SEGMENT_POWER_REQUIRED_PER_ENGINE: 799161.75 WATTS

SEGMENT_RANGE: 10580.33 METERS

TOTAL_FUEL_BURNED_ALL_ENGINES: 40.967037 KG

SEGMENT_TIME: 211.6066 SECOND

TOTAL_NOX_ALL_ENGINES: 0.12775812 KG

TOTAL_CO_ALL_ENGINES: 0.00022027978 KG

TOTAL_UHC_ALL_ENGINES: 0. KG

TOTAL_CO2_ALL_ENGINES: 131.32056 KG

TOTAL_H2O_ALL_ENGINES: 50.873386 KG

TOTAL_SEGMENT_TET: 1050. KELVIN

TOTAL_SEGMENT_ESFC: 84.7131 KG/KWATT

****

SEGMENT_NO: 6

SEGMENT_CONDITION:ForwClimb

SEGMENT_FINAL_LONGITUDE: 51.74579 DEGREES

SEGMENT_FINAL_LATITUDE: 32.990883 DEGREES

SEGMENT_INITIAL_ALT: 418.

SEGMENT_FINAL_ALT: 515.

SEGMENT_CLIMB_RATE: 0.4583978 METERS/SECOND

SEGMENT_FORWARD_VELOCITY: 50. METERS/SECOND

SEGMENT_POWER_REQUIRED_PER_ENGINE: 791817.8 WATTS

SEGMENT_RANGE: 10580.33 METERS

TOTAL_FUEL_BURNED_ALL_ENGINES: 40.67079 KG

SEGMENT_TIME: 211.6066 SECOND

TOTAL_NOX_ALL_ENGINES: 0.12571272 KG

TOTAL_CO_ALL_ENGINES: 0.00022604824 KG

TOTAL_UHC_ALL_ENGINES: 0. KG

TOTAL_CO2_ALL_ENGINES: 130.36057 KG

TOTAL_H2O_ALL_ENGINES: 50.501778 KG

TOTAL_SEGMENT_TET: 1050. KELVIN

TOTAL_SEGMENT_ESFC: 84.5535 KG/KWATT

****

SEGMENT_NO: 7

SEGMENT_CONDITION:ForwClimb

SEGMENT_FINAL_LONGITUDE: 51.754074 DEGREES

SEGMENT_FINAL_LATITUDE: 33.085697 DEGREES

SEGMENT_INITIAL_ALT: 515.

SEGMENT_FINAL_ALT: 612.

SEGMENT_CLIMB_RATE: 0.4583978 METERS/SECOND

SEGMENT_FORWARD_VELOCITY: 50. METERS/SECOND

SEGMENT_POWER_REQUIRED_PER_ENGINE: 784530.06 WATTS

SEGMENT_RANGE: 10580.33 METERS

TOTAL_FUEL_BURNED_ALL_ENGINES: 40.37454 KG

SEGMENT_TIME: 211.6066 SECOND

TOTAL_NOX_ALL_ENGINES: 0.123710215 KG

TOTAL_CO_ALL_ENGINES: 0.00023300147 KG

TOTAL_UHC_ALL_ENGINES: 0. KG

TOTAL_CO2_ALL_ENGINES: 129.40102 KG

TOTAL_H2O_ALL_ENGINES: 50.13026 KG

TOTAL_SEGMENT_TET: 1050. KELVIN

TOTAL_SEGMENT_ESFC: 84.3932 KG/KWATT

****

SEGMENT_NO: 8

SEGMENT_CONDITION:ForwClimb

SEGMENT_FINAL_LONGITUDE: 51.76236 DEGREES

SEGMENT_FINAL_LATITUDE: 33.18051 DEGREES

SEGMENT_INITIAL_ALT: 612.

SEGMENT_FINAL_ALT: 709.

SEGMENT_CLIMB_RATE: 0.4583978 METERS/SECOND

SEGMENT_FORWARD_VELOCITY: 50. METERS/SECOND

SEGMENT_POWER_REQUIRED_PER_ENGINE: 777298.3 WATTS

SEGMENT_RANGE: 10580.33 METERS

TOTAL_FUEL_BURNED_ALL_ENGINES: 40.120613 KG

SEGMENT_TIME: 211.6066 SECOND

TOTAL_NOX_ALL_ENGINES: 0.12163912 KG

TOTAL_CO_ALL_ENGINES: 0.00023225823 KG

TOTAL_UHC_ALL_ENGINES: 0. KG

TOTAL_CO2_ALL_ENGINES: 128.57542 KG

TOTAL_H2O_ALL_ENGINES: 49.81137 KG

TOTAL_SEGMENT_TET: 1050. KELVIN

TOTAL_SEGMENT_ESFC: 84.2453 KG/KWATT

****

SEGMENT_NO: 9

SEGMENT_CONDITION:ForwClimb

SEGMENT_FINAL_LONGITUDE: 51.770645 DEGREES

SEGMENT_FINAL_LATITUDE: 33.275322 DEGREES

SEGMENT_INITIAL_ALT: 709.

SEGMENT_FINAL_ALT: 806.

SEGMENT_CLIMB_RATE: 0.4583978 METERS/SECOND

SEGMENT_FORWARD_VELOCITY: 50. METERS/SECOND

SEGMENT_POWER_REQUIRED_PER_ENGINE: 770121.1 WATTS

SEGMENT_RANGE: 10580.33 METERS

TOTAL_FUEL_BURNED_ALL_ENGINES: 39.824364 KG

SEGMENT_TIME: 211.6066 SECOND

TOTAL_NOX_ALL_ENGINES: 0.119661614 KG

TOTAL_CO_ALL_ENGINES: 0.00023954353 KG

TOTAL_UHC_ALL_ENGINES: 0. KG

TOTAL_CO2_ALL_ENGINES: 127.6163 KG

TOTAL_H2O_ALL_ENGINES: 49.44003 KG

TOTAL_SEGMENT_TET: 1050. KELVIN

TOTAL_SEGMENT_ESFC: 84.0955 KG/KWATT

****

SEGMENT_NO: 10

SEGMENT_CONDITION:ForwClimb

SEGMENT_FINAL_LONGITUDE: 51.77893 DEGREES

SEGMENT_FINAL_LATITUDE: 33.370132 DEGREES

SEGMENT_INITIAL_ALT: 806.

SEGMENT_FINAL_ALT: 903.

SEGMENT_CLIMB_RATE: 0.4583978 METERS/SECOND

SEGMENT_FORWARD_VELOCITY: 50. METERS/SECOND

SEGMENT_POWER_REQUIRED_PER_ENGINE: 762999.3 WATTS

SEGMENT_RANGE: 10580.33 METERS

TOTAL_FUEL_BURNED_ALL_ENGINES: 39.570435 KG

SEGMENT_TIME: 211.6066 SECOND

TOTAL_NOX_ALL_ENGINES: 0.11767734 KG

TOTAL_CO_ALL_ENGINES: 0.00023936157 KG

TOTAL_UHC_ALL_ENGINES: 0. KG

TOTAL_CO2_ALL_ENGINES: 126.79136 KG

TOTAL_H2O_ALL_ENGINES: 49.12131 KG

TOTAL_SEGMENT_TET: 1050. KELVIN

TOTAL_SEGMENT_ESFC: 83.9377 KG/KWATT

****

SEGMENT_NO: 11

SEGMENT_CONDITION:ForwClimb

SEGMENT_FINAL_LONGITUDE: 51.787216 DEGREES

SEGMENT_FINAL_LATITUDE: 33.464943 DEGREES

SEGMENT_INITIAL_ALT: 903.

SEGMENT_FINAL_ALT: 1000.

SEGMENT_CLIMB_RATE: 0.4583978 METERS/SECOND

SEGMENT_FORWARD_VELOCITY: 50. METERS/SECOND

SEGMENT_POWER_REQUIRED_PER_ENGINE: 754078.75 WATTS

SEGMENT_RANGE: 10580.33 METERS

TOTAL_FUEL_BURNED_ALL_ENGINES: 39.274185 KG

SEGMENT_TIME: 211.6066 SECOND

TOTAL_NOX_ALL_ENGINES: 0.11574684 KG

TOTAL_CO_ALL_ENGINES: 0.00024679897 KG

TOTAL_UHC_ALL_ENGINES: 0. KG

TOTAL_CO2_ALL_ENGINES: 125.83268 KG

TOTAL_H2O_ALL_ENGINES: 48.750137 KG

TOTAL_SEGMENT_TET: 1050. KELVIN

TOTAL_SEGMENT_ESFC: 83.7943 KG/KWATT

****

SEGMENT_NO: 12

SEGMENT_CONDITION:ForwFlight

SEGMENT_FINAL_LONGITUDE: 51.7955 DEGREES

SEGMENT_FINAL_LATITUDE: 33.559753 DEGREES

SEGMENT_INITIAL_ALT: 1000.

SEGMENT_FINAL_ALT: 1000.

SEGMENT_CLIMB_RATE: 0. METERS/SECOND

SEGMENT_FORWARD_VELOCITY: 70. METERS/SECOND

SEGMENT_POWER_REQUIRED_PER_ENGINE: 1120482.6 WATTS

SEGMENT_RANGE: 22014.518 METERS

TOTAL_FUEL_BURNED_ALL_ENGINES: 59.3134 KG

SEGMENT_TIME: 314.4931 SECOND

TOTAL_NOX_ALL_ENGINES: 0.17956461 KG

TOTAL_CO_ALL_ENGINES: 0.00029318617 KG

TOTAL_UHC_ALL_ENGINES: 0. KG

TOTAL_CO2_ALL_ENGINES: 190.02354 KG

TOTAL_H2O_ALL_ENGINES: 73.621796 KG

TOTAL_SEGMENT_TET: 1054. KELVIN

TOTAL_SEGMENT_ESFC: 82.9577 KG/KWATT

****

SEGMENT_NO: 13

SEGMENT_CONDITION:ForwFlight

SEGMENT_FINAL_LONGITUDE: 51.823204 DEGREES

SEGMENT_FINAL_LATITUDE: 33.755825 DEGREES

SEGMENT_INITIAL_ALT: 1000.

SEGMENT_FINAL_ALT: 1000.

SEGMENT_CLIMB_RATE: 0. METERS/SECOND

SEGMENT_FORWARD_VELOCITY: 70. METERS/SECOND

SEGMENT_POWER_REQUIRED_PER_ENGINE: 1115833.9 WATTS

SEGMENT_RANGE: 22014.518 METERS

TOTAL_FUEL_BURNED_ALL_ENGINES: 58.621513 KG

SEGMENT_TIME: 314.4931 SECOND

TOTAL_NOX_ALL_ENGINES: 0.176073 KG

TOTAL_CO_ALL_ENGINES: 0.00037916395 KG

TOTAL_UHC_ALL_ENGINES: 0. KG

TOTAL_CO2_ALL_ENGINES: 187.82251 KG

TOTAL_H2O_ALL_ENGINES: 72.763016 KG

TOTAL_SEGMENT_TET: 1050. KELVIN

TOTAL_SEGMENT_ESFC: 83.1711 KG/KWATT

****

SEGMENT_NO: 14

SEGMENT_CONDITION:ForwFlight

SEGMENT_FINAL_LONGITUDE: 51.850906 DEGREES

SEGMENT_FINAL_LATITUDE: 33.951893 DEGREES

SEGMENT_INITIAL_ALT: 1000.

SEGMENT_FINAL_ALT: 1000.

SEGMENT_CLIMB_RATE: 0. METERS/SECOND

SEGMENT_FORWARD_VELOCITY: 70. METERS/SECOND

SEGMENT_POWER_REQUIRED_PER_ENGINE: 1111258.4 WATTS

SEGMENT_RANGE: 22014.518 METERS

TOTAL_FUEL_BURNED_ALL_ENGINES: 58.621513 KG

SEGMENT_TIME: 314.4931 SECOND

TOTAL_NOX_ALL_ENGINES: 0.176073 KG

TOTAL_CO_ALL_ENGINES: 0.00037916395 KG

TOTAL_UHC_ALL_ENGINES: 0. KG

TOTAL_CO2_ALL_ENGINES: 187.82251 KG

TOTAL_H2O_ALL_ENGINES: 72.763016 KG

TOTAL_SEGMENT_TET: 1050. KELVIN

TOTAL_SEGMENT_ESFC: 83.1711 KG/KWATT

****

SEGMENT_NO: 15

SEGMENT_CONDITION:ForwFlight

SEGMENT_FINAL_LONGITUDE: 51.87861 DEGREES

SEGMENT_FINAL_LATITUDE: 34.147957 DEGREES

SEGMENT_INITIAL_ALT: 1000.

SEGMENT_FINAL_ALT: 1000.

SEGMENT_CLIMB_RATE: 0. METERS/SECOND

SEGMENT_FORWARD_VELOCITY: 70. METERS/SECOND

SEGMENT_POWER_REQUIRED_PER_ENGINE: 1106701.5 WATTS

SEGMENT_RANGE: 22014.518 METERS

TOTAL_FUEL_BURNED_ALL_ENGINES: 58.621513 KG

SEGMENT_TIME: 314.4931 SECOND

TOTAL_NOX_ALL_ENGINES: 0.176073 KG

TOTAL_CO_ALL_ENGINES: 0.00037916395 KG

TOTAL_UHC_ALL_ENGINES: 0. KG

TOTAL_CO2_ALL_ENGINES: 187.82251 KG

TOTAL_H2O_ALL_ENGINES: 72.763016 KG

TOTAL_SEGMENT_TET: 1050. KELVIN

TOTAL_SEGMENT_ESFC: 83.1711 KG/KWATT

****

SEGMENT_NO: 16

SEGMENT_CONDITION:ForwFlight

SEGMENT_FINAL_LONGITUDE: 51.90631 DEGREES

SEGMENT_FINAL_LATITUDE: 34.344017 DEGREES

SEGMENT_INITIAL_ALT: 1000.

SEGMENT_FINAL_ALT: 1000.

SEGMENT_CLIMB_RATE: 0. METERS/SECOND

SEGMENT_FORWARD_VELOCITY: 70. METERS/SECOND

SEGMENT_POWER_REQUIRED_PER_ENGINE: 1102163.4 WATTS

SEGMENT_RANGE: 22014.518 METERS

TOTAL_FUEL_BURNED_ALL_ENGINES: 58.621513 KG

SEGMENT_TIME: 314.4931 SECOND

TOTAL_NOX_ALL_ENGINES: 0.176073 KG

TOTAL_CO_ALL_ENGINES: 0.00037916395 KG

TOTAL_UHC_ALL_ENGINES: 0. KG

TOTAL_CO2_ALL_ENGINES: 187.82251 KG

TOTAL_H2O_ALL_ENGINES: 72.763016 KG

TOTAL_SEGMENT_TET: 1050. KELVIN

TOTAL_SEGMENT_ESFC: 83.1711 KG/KWATT

****

SEGMENT_NO: 17

SEGMENT_CONDITION:ForwFlight

SEGMENT_FINAL_LONGITUDE: 51.93401 DEGREES

SEGMENT_FINAL_LATITUDE: 34.540073 DEGREES

SEGMENT_INITIAL_ALT: 1000.

SEGMENT_FINAL_ALT: 1000.

SEGMENT_CLIMB_RATE: 0. METERS/SECOND

SEGMENT_FORWARD_VELOCITY: 70. METERS/SECOND

SEGMENT_POWER_REQUIRED_PER_ENGINE: 1097643.5 WATTS

SEGMENT_RANGE: 22014.518 METERS

TOTAL_FUEL_BURNED_ALL_ENGINES: 58.621513 KG

SEGMENT_TIME: 314.4931 SECOND

TOTAL_NOX_ALL_ENGINES: 0.176073 KG

TOTAL_CO_ALL_ENGINES: 0.00037916395 KG

TOTAL_UHC_ALL_ENGINES: 0. KG

TOTAL_CO2_ALL_ENGINES: 187.82251 KG

TOTAL_H2O_ALL_ENGINES: 72.763016 KG

TOTAL_SEGMENT_TET: 1050. KELVIN

TOTAL_SEGMENT_ESFC: 83.1711 KG/KWATT

****

SEGMENT_NO: 18

SEGMENT_CONDITION:ForwFlight

SEGMENT_FINAL_LONGITUDE: 51.961708 DEGREES

SEGMENT_FINAL_LATITUDE: 34.736126 DEGREES

SEGMENT_INITIAL_ALT: 1000.

SEGMENT_FINAL_ALT: 1000.

SEGMENT_CLIMB_RATE: 0. METERS/SECOND

SEGMENT_FORWARD_VELOCITY: 70. METERS/SECOND

SEGMENT_POWER_REQUIRED_PER_ENGINE: 1093142.5 WATTS

SEGMENT_RANGE: 22014.518 METERS

TOTAL_FUEL_BURNED_ALL_ENGINES: 58.621513 KG

SEGMENT_TIME: 314.4931 SECOND

TOTAL_NOX_ALL_ENGINES: 0.176073 KG

TOTAL_CO_ALL_ENGINES: 0.00037916395 KG

TOTAL_UHC_ALL_ENGINES: 0. KG

TOTAL_CO2_ALL_ENGINES: 187.82251 KG

TOTAL_H2O_ALL_ENGINES: 72.763016 KG

TOTAL_SEGMENT_TET: 1050. KELVIN

TOTAL_SEGMENT_ESFC: 83.1711 KG/KWATT

****

SEGMENT_NO: 19

SEGMENT_CONDITION:ForwFlight

SEGMENT_FINAL_LONGITUDE: 51.989407 DEGREES

SEGMENT_FINAL_LATITUDE: 34.93217 DEGREES

SEGMENT_INITIAL_ALT: 1000.

SEGMENT_FINAL_ALT: 1000.

SEGMENT_CLIMB_RATE: 0. METERS/SECOND

SEGMENT_FORWARD_VELOCITY: 70. METERS/SECOND

SEGMENT_POWER_REQUIRED_PER_ENGINE: 1088659.8 WATTS

SEGMENT_RANGE: 22014.518 METERS

TOTAL_FUEL_BURNED_ALL_ENGINES: 58.621513 KG

SEGMENT_TIME: 314.4931 SECOND

TOTAL_NOX_ALL_ENGINES: 0.176073 KG

TOTAL_CO_ALL_ENGINES: 0.00037916395 KG

TOTAL_UHC_ALL_ENGINES: 0. KG

TOTAL_CO2_ALL_ENGINES: 187.82251 KG

TOTAL_H2O_ALL_ENGINES: 72.763016 KG

TOTAL_SEGMENT_TET: 1050. KELVIN

TOTAL_SEGMENT_ESFC: 83.1711 KG/KWATT

****

SEGMENT_NO: 20

SEGMENT_CONDITION:ForwFlight

SEGMENT_FINAL_LONGITUDE: 52.017105 DEGREES

SEGMENT_FINAL_LATITUDE: 35.128212 DEGREES

SEGMENT_INITIAL_ALT: 1000.

SEGMENT_FINAL_ALT: 1000.

SEGMENT_CLIMB_RATE: 0. METERS/SECOND

SEGMENT_FORWARD_VELOCITY: 70. METERS/SECOND

SEGMENT_POWER_REQUIRED_PER_ENGINE: 1084195.5 WATTS

SEGMENT_RANGE: 22014.518 METERS

TOTAL_FUEL_BURNED_ALL_ENGINES: 58.621513 KG

SEGMENT_TIME: 314.4931 SECOND

TOTAL_NOX_ALL_ENGINES: 0.176073 KG

TOTAL_CO_ALL_ENGINES: 0.00037916395 KG

TOTAL_UHC_ALL_ENGINES: 0. KG

TOTAL_CO2_ALL_ENGINES: 187.82251 KG

TOTAL_H2O_ALL_ENGINES: 72.763016 KG

TOTAL_SEGMENT_TET: 1050. KELVIN

TOTAL_SEGMENT_ESFC: 83.1711 KG/KWATT

****

SEGMENT_NO: 21

SEGMENT_CONDITION:ForwFlight

SEGMENT_FINAL_LONGITUDE: 52.044804 DEGREES

SEGMENT_FINAL_LATITUDE: 35.32425 DEGREES

SEGMENT_INITIAL_ALT: 1000.

SEGMENT_FINAL_ALT: 1000.

SEGMENT_CLIMB_RATE: 0. METERS/SECOND

SEGMENT_FORWARD_VELOCITY: 70. METERS/SECOND

SEGMENT_POWER_REQUIRED_PER_ENGINE: 1079749.5 WATTS

SEGMENT_RANGE: 22014.518 METERS

TOTAL_FUEL_BURNED_ALL_ENGINES: 58.621513 KG

SEGMENT_TIME: 314.4931 SECOND

TOTAL_NOX_ALL_ENGINES: 0.176073 KG

TOTAL_CO_ALL_ENGINES: 0.00037916395 KG

TOTAL_UHC_ALL_ENGINES: 0. KG

TOTAL_CO2_ALL_ENGINES: 187.82251 KG

TOTAL_H2O_ALL_ENGINES: 72.763016 KG

TOTAL_SEGMENT_TET: 1050. KELVIN

TOTAL_SEGMENT_ESFC: 83.1711 KG/KWATT

****

SEGMENT_NO: 22

SEGMENT_CONDITION:ForwDesc

SEGMENT_FINAL_LONGITUDE: 52.072502 DEGREES

SEGMENT_FINAL_LATITUDE: 35.520283 DEGREES

SEGMENT_INITIAL_ALT: 1000.

SEGMENT_FINAL_ALT: 903.

SEGMENT_CLIMB_RATE: -0.5974319 METERS/SECOND

SEGMENT_FORWARD_VELOCITY: 50.000004 METERS/SECOND

SEGMENT_POWER_REQUIRED_PER_ENGINE: 754005.44 WATTS

SEGMENT_RANGE: 8118.0806 METERS

TOTAL_FUEL_BURNED_ALL_ENGINES: 30.134314 KG

SEGMENT_TIME: 162.3616 SECOND

TOTAL_NOX_ALL_ENGINES: 0.08881029 KG

TOTAL_CO_ALL_ENGINES: 0.00018936403 KG

TOTAL_UHC_ALL_ENGINES: 0. KG

TOTAL_CO2_ALL_ENGINES: 96.54895 KG

TOTAL_H2O_ALL_ENGINES: 37.405025 KG

TOTAL_SEGMENT_TET: 1050. KELVIN

TOTAL_SEGMENT_ESFC: 83.7943 KG/KWATT

****

SEGMENT_NO: 23

SEGMENT_CONDITION:ForwDesc

SEGMENT_FINAL_LONGITUDE: 52.072502 DEGREES

SEGMENT_FINAL_LATITUDE: 35.59329 DEGREES

SEGMENT_INITIAL_ALT: 903.

SEGMENT_FINAL_ALT: 806.

SEGMENT_CLIMB_RATE: -0.5974319 METERS/SECOND

SEGMENT_FORWARD_VELOCITY: 50.000004 METERS/SECOND

SEGMENT_POWER_REQUIRED_PER_ENGINE: 759968.3 WATTS

SEGMENT_RANGE: 8118.0806 METERS

TOTAL_FUEL_BURNED_ALL_ENGINES: 30.361622 KG

SEGMENT_TIME: 162.3616 SECOND

TOTAL_NOX_ALL_ENGINES: 0.090291515 KG

TOTAL_CO_ALL_ENGINES: 0.00018365745 KG

TOTAL_UHC_ALL_ENGINES: 0. KG

TOTAL_CO2_ALL_ENGINES: 97.28453 KG

TOTAL_H2O_ALL_ENGINES: 37.68982 KG

TOTAL_SEGMENT_TET: 1050. KELVIN

TOTAL_SEGMENT_ESFC: 83.9377 KG/KWATT

****

SEGMENT_NO: 24

SEGMENT_CONDITION:ForwDesc

SEGMENT_FINAL_LONGITUDE: 52.072502 DEGREES

SEGMENT_FINAL_LATITUDE: 35.666294 DEGREES

SEGMENT_INITIAL_ALT: 806.

SEGMENT_FINAL_ALT: 709.

SEGMENT_CLIMB_RATE: -0.5974319 METERS/SECOND

SEGMENT_FORWARD_VELOCITY: 50.000004 METERS/SECOND

SEGMENT_POWER_REQUIRED_PER_ENGINE: 765985.8 WATTS

SEGMENT_RANGE: 8118.0806 METERS

TOTAL_FUEL_BURNED_ALL_ENGINES: 30.556454 KG

SEGMENT_TIME: 162.3616 SECOND

TOTAL_NOX_ALL_ENGINES: 0.09181402 KG

TOTAL_CO_ALL_ENGINES: 0.00018379706 KG

TOTAL_UHC_ALL_ENGINES: 0. KG

TOTAL_CO2_ALL_ENGINES: 97.917496 KG

TOTAL_H2O_ALL_ENGINES: 37.93437 KG

TOTAL_SEGMENT_TET: 1050. KELVIN

TOTAL_SEGMENT_ESFC: 84.0955 KG/KWATT

****

SEGMENT_NO: 25

SEGMENT_CONDITION:ForwDesc

SEGMENT_FINAL_LONGITUDE: 52.072502 DEGREES

SEGMENT_FINAL_LATITUDE: 35.7393 DEGREES

SEGMENT_INITIAL_ALT: 709.

SEGMENT_FINAL_ALT: 612.

SEGMENT_CLIMB_RATE: -0.5974319 METERS/SECOND

SEGMENT_FORWARD_VELOCITY: 50.000004 METERS/SECOND

SEGMENT_POWER_REQUIRED_PER_ENGINE: 772058.4 WATTS

SEGMENT_RANGE: 8118.0806 METERS

TOTAL_FUEL_BURNED_ALL_ENGINES: 30.783762 KG

SEGMENT_TIME: 162.3616 SECOND

TOTAL_NOX_ALL_ENGINES: 0.09333132 KG

TOTAL_CO_ALL_ENGINES: 0.0001782072 KG

TOTAL_UHC_ALL_ENGINES: 0. KG

TOTAL_CO2_ALL_ENGINES: 98.653404 KG

TOTAL_H2O_ALL_ENGINES: 38.21929 KG

TOTAL_SEGMENT_TET: 1050. KELVIN

TOTAL_SEGMENT_ESFC: 84.2453 KG/KWATT

****

SEGMENT_NO: 26

SEGMENT_CONDITION:ForwDesc

SEGMENT_FINAL_LONGITUDE: 52.072502 DEGREES

SEGMENT_FINAL_LATITUDE: 35.812305 DEGREES

SEGMENT_INITIAL_ALT: 612.

SEGMENT_FINAL_ALT: 515.

SEGMENT_CLIMB_RATE: -0.5974319 METERS/SECOND

SEGMENT_FORWARD_VELOCITY: 50.000004 METERS/SECOND

SEGMENT_POWER_REQUIRED_PER_ENGINE: 778185.56 WATTS

SEGMENT_RANGE: 8118.0806 METERS

TOTAL_FUEL_BURNED_ALL_ENGINES: 30.978594 KG

SEGMENT_TIME: 162.3616 SECOND

TOTAL_NOX_ALL_ENGINES: 0.09492043 KG

TOTAL_CO_ALL_ENGINES: 0.00017877747 KG

TOTAL_UHC_ALL_ENGINES: 0. KG

TOTAL_CO2_ALL_ENGINES: 99.286865 KG

TOTAL_H2O_ALL_ENGINES: 38.463966 KG

TOTAL_SEGMENT_TET: 1050. KELVIN

TOTAL_SEGMENT_ESFC: 84.3932 KG/KWATT

****

SEGMENT_NO: 27

SEGMENT_CONDITION:ForwDesc

SEGMENT_FINAL_LONGITUDE: 52.072502 DEGREES

SEGMENT_FINAL_LATITUDE: 35.885307 DEGREES

SEGMENT_INITIAL_ALT: 515.

SEGMENT_FINAL_ALT: 418.

SEGMENT_CLIMB_RATE: -0.5974319 METERS/SECOND

SEGMENT_FORWARD_VELOCITY: 50.000004 METERS/SECOND

SEGMENT_POWER_REQUIRED_PER_ENGINE: 784368.25 WATTS

SEGMENT_RANGE: 8118.0806 METERS

TOTAL_FUEL_BURNED_ALL_ENGINES: 31.205902 KG

SEGMENT_TIME: 162.3616 SECOND

TOTAL_NOX_ALL_ENGINES: 0.09645691 KG

TOTAL_CO_ALL_ENGINES: 0.0001734424 KG

TOTAL_UHC_ALL_ENGINES: 0. KG

TOTAL_CO2_ALL_ENGINES: 100.02312 KG

TOTAL_H2O_ALL_ENGINES: 38.749027 KG

TOTAL_SEGMENT_TET: 1050. KELVIN

TOTAL_SEGMENT_ESFC: 84.5535 KG/KWATT

****

SEGMENT_NO: 28

SEGMENT_CONDITION:ForwDesc

SEGMENT_FINAL_LONGITUDE: 52.072502 DEGREES

SEGMENT_FINAL_LATITUDE: 35.95831 DEGREES

SEGMENT_INITIAL_ALT: 418.

SEGMENT_FINAL_ALT: 321.

SEGMENT_CLIMB_RATE: -0.5974319 METERS/SECOND

SEGMENT_FORWARD_VELOCITY: 50.000004 METERS/SECOND

SEGMENT_POWER_REQUIRED_PER_ENGINE: 790605.4 WATTS

SEGMENT_RANGE: 8118.0806 METERS

TOTAL_FUEL_BURNED_ALL_ENGINES: 31.433207 KG

SEGMENT_TIME: 162.3616 SECOND

TOTAL_NOX_ALL_ENGINES: 0.098026305 KG

TOTAL_CO_ALL_ENGINES: 0.00016901636 KG

TOTAL_UHC_ALL_ENGINES: 0. KG

TOTAL_CO2_ALL_ENGINES: 100.75969 KG

TOTAL_H2O_ALL_ENGINES: 39.034153 KG

TOTAL_SEGMENT_TET: 1050. KELVIN

TOTAL_SEGMENT_ESFC: 84.7131 KG/KWATT

****

SEGMENT_NO: 29

SEGMENT_CONDITION:ForwDesc

SEGMENT_FINAL_LONGITUDE: 52.072502 DEGREES

SEGMENT_FINAL_LATITUDE: 36.03131 DEGREES

SEGMENT_INITIAL_ALT: 321.

SEGMENT_FINAL_ALT: 224.

SEGMENT_CLIMB_RATE: -0.5974319 METERS/SECOND

SEGMENT_FORWARD_VELOCITY: 50.000004 METERS/SECOND

SEGMENT_POWER_REQUIRED_PER_ENGINE: 796897.3 WATTS

SEGMENT_RANGE: 8118.0806 METERS

TOTAL_FUEL_BURNED_ALL_ENGINES: 31.628042 KG

SEGMENT_TIME: 162.3616 SECOND

TOTAL_NOX_ALL_ENGINES: 0.09963048 KG

TOTAL_CO_ALL_ENGINES: 0.00016889375 KG

TOTAL_UHC_ALL_ENGINES: 0. KG

TOTAL_CO2_ALL_ENGINES: 101.393524 KG

TOTAL_H2O_ALL_ENGINES: 39.279034 KG

TOTAL_SEGMENT_TET: 1050. KELVIN

TOTAL_SEGMENT_ESFC: 84.8783 KG/KWATT

****

SEGMENT_NO: 30

SEGMENT_CONDITION:ForwDesc

SEGMENT_FINAL_LONGITUDE: 52.072502 DEGREES

SEGMENT_FINAL_LATITUDE: 36.104313 DEGREES

SEGMENT_INITIAL_ALT: 224.

SEGMENT_FINAL_ALT: 127.

SEGMENT_CLIMB_RATE: -0.5974319 METERS/SECOND

SEGMENT_FORWARD_VELOCITY: 50.000004 METERS/SECOND

SEGMENT_POWER_REQUIRED_PER_ENGINE: 803244.8 WATTS

SEGMENT_RANGE: 8118.0806 METERS

TOTAL_FUEL_BURNED_ALL_ENGINES: 31.855347 KG

SEGMENT_TIME: 162.3616 SECOND

TOTAL_NOX_ALL_ENGINES: 0.10118972 KG

TOTAL_CO_ALL_ENGINES: 0.00016421432 KG

TOTAL_UHC_ALL_ENGINES: 0. KG

TOTAL_CO2_ALL_ENGINES: 102.13029 KG

TOTAL_H2O_ALL_ENGINES: 39.564293 KG

TOTAL_SEGMENT_TET: 1050. KELVIN

TOTAL_SEGMENT_ESFC: 85.0508 KG/KWATT

****

SEGMENT_NO: 31

SEGMENT_CONDITION:ForwDesc

SEGMENT_FINAL_LONGITUDE: 52.072502 DEGREES

SEGMENT_FINAL_LATITUDE: 36.177315 DEGREES

SEGMENT_INITIAL_ALT: 127.

SEGMENT_FINAL_ALT: 30.

SEGMENT_CLIMB_RATE: -0.5974319 METERS/SECOND

SEGMENT_FORWARD_VELOCITY: 50.000004 METERS/SECOND

SEGMENT_POWER_REQUIRED_PER_ENGINE: 809646.75 WATTS

SEGMENT_RANGE: 8118.0806 METERS

TOTAL_FUEL_BURNED_ALL_ENGINES: 32.050182 KG

SEGMENT_TIME: 162.3616 SECOND

TOTAL_NOX_ALL_ENGINES: 0.10284195 KG

TOTAL_CO_ALL_ENGINES: 0.00016387258 KG

TOTAL_UHC_ALL_ENGINES: 0. KG

TOTAL_CO2_ALL_ENGINES: 102.76445 KG

TOTAL_H2O_ALL_ENGINES: 39.80931 KG

TOTAL_SEGMENT_TET: 1050. KELVIN

TOTAL_SEGMENT_ESFC: 85.2232 KG/KWATT

****

SEGMENT_NO: 32

SEGMENT_CONDITION:Hover

SEGMENT_FINAL_LONGITUDE: 52.072502 DEGREES

SEGMENT_FINAL_LATITUDE: 36.250317 DEGREES

SEGMENT_INITIAL_ALT: 30.

SEGMENT_FINAL_ALT: 30.

SEGMENT_CLIMB_RATE: 0. METERS/SECOND

SEGMENT_FORWARD_VELOCITY: 0. METERS/SECOND

SEGMENT_POWER_REQUIRED_PER_ENGINE: 522167.84 WATTS

SEGMENT_RANGE: 0. METERS

TOTAL_FUEL_BURNED_ALL_ENGINES: 70.56 KG

SEGMENT_TIME: 360. SECOND

TOTAL_NOX_ALL_ENGINES: 0.2188242 KG

TOTAL_CO_ALL_ENGINES: 0.00034743742 KG

TOTAL_UHC_ALL_ENGINES: 0. KG

TOTAL_CO2_ALL_ENGINES: 226.23146 KG

TOTAL_H2O_ALL_ENGINES: 87.6454 KG

TOTAL_SEGMENT_TET: 1050. KELVIN

TOTAL_SEGMENT_ESFC: 84.3019 KG/KWATT

****